

Stochastic Control Strategies for Residential Microgrids

Potential Benefits of Micro-CHP Installation in Multifamily Buildings

Domenico Laudiero

Master of Science Thesis

Stochastic Control Strategies for Residential Microgrids

Potential Benefits of Micro-CHP Installation in Multifamily Buildings

MASTER OF SCIENCE THESIS

For the degree of Master of Science in Systems and Control at Delft
University of Technology

Domenico Laudiero

May 21, 2018

Faculty of Mechanical, Maritime and Materials Engineering (3mE) · Delft University of
Technology



Copyright © Delft Center for Systems and Control (DCSC)
All rights reserved.



Abstract

Fast depleting fossil fuels and growing awareness for environmental protection have led us to the urgency of a long-term energy planning where reduction of emissions, integration of renewable supply, and energy efficiency improvement represent the main targets of a ‘smarter’ employment of primary resources. Research is needed nowadays to drive a transient phase towards the construction of future ‘smart grids’, where multiple actors will be able to communicate with each other and efficiently adapt their production/consumption with respect to the dynamic evolution of the increasingly complex power network. In this scenario, operational management of small, local electricity networks (microgrids) and their two-way interconnection to the main grid are creating new opportunities and, at the same time, new technological challenges. Advanced control schemes are being investigated to smoothen the integration of distributed generation and to achieve optimal operation at microgrid level, through coordination and dispatching of power generation, flexible loads, and storage elements.

The residential sector is responsible for about 30% of the global energy consumption and has historically played a passive role in the unidirectional centralised power infrastructure. A residential microgrid that utilises controllable prime movers, such as gas engines, to compensate fluctuating demand and output of renewable energy would represent a fundamental step towards a more economic, efficient, and environment friendly energy infrastructure. This MSc thesis project focuses on the design of energy management systems in residential buildings where micro-Combined Heat and Power (CHP) generators are installed. Micro-CHP technology is able to produce electrical energy locally in a controllable way, having at the same time the advantage of efficiently employing by-product heat to satisfy thermal demand of the building where it is located. The purpose of our work is an economic analysis regarding the profitability of investment in distributed energy resources for Dutch households and a subsequent investigation about the benefits that advanced control techniques would lead to microgrid operation on the long run. For this reason, specific case studies are built based on real data of thermal and electric consumption, which have been collected through smart meters in various Dutch houses. Two different versions of the microgrid are considered: a first case only involves micro-CHP and thermal energy storage, whereas a second one is expanded to include solar panels.

Advanced techniques employed for supervisory control of power flows in microgrids generally

aim to take into account relevant information about the consequences of choosing specific actions, by considering future predictions of system evolution. Model Predictive Control (MPC) is a well-known, established and widely used control technique that is often considered as a natural approach to adopt in microgrids. Its main strength is the ability to turn a control problem into an optimisation problem; therefore the capability of including operational constraints arises naturally. However, high volatility of small-scale demand and intrinsic stochasticity of renewable energy supply lead to the hard challenge of integrating appropriate forecasting models into the decision-making strategy. When deterministic approaches relying on the certainty equivalence paradigm are applied in residential microgrids, frequent violations of thermal comfort constraints occur due to poor prediction accuracy of the stochastic processes involved. The possibility to explicitly take into account the uncertainty affecting the controlled system extends the effectiveness of the predictive control strategies, at the cost of increased complexity. Therefore, suitable probabilistic formulation of the forecasting models for stochastic processes and subsequent control strategies in the MPC framework are studied in our work. Different stochastic approaches recently studied in the scientific literature, i.e. scenario based and tree based, are implemented and compared for the defined case studies. Their performance is evaluated in terms of economic savings, primary energy consumption, and violation of thermal comfort constraints for the households.

The results of our work show the profitability of investment in residential microgrids for average Dutch households willing to share the installation of distributed energy resources in multifamily buildings, even in absence of government subsidies. Moreover, the employment of predictive strategies for local generation scheduling results in slightly improved performance with respect to traditional rule-based controllers. The poor prediction accuracy of demand forecasting on small spatial scale still represents the main difficulty to overcome in order to fill the gap with the theoretical potential benefits of ‘optimal’ predictive strategies. However, in the investigated context, the need for a stochastic framework is motivated and highlighted with respect to the usage of deterministic tools due to the large variance of uncertainty in system dynamics.

Table of Contents

Acknowledgements	vii
1 Introduction	1
1-1 Residential Microgrids: Motivation	2
1-2 Residential Microgrids: Challenges	3
1-3 Research Objectives	5
1-4 Thesis Contribution	6
1-5 Thesis Outline	6
2 Microgrid: Description and Modelling	9
2-1 Distributed Generation in Smart Grids	9
2-1-1 Centralised Electricity Infrastructure	10
2-1-2 Decentralisation of Power Generation	11
2-1-3 Local Energy Management System (EMS)	12
2-2 Available Technologies: Elements of a Residential Microgrid	14
2-2-1 Micro-CHP Technologies	14
2-2-2 Gas-Fired Boiler	16
2-2-3 Thermal Energy Storage (TES)	17
2-2-4 PhotoVoltaic (PV) Systems	17
2-3 Microgrid Modelling	18
2-3-1 Power Balance	19
2-3-2 Operational Constraints	20
2-3-3 Stochastic Formulation	21
2-3-4 Performance Indices	22
2-4 Conclusions	24

3	Economic Profitability: Investment in Residential Microgrids	25
3-1	Analysis of Energy Demand	25
3-2	Initial Economic Assessment for the Dutch Scenario	27
3-2-1	Potential Benefits of Micro-CHP	28
3-2-2	Potential Benefits of Solar Panels	32
3-3	Optimal Sizing of Energy Resources	35
3-3-1	Selection of Typical Days	35
3-3-2	Sizing Problem	38
3-3-3	Definition of Case Studies	39
3-4	Conclusions	40
4	Forecasting of Stochastic Processes	41
4-1	Literature Background	41
4-1-1	Point Forecasting	42
4-1-2	Probabilistic Forecasting	45
4-2	Energy Consumption Patterns	48
4-2-1	Prediction Factors	49
4-2-2	Benchmark: Naive Forecasting	52
4-2-3	Point Forecasting Models	53
4-2-4	Probabilistic Forecasting	54
4-3	Photovoltaic Generation	58
4-3-1	Clear Sky Model	58
4-3-2	Forecasting Model	60
4-4	Conclusions	61
5	Control Strategies for Energy Management Systems	63
5-1	Literature Background: Model Predictive Control	63
5-1-1	Classic MPC	64
5-1-2	Robust MPC	66
5-1-3	Stochastic MPC	67
5-2	Benchmark Strategy: Rule-Based Control	70
5-3	Certainty Equivalence: MPC	71
5-3-1	Deterministic Formulation	72
5-3-2	Practical Disadvantages	73
5-4	Stochastic Reformulation	74
5-4-1	Scenario-Based Approach	74
5-4-2	Tree-Based Approach	76
5-5	Conclusions	78
6	Simulation and Comparison	79
6-1	Case Study 'A': Micro-CHP	80
6-2	Case Study 'B': Micro-CHP and PV Generation	84
6-3	Conclusions	84

7 Conclusions & Recommendations	89
7-1 Summary	89
7-2 Conclusions	90
7-3 Future Work	91
Bibliography	93
Glossary	101
List of Acronyms	101
List of Symbols	101

Acknowledgements

I would like to especially thank my daily supervisor T. Pippia for his assistance during the long work of this year. It has been an hard challenge for me to achieve this final goal, and you were kind to understand my difficulties and push me forward.

I would like to acknowledge my supervisor prof.dr.ir. B. De Schutter for his guidance and assistance which helped me to complete this thesis. Your meticulous attitude to my work had certainly helped me to improve my final report.

I want to deeply thank my family. Without your support all of this would have never been possible. I thank you for bearing my long and evading silences with patience and unconditional love. Thanks to my grandma, I would love to reach your age with at least 1% of the same open-mindedness, wiseness and tolerant fondness that characterizes you.

Thanks to my Italian-Dutch friends. Kneppelhoutstraat has been my second home in the Netherlands, every time I needed a warm and cosy place where to find friends your doors were open. Thanks Edo, for our endless conversations and your sparky spirit that often helped me to distract and stimulate my mind. And, even though I have not been very present for you, both physically and mentally, 'Azzurri Delft', you were the best Sunday companions I could have asked. Thanks Luche' for being an unforgettable house mate.

Thanks to my Neapolitan friends, spread all over the world. I know we will always be heartily inseparable. Aldo and Bob, your presence during the writing of this thesis meant to me a lot more than you could expect. Thanks to Miranda for her sudden and fool proposals, I hope we keep on sharing our huge passion for travelling.

A special thank to the person who I will always admire, and who helped me to come back on my path and complete this struggling battle. I cannot stop to consider you as a living part of me.

To my grandparents, I feel you smile with me today.

Delft, University of Technology
May 21, 2018

Domenico Laudiero

“La facoltà d’illuderci che la realtà d’oggi sia la sola vera, se da un canto ci sostiene, dall’altro ci precipita in un vuoto senza fine, perché la realtà d’oggi è destinata a scoprire l’illusione domani. E la vita non conclude. Non può concludere. Se domani conclude, è finita.”

— *Luigi Pirandello*

Chapter 1

Introduction

During the first development of the electrical industry, back in 1882, centrally controlled electrical network was not developed yet and the company led by Thomas Edison was installing steam-powered plants with dedicated local loads. When the economical benefits related to the usage of large-scale centralised plants drove modern society to the power infrastructure that we have nowadays, the idea of independent and locally balanced small networks was left apart and not considered anymore for a long time. However, as power infrastructure grew bigger and bigger, it became progressively more complex to control and manage.

Today urban population is increasingly growing and more energy intensive activities represent the consequences of a healthier and richer urbanised society. According to the main scenario of the World Energy Outlook 2017 [39], by 2040, the global energy demand is predicted to add the equivalent of today's China and India consumption to the current needs. The growing electrification of energy and the shift to a more service-oriented economy create new challenges for the conventional power infrastructure and the system of centralised power generation. Furthermore, the rapid deployment and falling costs of clean energy technologies, pushed by the necessity to reduce anthropogenic carbon emissions, is introducing in the network a large share of hardly controllable and intermittent sources of power, which makes the management of this increasingly complex system a challenging task to achieve.

Hence, through a mature analysis of the many drawbacks linked to the extreme centralised structure of power generation, that original idea by Edison has caused new interests in industry and society. The development of small local electricity networks, named **microgrids**, has been investigated in the recent years with the purpose to facilitate the integration of renewable energy resources for a cleaner energy mix, and improve efficiency of generation and transmission processes. The diffusion of microgrids on the market has been aided by the huge development in power electronics, which provides useful tools for control and conversion of electric power and allows a bidirectional interconnection between microgrids and the utility grid, distributed energy technologies, whose decreasing investment costs have encouraged their installation on small-scale systems, and Information and Communication Technologies (ICT), which made easier the communication between the many different components of a microgrid and their coordination through advanced control schemes [64]. For these reasons the installation of microgrids is spreading worldwide and, according to Navigant Research [60], global

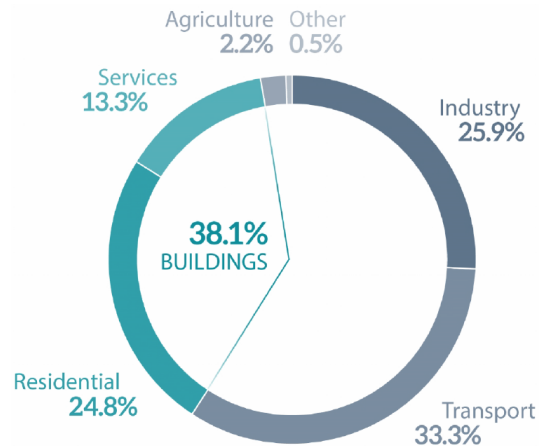


Figure 1-1: Finally energy consumption by sector in EU in 2014 [22]

microgrid capacity is expected to grow from 1.4 GW in 2015 to 7.6 GW in 2024 under a base scenario.

1-1 Residential Microgrids: Motivation

In the European Union, buildings account for 40% of final energy consumption and contribute about 36% of greenhouse gas emissions (as shown in Figure 1-1, [22]). Consequently, it seems noticeable that buildings could represent a fundamental key factor in order to achieve the main objectives of EU energy policies related to emissions cutting and overall energy efficiency improvement.

Aware of the huge benefits that a smart and efficient management of domestic consumption could lead to the modern power system, in our work we decided to focus on the residential sector and, specifically, on the potential benefits of microgrid integration in residential buildings.

Two more reasons are deeply related to the motivation of this thesis topic:

- The conspicuous thermal consumption associated with electric demand in residential buildings provides room for a notable drive in efficiency improvement by means of **micro-cogeneration** processes. Micro-cogeneration technology, known as Combined Heat and Power (CHP), aims to capture the by-product heat usually wasted in conventional power generation and allows its usage directly on site, thus greatly decreasing primary energy consumption. In northern cold countries, such as the Netherlands, where space heating in average houses represents about 70% of total consumption [20], the motivation for micro-cogeneration systems is even stronger.
- The lowering market price of distributed energy technologies encourage private customers to invest in their installation, pushed by economic incentives realized in bill reduction, and motivate their integration in energy networks as small as single houses. Specifically, together with the micro-CHP engines, we focused our attention on the renewable technology whose market has experienced one of the most rapid expansion in the last decades: PhotoVoltaic (PV) systems.

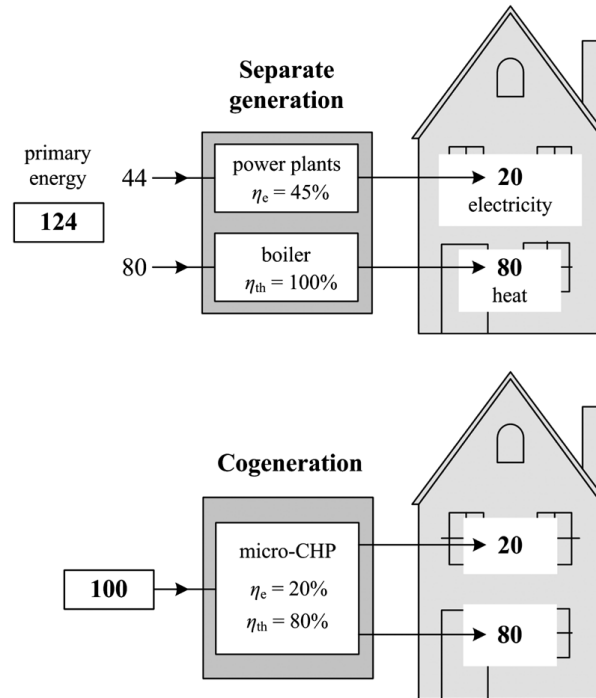


Figure 1-2: Primary energy resources. Comparison between cogeneration and separate generation [38]

Before presenting further details of our work, in order to better explain how the efficiency of domestic energy use is substantially improved when a micro-cogeneration system is integrated in a residential environment, we want to briefly provide a simplified comparison with the conventional case of separate generation. We take into consideration a single household whose electrical and thermal demand are 20 and 80 units, respectively. In standard houses, thermal demand is provided through the utilization of high-efficiency boilers that convert the calorific value of natural gas into heating, while, on the other hand, electrical demand is supplied by transmission and distribution lines which connect large power plants directly to our houses. As showed in Figure 1-2, if we substituted the boiler with a high-efficiency micro-CHP of comparable size, we would achieve primary energy savings of 24 units, corresponding to 19% of total conventional consumption.

1-2 Residential Microgrids: Challenges

In order to allow penetration of flexible distributed generation, the structure of the actual utility grid has to radically change, going from a passive unidirectional infrastructure towards an active distribution system where electricity can flow bidirectionally from the distribution network to the interconnected microgrids and vice versa. Indeed, the user of a microgrid can become a net producer for some periods of the day, when local supply exceeds demand. In this way the new figure of ‘prosumer’ starts emerging, who plays the double role of producer and consumer of electric power. Hence, a new market should be defined in order to regulate and balance the power flows in this dynamic power grid: on one hand, the prosumers have

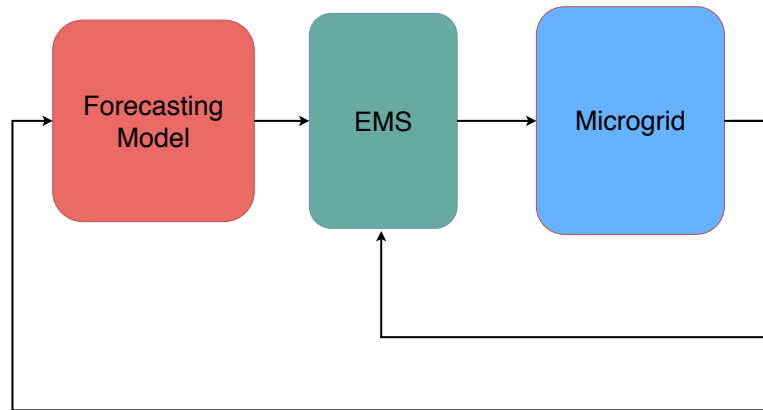


Figure 1-3: Control scheme for the Energy Management System (EMS) in a residential microgrid

to provide a substantial self-supply and avoid to become an obstacle for the management of distribution networks, while, on the other hand, as investors, they want to maximise their profits in terms of either revenues or cost savings in electricity. Consequently, it is fundamental for the retailers to set an appropriate electricity pricing policy which takes into account both the interests of the distribution system operators and those of the prosumers [67]. On our side, we focus on the **management of residential microgrids and their energy resources**, thus assuming that the trading between the prosumers and the distribution network has already been solved and the decisions of prosumers have to deal with a fixed pricing scheme. In this context, an Energy Management System (EMS) has the purpose to make optimal decisions during microgrid operation and maximise the cost savings of the prosumer. An EMS operating in interconnected microgrids should, therefore, employ intelligent control techniques in order to optimally choose and schedule the production of the micro-sources integrated in the local network.

Forecasting The supervisory control problem in a microgrid deals with the satisfaction of electrical and thermal demand of the local consumers, under economical and technical conditions, despite the uncertainties and disturbances that might appear in the system. In this sense, residential microgrid management can considerably benefit from accurate **short-term forecasting** of local demand or uncontrollable renewable supply, since, in order to guarantee continuous balance between supply and demand, economy of operations is quite sensitive to information regarding the future behaviour of the network. Consequently, the general control scheme employed in many scientific works is compactly represented in Figure 1-3. Here, a first block containing the forecasting model of microgrid uncontrollable dynamics (i.e. local energy demand or renewable supply) is clearly highlighted and provides the necessary input for the EMS.

While traditional forecasting techniques have been widely applied in the power sector to estimate future load profiles of aggregated consumption on national or regional scale, the intrinsic stochastic behaviour of the end users becomes more relevant and, consequently, the

accuracy of prediction deteriorates, as the spatial scale of forecasting decreases (disaggregated consumption) [33]. A large amount of data, highly granular both temporally and spatially, is requested for the identification of appropriate forecasting models on small-scale environments. Timely, the smart meter deployment over the past decade is providing the industry with the necessary datasets, even though their public availability for research purposes seems to be still limited.

Control In the scientific literature and in many industrial processes, **Model Predictive Control (MPC)** is the most widespread control strategy applied for solving high-level supervisory problems where constraints on the manipulated and controlled variables have to be considered in the control design [52]. The MPC framework seems to perfectly suit the purpose of an EMS in order to control and schedule set-points for dispatchable energy resources within a microgrid.

However, even though classic deterministic MPC has been widely applied in the microgrid literature [68, 38, 65, 12, 10], many issues are kept unsolved in its employment for residential environments. High volatility of small-scale demand leads to the necessity of explicitly taking into account the uncertainty affecting the system under study. Moreover, possible integration of renewable power sources, such as PV modules, introduces a further degree of stochasticity due to their intermittent and uncontrollable power generation. Appropriate probabilistic formulation of the forecasting models for the mentioned stochastic processes and subsequent control strategies in the MPC framework are therefore researched and analysed in this work. In the considered field of stochastic optimization, great improvements were led in the recent years through the inclusion of uncertainty models in the formulation of the optimization problems [24, 55]. However, the method to acquire or define the exact probability distributions, which should be accurate enough for planners to rely on, is still a tough and unsolved problem. Often, the probabilistic distributions of stochastic variables associated with solar irradiation and electrical or thermal loads have been assumed as already known in scientific works [85, 30, 17]. For this reason, the use of stochastic MPC in real world problems or in other applications is still limited or not fully explored.

1-3 Research Objectives

In the presented context, we focused our thesis work on the actual conditions for investment in microgrid technologies in the Dutch residential sector, with the aim to provide practical results to quantify and evaluate the economic profitability granted during the lifetime operation of the microgrid under a suitable control strategy.

To this purpose we advance the two following objectives:

- 1. Assess economic profitability of investment in a residential microgrid*
- 2. Evaluate the impact of stochastic control strategies in order to minimise operational costs in a residential microgrid*

Target ‘1’ is pursued through an economical investigation focused on the distributed energy resources presently available on the market and the analysis of energy demand of average

Dutch customers. It is then concluded at the end of Chapter 3 with the definition of **two case studies** ('A' and 'B'), whose components are optimally sized with respect to the economic objective. The main difference between the two considered examples is represented by the employment of solar panels in the second case, which introduces a source of uncertainty on the supply side, besides to the intrinsic uncertainty in the energy demand.

On the other hand, target '2' is considered in the second part of this thesis and deals with the implementation of control strategies in the EMS to optimally operate the residential microgrids previously defined. Specifically, our aim is to evaluate the potential benefits of stochastic strategies with respect to the traditional deterministic framework in the field of optimal power flows. Indeed, stochastic formulation of the control problem explicitly considers and models the uncertainties related to the volatile external processes perturbing the system, i.e. energy consumption of the households and PV intermittent generation, thus adding a degree of complexity which is expected to pay off in terms of economic performance.

1-4 Thesis Contribution

This thesis work has been guided by the purpose to evaluate the benefits of actual technologies and employment of intelligent control strategies for microgrid management in real life conditions. Moreover, we focused our attention on the specific context of the Netherlands.

For these reasons, we decided to build case studies inspired by **real datasets**, and we avoided any theoretical assumptions about the processes affecting microgrid operation. Hence, forecasting models for the volatile stochastic processes appearing in the system dynamics are identified based on the mentioned real datasets.

Moreover, different stochastic approaches recently studied in the scientific literature, i.e. scenario-based [76] and tree-based [49] MPC, have been adapted, implemented and compared on the defined case studies. Finally, performance of the control strategies have been evaluated in terms of economic savings, primary energy consumption and potential violations of thermal comfort constraints for the households. Indeed, in the small scale context of a residential microgrid, a conventional deterministic framework is strongly affected by the uncertainty of forecasting models and, consequently, leads to aggressive decisions that easily incur in several constraint violations of the thermal comfort bounds for the households. Subsequently, when the effects of these violations are practically considered, it emerges that stochastic strategies can actively control the violation limit and offer the best performance between the tested algorithms.

1-5 Thesis Outline

This thesis report comprises 7 chapters, including the current chapter. A detailed outline of the work is presented as follows:

Chapter 2 introduces the scenario of decentralised generation in which residential microgrids have the opportunity to expand. The technologies having the potentiality to be integrated in small-scale networks are separately analysed and their usefulness is discussed in detail. Finally, the concept of a microgrid as a controllable unit of grouped micro-sources, storage

systems and local loads is provided and the mathematical model employed for its control is formulated.

Chapter 3 performs an investigation on the economic profitability for investment in distributed energy resources for Dutch households. Hence the microgrids representing our case studies are defined in terms of technologies and typology of customers through economic motivation. Finally, a method to select the size of each energy resource, based on the potential economical savings led by microgrid operation, is discussed and the two definitive case studies are presented.

Chapter 4 deals with the identification of forecasting models to predict demand and supply behaviour in the microgrid. Firstly, state-of-the-art forecasting methodologies and techniques are analysed looking at the concerning scientific literature. Then, more attention is given to the specific models of forecasting for residential energy demand and solar power generation.

Chapter 5 analyses predictive strategies that can be applied to control microgrid operation with the specified objective to reduce operational costs. After an exhaustive presentation of MPC strategies from a theoretical perspective, deterministic and stochastic techniques are applied and adapted to our case studies.

Chapter 6 provides a detailed performance comparison between the previously described algorithms when implemented to control the power flows in the microgrids representing our case studies. A single section is dedicated to each of the two case studies of our work.

Chapter 7 summarizes the thesis with a discussion and contributes with recommendations for future work.

Microgrid: Description and Modelling

Domestic energy consumption in the residential sector is differentiated into electrical and thermal demand, which are respectively satisfied in conventional conditions by centralised power and gas infrastructures. As regards residential heating systems, two main categories can be analysed: domestic hot water and space heating. In most of the cases, in standard houses, both demands are provided through the utilization of high-efficiency boilers that convert the calorific value of natural gas into heating. On the other hand, electrical demand is supplied by transmission and distribution lines which connect large power plants directly to our houses.

In this chapter we want to present a deeply researched alternative to the conventional generation scenario: the interconnection of many small-scale electricity networks, where supply and demand are aimed to be locally balanced, and which have the potential to transform actual power infrastructure in a more efficient and dynamic ‘smart grid’. In Section 2-1 we introduce the framework of distributed generation in which residential microgrids have the opportunity to expand. In Section 2-2 the technologies that can be integrated in small-scale networks are separately analysed and their usefulness is discussed in detail. Finally, in Section 2-3 a complete mathematical model of the residential microgrid we consider in this thesis is formulated.

2-1 Distributed Generation in Smart Grids

Nowadays, new technologies are emerging on the market with the capability to either increase overall efficiency of energy generation or deeply reduce the emissions of the generation process: two main objectives for the climate challenge that we are facing. The first category of technologies is represented by micro-cogeneration systems, which can capture the by-product heat usually wasted in the conventional power generation and make it directly usable on site. The second category is related to renewable energy sources, which are based on regenerative natural resources and convert the energy of the latter into disposable electricity. Both of them, however, have the potential benefit to be installed with low investment on small-scale

systems and close to the required source of demand, avoiding any transmission losses due to energy delivery and aiming to locally balance power flows within the network where they are integrated.

In this section we want to analyse the main differences between the conventional centralised power generation and the more complex infrastructure of a smart grid where distributed energy resources are interconnected.

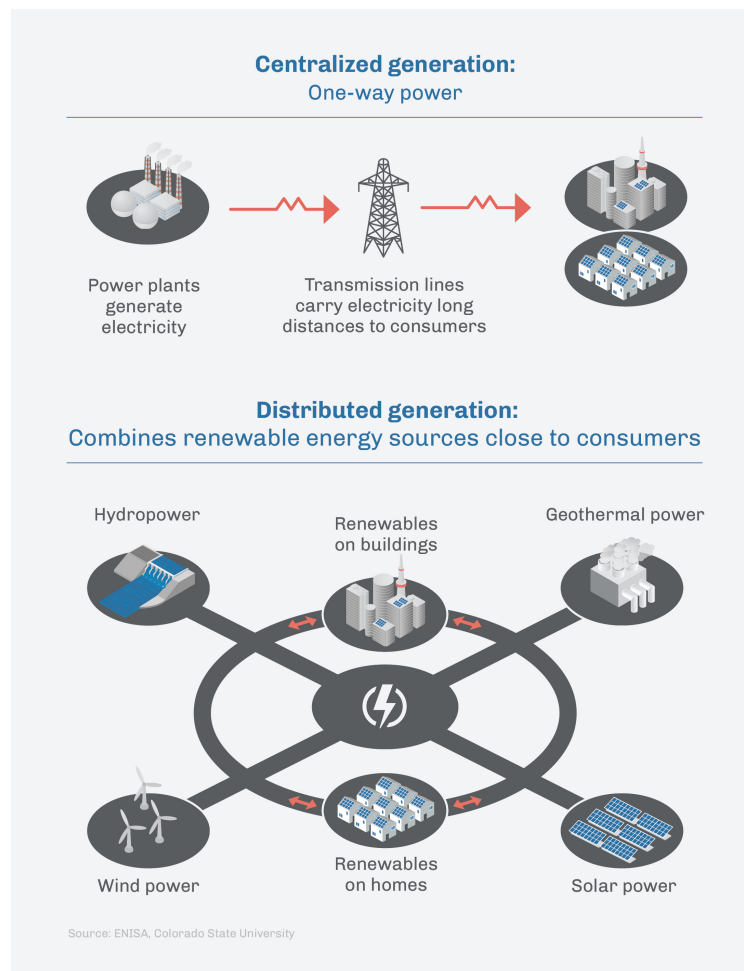


Figure 2-1: Centralised/Distributed generation in power infrastructure [78]

2-1-1 Centralised Electricity Infrastructure

Electricity generation in the classical model of electric power systems is centralised in a very small number of elements, big power plants, which are normally located far away from final users. As example, the Dutch power plant park is characterised by a high share of fossil-fuel based generation units, the majority of which are gas-fired (Figure 2-2). Generation companies produce electricity and sell it to the markets. Large industrial consumers buy the electricity directly from the market, whereas domestic and commercial users acquire it through retail companies (energy suppliers) working at the distribution level. At the same time, power lines are managed by transmission and distribution system operators, whose

objective is to guarantee system reliability and energy balance in each specific control zone. Hence, power networks that supply our houses with the necessary requested demand are based on unidirectional flow from generators to loads and are vertically structured. In this way, historically, the final consumers have not been taken into account in the power system except for when it comes to pay the bill. Their aggregated consumption is mainly measured by means of manual metering readings on monthly or yearly intervals.

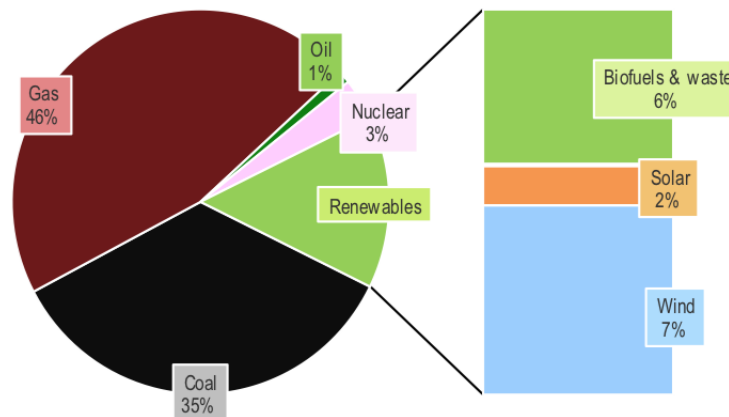


Figure 2-2: Power generation in the Netherlands according to the International Energy Agency (IEA), 2016 [2]

Traditionally, scheduling plans of production for fossil-fuel power plants can easily be determined one-day in advance, since present infrastructure allows demand prediction to be made on aggregated scale where the behaviours of single customers are smoothed due to averaging effects. However, the larger penetration of renewable energy sources is characterised by intermittent and stochastic nature of power generation, that strongly contrasts with the long reaction times of the network for adaptation to dynamic requirements. Hence, the major negative consequence of the new emission-free power generation systems is the high complex control system that should be designed to manage network operation. The growing electrical demand related to high-consuming appliances will therefore need a mixed combination of fuel-based and renewable generation sources. Therefore, an ideal solution would be to use the strengths and disadvantages of each source to counterbalance those of the others in a more distributed scenario of power generation.

2-1-2 Decentralisation of Power Generation

Distributed generation offers the possibility to produce energy close to the demand, enhancing reliability and power quality of the delivered electricity, while improving overall efficiency of the energy infrastructure. Significant benefits are offered in the distributed generation scenario for both the single customers and the utility grid as a whole (at least potentially). From an economical perspective, energy policies of every agent in the decentralised grid would be more cost effective due to its possibility of efficiently responding to real-time market prices

and react to the dynamics of the whole network. Secondly, primary energy consumption would be reduced by avoiding transmission losses in the power lines and by using highly efficient or renewable-based generation systems. Finally, one of the most important effects would be related to environmental conservation: penetration of controllable distributed generators makes easier to invest in renewable green energy and helps the transition to a more sustainable energetic infrastructure [64]. Associated savings of CO₂ emissions and primary resources in the distributed scenario highly depend on the fuel mix with which power is centrally generated, consumption of the privates willing to invest in distributed energy resources, typologies of generation and storage technologies employed, and control strategies implemented in the small-scale network.

Distributed energy resources are usually grouped in local controllable units, which play the role of single actors in the smart grid. These small-scale local energy grids are called **microgrids** and have the purpose to generate and regulate the flow of power according to their internal demand. Microgrids can be interfaced with the main grid through smart switches, thus allowing microgrid to function both in interconnected and isolated configuration. The interconnection with the power network guarantees that electric demand can be satisfied at any time instant.

In order to allow penetration of distributed generation, however, the structure of the utility grid has to change radically, going from a passive system towards an active distribution system. When generation exceeds demand in an interconnected microgrid, the electricity surplus can flow back in the distribution network so that the owner can become a net producer in some intervals of the day. In this way the energy market system becomes far more dynamic and interactive with the new emerging figure of ‘prosumers’, who play the double role of producers and consumers of electric power.

Local markets could arise where different prosumers trade energy among each other and new business opportunities could emerge for retailers [67]. Distribution system operators can thus have the possibility to expand their role, since they can no longer remain passive when it comes to managing the energy flows on their systems. Hence, they should manage the key activity to make the distributed supply cooperate with the centralised system, since the production of electricity in the distribution network can become highly unpredictable when many renewable sources are employed by prosumers. However, controllable microgrids aim to make the impact of extreme situations less severe for the operator as their functionality allows supply and demand to be balanced before the meter.

2-1-3 Local Energy Management System (EMS)

This thesis is focused on the interests of single prosumers willing to invest in residential microgrids and enter the current market of a smart grid. While, on one side, the initial installation of distributed energy resources in a residential building represents the highest cost for this investor, it is fundamental, at the same time, to manage the use of these resources in a cost-effective manner during daily operation.

Accordingly, an Energy Management System (EMS) serves the purpose to minimise the running costs of a single microgrid, while continuously balancing local demand and supply [64]. In order to achieve this goal, the operational strategy that an EMS implements has the objective to make decisions about the power flowing in the local network. In this section we

analyse the three energy aspects which can be controlled (completely or partially) on high level from an EMS: supply, demand, and storage.

Supply The main distinguishing characteristic among all types of distributed generation technologies is the possibility to actively control their power output.

Dispatchable units can follow the optimal scheduling plan produced by the EMS. They are subject to technical constraints and are crucial for microgrid self-supply, by offering a certain amount of flexibility in power generation. Depending on the type of fuel, dispatchable generators can be more or less polluting, but they are necessary in order to compensate for local net imbalance in the microgrid in moment of high fluctuation in demand or renewable supply. Non-dispatchable units, on the other hand, are mainly renewable generators, characterised by intermittency and volatility. Control can be applied with the only objective to maximise their production, but their input source (sun, wind) is clearly uncontrollable.

For the purpose of this thesis, where an optimal control strategy has to be developed in order to schedule the generation plan in the microgrid, larger interest has clearly been directed to the study of dispatchable units. However, the available technologies for solar power generation are also discussed with the aim to integrate solar panels in case study 'B' of our work.

Demand Loads in a microgrid are commonly categorised into fixed and flexible ones, according to the comfort choices defined by the user. Flexible loads can be controlled by the smart system with the purpose to respond to economic targets, and become part of control techniques of demand side management, in which residents willing to decrease their comfort level allow less restrictive constraints for the EMS [64].

Flexibility options in electrical demand consist of load curtailment, when the supplied power can be shedded (e.g. lighting), or deferment, when demand is allowed to be shifted in off-peak hours at the price of reduced bill for the customer (e.g. washers, dish-washers, dryers). As regards thermal consumption, flexibility can be assumed on space heating when households allow the system to control internal building temperature within a predefined comfort range. However, in order to introduce this extra degree of flexibility a detailed model of the building as a thermal load would be required [12].

Demand side management could further modify energy consumption patterns in the future, but it will not be taken into account any further in this thesis project. Only fixed loads, both thermal and electrical, will be considered in the next.

Storage Storage systems can be useful in order to guarantee a certain degree of flexibility in the local production, by decoupling supply and demand. Indeed, when storage systems are installed, the effects of requested power variability can be mitigated, allowing the generation to be less restricted to balance the instantaneous demand.

However, a great distinction should be made between electrical and thermal storage systems. On one hand, the option to store heat is the main enabler for flexible operation in smart buildings, since generated heat has necessarily to be consumed locally, otherwise the effort of the generation would be totally wasted. Moreover, from an economic point of view, the relatively low initial investment for a thermal storage is expected to be paid-back in short time. Indeed, in some cases, hot water tanks are already present in conventional houses.

On the other hand, the usage of domestic batteries will most probably not lead to acceptable

investments at the present time due to their high cost and to the risk of short lifetime due to irregular cycles of charge/discharge [37]. For this reason, in the further development of this thesis electric batteries are not included in the constitutive elements of a residential microgrid. However, we observe that, with the advent of electrical vehicles, the possibility to integrate the usage of their batteries in intelligent control schemes via vehicle-to-grid technology is under investigation in the recent years [3]. The level of profitability for electrical storage could grow dramatically in this case, since the stored energy would serve as a buffer by supplying loads during the peak hours, when the market price is high.

2-2 Available Technologies: Elements of a Residential Microgrid

In the next sections we want to investigate the available energy resources that can be integrated in the design of a residential microgrid. Techno-economical aspects are evaluated in order to motivate the choice of their usefulness in the operation of a microgrid.

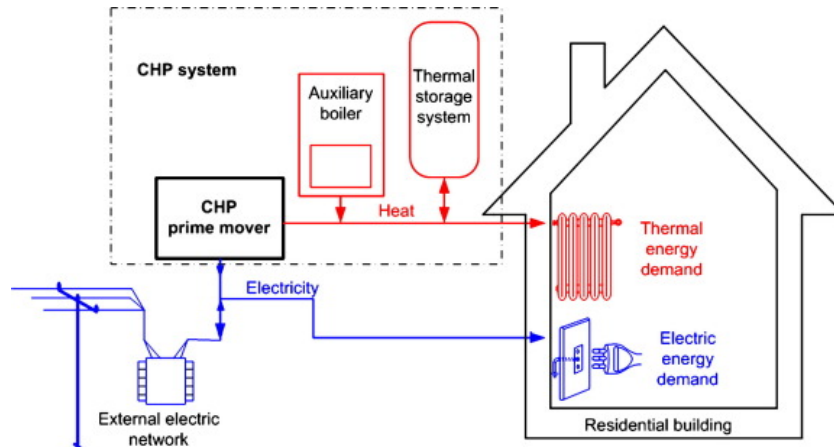


Figure 2-3: Micro-CHP system [9]

2-2-1 Micro-CHP Technologies

The miniaturization of cogeneration systems into small and micro units is an important topic of interest today. Combined Heat and Power (CHP) systems generate electricity locally and utilize the co-produced heat to satisfy thermal demand at the same time. The two typologies of power outputs are provided through different energy conversion mechanisms of the primary resource (usually natural gas). The portability and simplicity of CHP technologies should allow their installation in millions of homes, particularly where there is a huge market for heating fuel [50]. Their availability in the residential sector is expected to play a major role in curbing CO₂ emissions and reducing primary energy consumption for space heating, domestic hot water supply and electricity in the next future.

Complete micro-CHP systems are usually intended as a combination of a prime mover technology, a thermal storage system and an auxiliary boiler, as depicted in Figure 2-3. For a given scenario, the profitability of a micro-CHP system depends on the choice of prime mover technology and size, and of the proper thermal storage system.

Technology	$\eta_{\text{CHP, el}}$	C	$\eta_{\text{CHP, tot}}$	Engine Size	Market availability
Internal Combustion Engine	20-30 %	0.3-0.4	85-90 %	1-5 kW	Well-established
Micro Gas Turbine	12-16 %	0.2-0.3	80-90 %	≥ 3 kW	Prototype
Stirling Engine	13-20 %	0.15-0.3	85-95 %	1-9 kW	Available
Fuel Cell	$\approx 40-50$ %	1	80-90 %	1-3 kW	High cost / R&D

Table 2-1: Comparison of prime mover technologies for micro-CHP [50, 57]

Prime movers employed in the residential sector are developed with electrical capacities of up to 5 kW_e, and heat capacity, depending on technology, of up to 20 kW_{th}. Electricity production (P_{CHP}) and heat generation (Q_{CHP}) of the prime mover in a micro-CHP system are strongly correlated at any time instant, as explained by the following mathematical formulation:

$$P_{\text{CHP}}(t) = \eta_{\text{CHP, el}} \cdot f_{\text{CHP}}(t) = \underbrace{\eta_{\text{CHP, th}}}_C \cdot Q_{\text{CHP}}(t) \quad (2-1)$$

In the above equation f_{CHP} stands for the amount of fuel (usually natural gas) burned in CHP, here expressed by its energetic value, whereas $\eta_{\text{CHP, th}}$ and $\eta_{\text{CHP, el}}$ represent respectively thermal and electrical efficiency of the CHP. Power-to-heat ratio (C) is the fundamental physical parameter that distinguishes the technologies of prime mover, together with the overall efficiency:

$$\eta_{\text{CHP, tot}} = \eta_{\text{CHP, el}} + \eta_{\text{CHP, th}} \quad (2-2)$$

In the next paragraphs we will discuss about the prime mover technologies presently available on the market (even though not widespread or industrialised). A summarised comparison among the main characteristics of each technology is showed in Table 2-1, while more complete reviews can be found in the literature [50, 57].

Internal Combustion Engine (ICE) Micro-CHP systems based on internal combustion engines are commercially widespread and the most well-established technology for CHP applications worldwide [34, 83]. They are similar to vehicle engines modified to run on natural gas or compression-ignition diesel. Considerable works have been carried out in the last decade, by taking advantage of research coming from the automotive sector, for improving performance, lowering emissions, and reducing the cost of micro-CHP systems based on ICE. Their electric efficiency ranges from 20% to 30%, with the power-to-heat ratio generally increasing with size and a potential total efficiency up to 90%.

Micro Gas Turbines Gas turbines are a well-established technology for power output higher than 30 kW_e, whereas some disadvantages related to small-scale effects and investment costs make commercial development of micro turbines quite complicated [50]. However, recently EnerTwin has been testing a 3 kW_e micro turbine [21], even though the commercial price has not been announced yet. All the thermal power recovered in gas turbines is at a high temperature, coming from the exhaust gases (micro turbines cannot be used for cooling generation). Positive benefits of their usage are low maintenance request, multi-fuel usage, long lifetime, and very low emissions. It is considered that micro turbines could be suitable

to meet the electrical and thermal requirements of multifamily residential, commercial, and educational buildings. Their electric efficiencies mainly depend on the size: target values for residential sector are not higher than 20%.

Stirling Engines Stirling engines are external combustion engines, working by the repeated heating and cooling of a sealed working gas that is moved by a piston between hot and cold heat exchangers. Stirling engines indicate an interesting application for the household sector, thanks to their features of having a simple design, producing minimal noise and vibration, and allowing multi-fuel flexibility. They have relatively low electric efficiencies of around 13-20%, leading to high heat-to-power ratio. It seems a promising technology for the usage in small residential microgrids, since its advantages with respect to other technologies increase as power range decreases. The commercial price of Stirling engines is still high, but many companies are investing in their development [80].

Fuel Cells Fuel cell systems are electrochemical devices that directly convert chemical energy into electricity, while a fraction of the unused energy becomes available as heat. They are the most promising technologies for local supply of electricity thanks to their high power-to-heat ratio, but the large investment cost appears to be the main barrier to their widespread application. Typically the used fuel is hydrogen, but with the use of reforming processes many other hydrocarbons can be used, e.g. natural gas. We can distinguish between two completely different technologies, according to the operating temperature of the fuel cell.

- The polymer-electrolyte-membrane fuel cell, which operates around 80 °C and is based on the use of a specific polymer able to conduct hydrogen atoms.
- The solid-oxide fuel cell, which operates between 500 and 1000 °C, and allows the fuel reforming to happen internally, thanks to the high fuel cell operating temperature.

The appropriate choice of micro-CHP prime mover for our case study will be treated in more detail in Chapter 3.

2-2-2 Gas-Fired Boiler

An auxiliary boiler is usually included in any residential microgrid in order to meet thermal demand peaks that cannot be satisfied by both the CHP and the thermal storage system, or in cases in which the CHP prime mover is idle due to operational constraints. Gas-fired boilers are already installed in most of the houses connected to the gas grid and are used to satisfy thermal demand when no decentralised power generation is assumed. They are characterised by high levels of efficiency in the burning process ($\eta_{\text{BOIL}} \approx 100\%$), and by a fast dynamics able to react to quick changes in hot water demand [38]. The conversion process can be easily modelled as follows:

$$Q_{\text{BOIL}}(t) = \eta_{\text{BOIL}} \cdot f_{\text{BOIL}}(t) \quad (2-3)$$

where f_{BOIL} represents the amount of natural gas burned in the boiler, expressed by its energetic value.

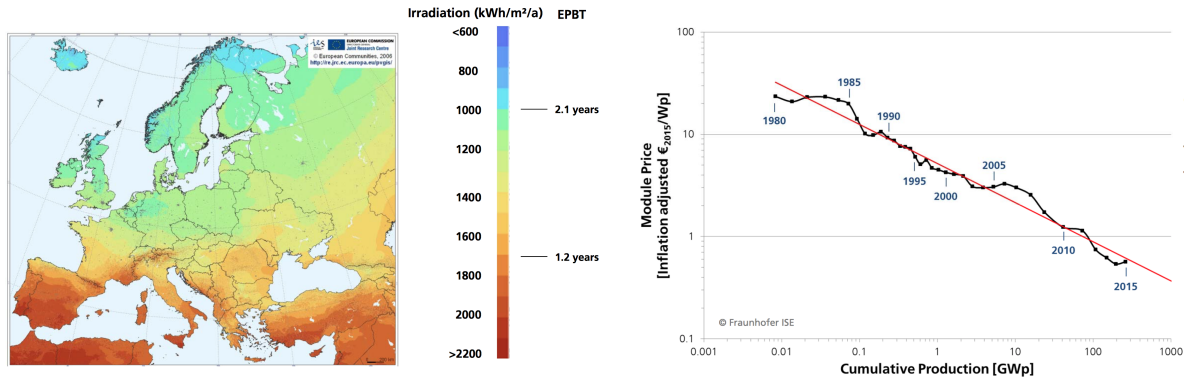


Figure 2-4: Data from Fraunhofer ISE, 2016 [27]. Left - Expected pay-back time of PV rooftop systems in Europe. Right - Commercial prices for PV modules [€/W_p].

2-2-3 Thermal Energy Storage (TES)

Generated heat can be efficiently stored in insulated water tanks. Indeed, water is a convenient heat storage medium, thanks to its high specific heat capacity and low cost. Cold water supply is heated by micro-CHP prime mover or auxiliary boiler and flows in the tank in order to keep its stored energy in the form of temperature level. When water flows out from the tank water releases its heat, which can be used for space heating and hot water demand. Through stratification, water at different temperatures can be stored in the same tank having a temperature gradient profile throughout its length and used for different thermal needs [75]. Nevertheless, in our simplified model we assume the temperature in the water tank to be homogeneously represented by its average value.

The amount of stored heat in the tank (ΔQ_{TES}) is physically linked to the difference in temperature between stored hot water and cold water supply (ΔT_{TES}), according to the formula

$$\Delta Q_{\text{TES}}(t) = c_{\text{H}_2\text{O}} \rho_{\text{H}_2\text{O}} V_{\text{TES}} \Delta T_{\text{TES}}(t) \quad (2-4)$$

where $c_{\text{H}_2\text{O}}$ and $\rho_{\text{H}_2\text{O}}$ represent unit thermal capacity and mass density of water, respectively. Hence, the capacity of the thermal energy storage is strictly related to the volume of the tank V_{TES} . As example, if the insulated tank keeps water at the average value of 60°C (50°C higher than temperature of cold water supply), the energy density of the thermal energy storage is approximately 70 Wh/litre.

2-2-4 PhotoVoltaic (PV) Systems

The application of renewable energy sources in microgrids is one of the extensively studied topics in the recent literature. Nevertheless, in regions with relatively weak natural energy a necessary compensation between micro-sources should be developed to mitigate the effects of high variability in the renewable power output. Including a diverse set of renewable energy generation technologies and optimizing the mix of renewable units could potentially reduce energy balance fluctuations in a small-scale microgrid [64].

However, in the residential environment the huge investment on a large mix of micro-sources can never be practically compensated by the economical savings due to operational management. Hence, here we only want to focus on the renewable technology whose market has

experienced one of the most rapid expansion in the last decades: PhotoVoltaic (PV) systems. As we can see from Figure 2-4, the trend towards a decreasing commercial price for PV technology makes the benefits of investment incredibly profitable even in less sunny countries as the Netherlands.

In order to better understand the average electricity yield from a certain PV array, we give here a brief explanation of its functioning. The PV system consists of a photovoltaic array which converts the light photons falling on its surface into electrons. This generates a direct current which has to be converted to deliver AC power to the loads through power electronic interface. The efficiency of a PV panel is strongly dependent on the ambient conditions, the most influential being the incident solar irradiance on the surface G_c and the solar cell temperature T_c [48]. Moreover, the cell temperature is in turn correlated to the global solar irradiance, which becomes the main influential parameter for the generated solar power.

Solar irradiance, representing the amount of solar energy received on a surface per unit time per unit area, is affected by solar elevation angle, haze effect, and cloud cover. While the elevation angle is deterministically defined by the latitudinal location and the specific time of the day/year [48], the cloud cover and the haze effect are stochastic. Consequently, the latter make solar power generation of a PV module highly unpredictable and lead a clear cause of uncertainty in microgrid operation.

A simple model for the PV power production is presented in [25]:

$$P_{PV}(t) = P_{STC} \frac{G_c(t)}{G_{STC}} \left[1 + \alpha(T_c(t) - T_{STC}) \right] \quad (2-5)$$

The nominal power P_{STC} , the cell temperature T_{STC} and the global irradiance G_{STC} under Standard Test Conditions (STC) (1000W/m², 25°C) are usually provided from the manufacturers, together with the power temperature coefficient α . The nominal power P_{STC} is related to the effective area of the installed module A_{PV} , together with the efficiency of the panels.

From a control perspective, the only action that can be performed on high level to maximise power generation of a solar panel is to alter the tilt angle in order to modify the radiation G_c incident on the surface. At a lower control level, for any value of solar radiation, there is a unique point on the current-voltage characteristic of the solar cells at which they generate maximum power. Hence, maximum power point tracking is a low-level control strategy used to make solar cells generate power always at this point, but it is often already integrated in the commercialised PV system, included the power electronics interface employed for the DC/AC conversion.

2-3 Microgrid Modelling

For the purpose to locally control residential microgrids, it is common to use a hierarchical control structure. In the literature this structure is often described by means of three broad layers: a primary control that stabilizes frequency and voltage in the electrical network using droop controllers, a secondary control that compensates the steady state deviations in voltage and frequency, and a tertiary control whose objective is to define a supervisory strategy that provides set-points to the main system components [64]. While primary and secondary controls are managed by low-level controllers for the individual energy resources, tertiary control

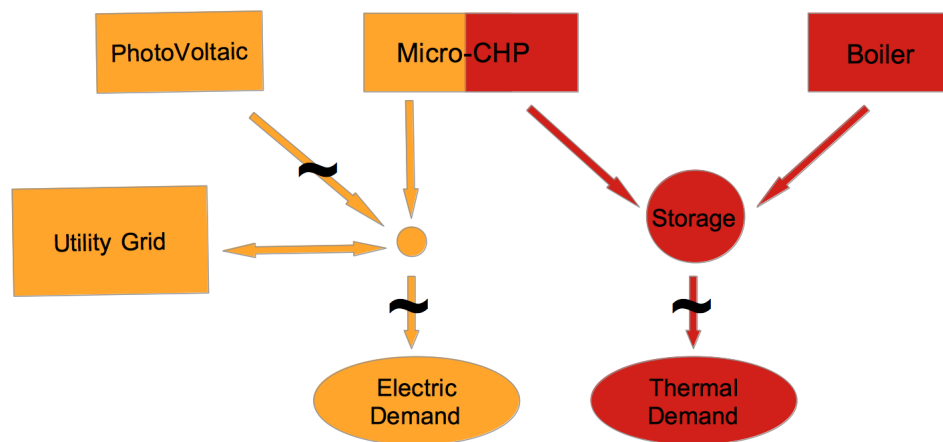


Figure 2-5: Model of residential microgrid. Electric ('yellow') and thermal ('red') networks. Symbol '~' represents uncertainty related to a stochastic process.

is implemented for a high-level centralized operator that deals with the medium-long term behaviour of the microgrid: the EMS previously discussed.

At high level, the elements composing a residential microgrid can be represented in a flow diagram (Figure 2-5). Each energy resource can be modelled separately and the instantaneous balance of their input/output power flows serves the purpose of their dynamic coupling.

The variables involved in the description of microgrid dynamics are intrinsically **hybrid** in nature. On one hand, discrete variables represent the functioning modes (on/off) of the controllable energy resources integrated in the microgrid, whereas, on the other hand, continuous variables describe the amount of production generated or exchanged with the storage elements at any time instant. A Mixed Logical Dynamical (MLD) system is usually employed with the purpose to model nonlinear microgrid dynamics in the literature [65, 38]. The procedure was originally proposed in [7] in order to deal with easier tractability of on-line optimization problems, due to MLD ability to convert all the nonlinear logical relations of an hybrid system into constraints which are linear in the new variables. Hence, the modelled system can be described by linear dynamic equations representing power balances within the microgrid and a set of inequalities involving real and integer variables that represent logical and technical constraints.

2-3-1 Power Balance

In the residential sector, when micro-CHPs are integrated in the system, the definition of microgrids is extended to deal with thermal energy flows exchanged within the network. Both electrical and thermal power have to be balanced in the microgrid at any time instant. However, while heat can only be generated locally and has to be consumed on site, electricity can flow back in the utility grid. Local balances of energy flows are expressed through the

following equations, representing a discrete-time model with sampling time T_s :

$$Q_{\text{TES}}(t+1) = Q_{\text{TES}}(t) + Q_{\text{CHP}}(t) \cdot T_s + Q_{\text{BOIL}}(t) \cdot T_s - D_Q(t) \quad (2-6)$$

$$G(t) = D_E(t) - P_{\text{CHP}}(t) \cdot T_s - P_{\text{PV}}(t) \cdot T_s \quad (2-7)$$

The two typologies of power output, P_{CHP} and Q_{CHP} , from the prime mover of the micro-CHP are correlated through (2-1). Together with the heat generated by the auxiliary boiler Q_{BOIL} , they are the only controllable inputs of the system, and are supplied uniformly during a single time step. The variables D_E and D_Q represent local demand of electricity and heat that have to be satisfied within the microgrid during any time step, while P_{PV} is the uncontrollable power output produced by the PV panels for each time step.

We can clearly distinguish the different behaviours of thermal and electrical network: on one hand, the dynamics of the thermal energy storage Q_{TES} is directly integrated in the model by means of heat balancing (2-6) and provides the useful degree of flexibility in the operation of the microgrid by decoupling thermal supply and demand, whereas, on the other hand, the utility grid works as a sort of potentially infinite electricity buffer, so that the amount of electrical energy exchanged with the grid G practically represents the local net imbalance (2-7). For the whole thesis we keep the convention that considers G as positive when the microgrid buys power from the main grid and negative when the microgrid sells power to it. A different way to impose satisfaction of heat demand could be to consider the heat required for residential space heating in terms of more relaxed thermal comfort constraints on desired indoor temperature [10]. However, an additional thermal load model of the building should be defined in this case to convert the heat variables in (2-6) in terms of temperature [82].

2-3-2 Operational Constraints

In the supervisory framework, fast dynamics of the generators are negligible, since the EMS operates at sampling times in the order of several minutes. A set of binary variables (δ_{CHP} , δ_{BOIL}) is used to model the discrete modes of the CHP and the auxiliary boiler, indicating whether the generation process is active or not. Moreover, the dispatchable generators and the storage system are forced to satisfy some technical constraints, which are presented in detail in the following.

Micro-CHP Prime Mover Power output of the micro-CHP is limited by the maximum generator capacity, depending on the choice of engine size. Furthermore, the generator is unable to produce electricity below a certain operative threshold. Since from 40% of their full capacity all the considered micro-CHP devices are able to modulate their power output, the minimum output of the generator can be defined as a fixed percentage of their engine size. The latter considerations lead to the following operational constraint for the micro-CHP device:

$$\min_{\text{CHP}} \cdot \delta_{\text{CHP}}(t) \leq P_{\text{CHP}}(t) \leq \max_{\text{CHP}} \cdot \delta_{\text{CHP}}(t) \quad (2-8)$$

where \min_{CHP} and \max_{CHP} respectively represent the minimum and maximum electrical energy that the engine is able to supply to the network within one sampling time. Moreover, the constraint (2-8) includes the logical implication that the generation mode ($\delta_{\text{CHP}}(t) = 1$) is equivalent to the effective power production ($P_{\text{CHP}}(t) > 0$), whereas the 'off' mode ($\delta_{\text{CHP}}(t) = 0$) implies a null power output.

No constraints about maximum amount of operational hours were found in the literature, since micro-CHP engines "must operate for as long as possible in order to improve the economic profitability of their implementation" [73]. However, a minimum running time can be set in order to avoid frequent on/off switching of the engines, which could deteriorate micro-CHP performance. The following constraints force minimum operation times (up time T^{UP} , down time T^{DOWN}) in which the generator has to be kept on/off after a switching [65] :

$$\delta_{\text{CHP}}(t) - \delta_{\text{CHP}}(t-1) \leq \delta_{\text{CHP}}(\tau) \quad \tau = t+1, \dots, t+T^{\text{UP}}-1 \quad (2-9)$$

$$\delta_{\text{CHP}}(t-1) - \delta_{\text{CHP}}(t) \leq 1 - \delta_{\text{CHP}}(\tau) \quad \tau = t+1, \dots, t+T^{\text{DOWN}}-1 \quad (2-10)$$

Indeed, the first constraint implies that, after a switching on of the micro-CHP ($\delta_{\text{CHP}}(t) = 1$, $\delta_{\text{CHP}}(t-1) = 0$), the engine has to keep working for T^{UP} time steps ($\delta_{\text{CHP}}(\tau) \geq 1$, for $\tau = t+1, \dots, t+T^{\text{UP}}-1$). Similarly, the second constraint implies that, after a switching off of the engine ($\delta_{\text{CHP}}(t-1) = 1$, $\delta_{\text{CHP}}(t) = 0$), the operating status of the prime mover has to be 'off' for T^{DOWN} time steps.

Gas-Fired Boiler The functioning of the auxiliary burner should also be modelled by means of binary variables (δ_{BOIL}) and continuous ones (Q_{BOIL}) describing the generated heating power. Then, operational constraints due to the limit on power output have to be considered as follows

$$\min_{\text{BOIL}} \cdot \delta_{\text{BOIL}}(t) \leq Q_{\text{BOIL}}(t) \leq \max_{\text{BOIL}} \cdot \delta_{\text{BOIL}}(t) \quad (2-11)$$

where \min_{BOIL} and \max_{BOIL} respectively represent the minimum and maximum thermal energy that can be generated by the boiler within one sampling time.

The up/down operation times for the auxiliary burner can be neglected, since it is assumed to have a very fast dynamics (within the sampling time). Differently, they could be modelled in the same way as for the micro-CHP prime mover.

Hot Water Tank For thermal energy storage, the main parameter to be assessed is water average temperature, since it is correlated to the energy density of the water tank according to (2-4). An average temperature of required hot water for domestic use can be assumed approximately 40-50 degrees higher than temperature of cold water supply (10 °C), according to the cited studies. Hence, water tank has to maintain its temperature in the range of 40-70°C. Consequently, the thermal energy in the water storage has to be kept between a minimum and maximum value, as follows:

$$\min_{\text{TES}} \leq Q_{\text{TES}}(t) \leq \max_{\text{TES}} \quad (2-12)$$

2-3-3 Stochastic Formulation

The residential microgrid has been treated up to now by analysing all its energy resources, and modelled as a MLD hybrid system. However, it is fundamental to highlight that the uncontrollable processes affecting system dynamics as external disturbances are intrinsically stochastic and their behaviour has to be modelled and identified in order to include prediction of the evolution of the whole system in the control strategy. Indeed, in Figure 2-3 the power flows related to domestic demand and supply from renewable generation are purposefully

marked by a ' \sim ' sign.

When the model defined by (2-1) and (2-6)-(2-12) is used to investigate the future evolution of power flows within the microgrid, heat and power demand (D_Q, D_E), together with the power generated by renewable sources P_{PV} , lead to the necessity to identify forecasting models able to capture the dynamics of their behaviour. Many scientific studies aim to build deterministic models of energy demand patterns and renewable generation that are unable to explain the degree of uncertainty related to the forecasting procedure. However, the analysis of our work aims to quantify the advantages for the control system when uncertainty is explicitly taken into account in appropriate formulation of the mentioned stochastic processes.

Hence, in stochastic formulation, the three processes are modelled by separating their future average value ($\hat{\cdot}$), deterministically forecast at each time step, from the additive uncertainty perturbing the prediction ($\tilde{\cdot}$):

$$\begin{aligned} D_E(t) &= \hat{D}_E(t) + \tilde{D}_E(t) \\ D_Q(t) &= \hat{D}_Q(t) + \tilde{D}_Q(t) \\ P_{PV}(t) &= \hat{P}_{PV}(t) + \tilde{P}_{PV}(t) \end{aligned} \quad (2-13)$$

2-3-4 Performance Indices

The control strategy implemented in the EMS aims should aim to maximise the operational benefits of microgrid operation with respect to the conventional working conditions of an household connected to the distribution network of electricity and natural gas. Performance indices regarding primary energy consumption, emission savings and cost reduction are discussed in the following. Their employment will be used in this thesis to quantify the positive impact of the installation of residential microgrids in the Netherlands. All the indices are computed by considering a time span of a single year of microgrid operation. Consequently, the yearly consumption for each of the energy needs is identified through a 'Y' superscript.

Primary Energy Savings Primary energy savings are computed by comparing efficiency of centralised power generation and local distributed generation when new technologies are employed in the microgrid. Efficiency of power supplied by the utility grid strongly depends on specific country infrastructure. In the Netherlands, centralised energy mix provides electricity with an efficiency of 44%, whereas transmission and distribution losses only count for 3.9% [19]. Therefore power delivered at our homes is supplied with a total grid efficiency $\eta_{GRID}=42.3\%$. The primary energy savings (PES) are analytically defined as the normalised difference between the primary energy consumed in conventional generation (PE_{STD}) and the primary energy consumed when a microgrid is installed (PE_{MG}), which will be better defined in the next chapters.

$$\begin{aligned} PES &= \frac{PE_{STD} - PE_{MG}}{PE_{STD}} \\ PE_{STD} &= \frac{D_E^Y}{\eta_{GRID}} + \frac{D_Q^Y}{\eta_{BOIL}} \end{aligned} \quad (2-14)$$

Emission Savings With a similar reasoning, we can compute emission savings when a microgrid operates (E_{MG}) with respect to conventional centralised generation (E_{STD}):

$$EmS = \frac{Em_{STD} - Em_{MG}}{Em_{STD}} \quad (2-15)$$

$$Em_{STD} = ef_{GRID} \cdot D_E^Y + ef_{GAS} \cdot D_Q^Y$$

The emission factor for electricity transmitted through the utility grid (ef_{GRID}) strictly depends on the energy mix of the considered country. Due to the highly dependence on natural gas (the ‘cleanest’ fossil fuel used for power generation), the emission factor of Dutch utility grid is relatively low compared to other European countries [1], even though a large share of the production is still handled by high-pollutant coal (Figure 2-2). On the other hand, gas-fired engines, as condensing boilers or CHP prime movers have emission factors (ef_{GAS}) related to the produced thermal energy [11]. The numerical values for the emission factors employed in this thesis are reported in Table 2-2.

ef_{GAS}	230	gCO_2/kWh_{th}
ef_{GRID}	384	gCO_2/kWh_e

Table 2-2: Emission factors for gas-fired engines and for electricity distributed through the utility grid [1, 11]

Cost Savings Economical benefits are the main factors that provide an incentive to customers to invest in residential microgrids. These are mainly related to the reduced use of primary resources during the operation of the microgrid. Standard costs in domestic energy consumption (C_{STD}) are computed by considering market prices for electricity and natural gas from the utility grid, and the correspondent cost savings are computed as follows:

$$CS = \frac{C_{STD} - C_{MG}}{C_{STD}} \quad (2-16)$$

$$C_{STD} = c_{EL} \cdot D_E^Y + c_{GAS} \cdot D_Q^Y$$

Since liberalisation of the energy market has created a range of different prices for each retailer, in this thesis we consider **average costs** in the Netherlands as defined in Table 2-3. Moreover, the prices are assumed fixed in time, independently from the hour of the day. Feed-in tariff is also included in this table to represent the price paid back from the retailer to the prosumer when electricity produced in the microgrid flows back in the utility grid. In this thesis we assume that this tariff is computed as the net price of supplied electricity from the grid, hence excluding taxes and transportation costs from the gross tariff.

Natural Gas	c_{GAS}	7	$c\text{€}/kWh_{th}$
Electricity	c_{EL}	18.5	$c\text{€}/kWh_e$
Feed-in Tariff	c_{FIT}	6.5	$c\text{€}/kWh_e$

Table 2-3: Average cost for domestic consumption in the Netherlands [84]

Cost savings will represent the main objective of the control strategies proposed in this thesis due to their direct incentive for private investors. Indeed, the only way to include more factors, such as fuel and emissions reduction, in the mindset of an investor, and subsequently push the expansion of residential microgrids, would be to convert and evaluate the previous performance indices in terms of economical subsidies or incentives.

2-4 Conclusions

In this chapter we have exploited the concept of residential microgrids. First, we have provided details on the distributed energy resources that can be installed in local networks to improve efficiency and reduce emissions of the generation process for both electrical and thermal energy. Later, we presented the high-level mathematical model employed by the EMS in order to make decisions about the reference set-points of supply for the local controllable generators. With this discussion in mind, we can now proceed to evaluate the benefits of residential microgrids in the actual Dutch market, starting by the choice of their correct sizing when average domestic demand has to be satisfied.

Economic Profitability: Investment in Residential Microgrids

High up-front investment costs in distributed technologies is an important obstacle to the spreading of residential microgrids. Therefore, when we evaluate the performance of a microgrid from an economical perspective, the initial investment cost represents a fundamental parameter to be compared with operational savings during lifetime of the resources.

A government subsidy could help the economic profitability of the investment, motivated by the reduction in CO₂ emissions and the increase in energetic efficiency when distributed resources are installed in Dutch houses. Indeed these factors can help in the direction to reach the targets of Paris agreement [59], at least as regards the efforts in the residential sector. Nevertheless, we did not investigate about actual subsidy policies in the Netherlands. Hence, the whole thesis makes no assumption on cost reduction for the analysed resources and only considers actual market prices.

This chapter is aimed to perform an investigation on the economic profitability for investment in distributed energy resources for Dutch households. Moreover, in order to consider appropriate case studies for the evaluation of control strategies in residential microgrids, the technologies and typology of customers are selected through economic motivation. The investigation starts from an analysis of domestic energy demand in the Netherlands in Section 3-1. Then, in Section 3-2, potential benefits of investment in micro-CHP and PV solar panels are evaluated for the Dutch scenario, and are employed to properly choose the customers and the technologies of our case studies. Finally, in Section 3-3 the size of each energy resource is selected, based on the potential economical savings led by microgrid operation, and two case studies are ultimately presented.

3-1 Analysis of Energy Demand

Energy consumption patterns in residential scenarios are highly time-dependent and unique for every household. They are characterised by high fluctuation of power demand on short

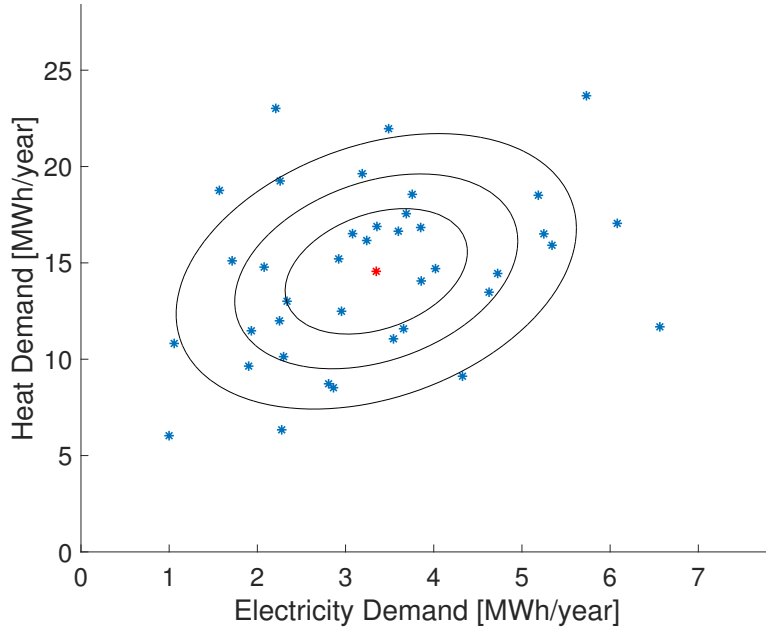


Figure 3-1: Scatter plot of yearly consumption for 39 clients in Amsterdam, from the Liander dataset [5]. Black ellipsis represent the contour plot of a bivariate Gaussian distribution having centre in the point indicated by the red mark.

time scale, due to the stochastic behaviour of households. These patterns will be deeply analysed in Section 4-2.

However, in this context, we are interested to highlight that the variability in power demand strongly affects the operation of the energy resources integrated in the microgrid. The aggregated measurements of consumed energy, usually available either on spatial or temporal scale, are unable to take into account peaks and oscillations of actual small-scale demand that could not be covered by the local supply during the operation of the controlled system.

For this reason, we started this thesis work by searching for granular data regarding actual energy consumption in Dutch houses. Indeed, since one of the main targets of this thesis is to analyse the practical implementation of an EMS on case studies inspired by real life, we decided to avoid data manipulation used to build simulated reference profiles.

Real data for residential consumption were obtained from open-source dataset by Liander, the largest utility company operating in the Netherlands [5]. The available data for gas and electricity cover a single year of measurements collected by smart meters installed in 80 houses in Amsterdam.

Electricity measurements are expressed in kWh consumed on 15-minutes scale, whereas gas consumption is measured in m^3 on an hourly basis. We assumed all the gas to be consumed for thermal needs (negligible cooking activities) and converted the used volume of gas to thermal demand. Net calorific value (ρ_{LHV}) of natural gas in the Netherlands is approximately equivalent to 38.05 MJ/m^3 ($=10.57 \text{ kWh/m}^3$) [18], whereas energy efficiency of gas-fired condensing boiler (η_{BOIL}) is assumed to be 100%, as explained in Section 2-2-2. Hence, the

conversion process can be expressed as follows:

$$D_Q(t) = \eta_{\text{BOIL}} \cdot \rho_{\text{LHV}} \cdot V_{\text{GAS}}(t) \quad (3-1)$$

where V_{GAS} is the hourly gas consumption collected in Liander dataset.

After this procedure, households have been characterised according to their yearly energy consumption (D_E^Y, D_Q^Y). In Figure 3-1 a scatter plot represents heat and electricity demand of the considered customers. Their correlation and distribution are approximated by a bivariate Gaussian distribution, whose contour plot is showed through elliptic black lines. The mean of the distribution is marked in red and represents average consumptions for Dutch households:

$$\bar{D}_E^Y = 3.5 \text{ MWh} \quad \bar{D}_Q^Y = 14 \text{ MWh}$$

In this thesis we decided to consider only households who are close to the average consumption, in order not to bias the subsequent discussion. Hence the clients from the Liander dataset are ordered by increasing Mahalanobis distance from the computed distribution and only the first elements of the sorting are analysed as potential investors in a residential microgrid. The Mahalanobis distance is a metric function employed to measure the distance of a single point from a probability distribution. Mathematically, it is defined for our case as:

$$M = \sqrt{(\vec{D}^Y - \bar{D}^Y)^T C^{-1} (\vec{D}^Y - \bar{D}^Y)} \quad (3-2)$$

where \bar{D}^Y and C represent the mean and the covariance of the demand distribution, while \vec{D}^Y is the vector containing yearly consumption of electrical and thermal energy for each customer.

Finally, we want to highlight here that, due to absence of more granular data from smart meters, we have been forced to employ a **sampling time T_s of one hour** to simulate and control the microgrid (modelled in Section 2-3) for the rest of the work. For this reason, the values of power supplied from the generators within a time step, expressed in kW, will be numerically equivalent to the delivered energy expressed in kWh.

3-2 Initial Economic Assessment for the Dutch Scenario

In this section, we want to quantify operational economical savings and perform an investigation on the economic profitability for investment in distributed energy resources for Dutch households.

The up-front investments (I) for microgrid technologies are usually approximated as costs that increase linearly with resource size (S). An investment is considered profitable if the pay-back period due to operational savings that the technology entails is shorter than the lifetime (l) of the considered resource. In order to compare the up-front costs and the benefits due to the installation, the ‘annualization’ procedure is used to rescale the investment on a single year of operation, in which the operational savings are computed [11]. Once defined an inflation rate ($r = 3\%$ per year), the annualized investment for a single resource can be approximated as follows:

$$I_{\text{ann}} = \underbrace{\left(\frac{r \cdot (1+r)^l}{(1+r)^l - 1} \right)}_{\text{annualization : } a(r,l)} \cdot I = a(r,l) \cdot I_u \cdot S \quad (3-3)$$

CHP Lifetime	l^{CHP}	15	years
CHP Investment	I_u^{CHP}	3000	€/kW _e
CHP Maintenance	$c_{\text{O\&M}}$	1.5	c€/kWh

Table 3-1: Economical parameters of micro-CHP engines [11]

where in the second equation we substituted the up-front investment (I) with the product between the unitary investment (per unity of resource, I_u) and the size of the considered resource (S).

3-2-1 Potential Benefits of Micro-CHP

Micro-cogeneration technologies reduce the amount of primary resources required to supply a fixed final energy use, due to their high overall efficiency, and, subsequently, they can lead to additional economic and environmental benefits. Indeed, when micro-CHP are installed in residential environments to provide local supply of both electrical and thermal demand, the final customer will consume a larger amount of gas with respect to traditional supply through domestic gas-fired boiler, whereas the electricity bill will be substantially reduced. Hence, economical benefits in the operation of a micro-CHP fundamentally depend on the price for gas and electricity in a specific country: the cheaper is the gas with respect to the electricity from the utility grid, the more convenient CHP operation would be.

We highlight that the more electric power is locally supplied by the micro-CHP during operation, the larger the economical savings for the owner of the microgrid are, since the customer avoids to buy it from the more utility grid.

Operational Savings In the following reasoning we assume that the heat produced by a micro-CHP cannot be dumped. Hence, the installation of a hot water tank is necessary to store the heat and reuse it when the household requires it. Furthermore, we assume infinite capacity of the thermal energy storage in order to neglect practical operational constraints and completely decouple thermal demand from thermal supply. This assumption simplifies the discussion regarding the choice of micro-CHP engine, whereas thermal storage is only reconsidered in Section 3-3-2.

When this situation occurs all the generated heat can be employed to satisfy the local demand D_Q , and we can compute the amount of extra gas (Δ_{GAS}) which has to be burned with respect to the standard thermal supply with an highly efficient boiler. In the equation below the efficiency η_{BOIL} is assumed to be unitary, while the fuel quantities f_{CHP} and f_{BOIL} are computed through formulas (2-1) and (2-3) in case of balance between supplied and demanded heat:

$$\begin{aligned} \Delta_{\text{GAS}} &:= f_{\text{CHP}} - f_{\text{BOIL}} = \\ &= \frac{D_Q}{\eta_{\text{CHP, th}}} - \frac{D_Q}{\eta_{\text{BOIL}}} = \frac{1 - \eta_{\text{CHP, th}}}{\eta_{\text{CHP, th}}} \cdot D_Q \end{aligned} \quad (3-4)$$

At the expense of burning Δ_{GAS} the micro-CHP system provides to the final customer the electric power P_{CHP} defined in (2-1), together with the generated $D_Q (= Q_{\text{CHP}} \cdot T_s)$. Hence, the net additional efficiency of the CHP can be defined as the ratio between provided electric

energy and additional burned gas :

$$\bar{\eta}_{\text{CHP}} := \frac{P_{\text{CHP}} \cdot T_s}{\Delta_{\text{GAS}}} = \frac{\eta_{\text{CHP, el}}}{1 - \eta_{\text{CHP, th}}} \quad (3-5)$$

Finally, unitary cost per kWh of the energy supplied by the CHP engine, can be computed as the sum of fuel cost and maintenance cost for engine operation:

$$c_{\text{CHP}} = c_{\text{FUEL}} + c_{\text{O\&M}} = \frac{1}{\bar{\eta}_{\text{CHP}}} \cdot c_{\text{GAS}} + c_{\text{O\&M}} \quad (3-6)$$

As analysed in the Section 2-2-1, the efficiency parameters highly vary with the prime mover technology of the system. However, in the following, total efficiency $\eta_{\text{CHP, tot}}$ (2-2) can be assumed fixed at 92% (top quality available engines [50]). In this case, the parameter $\bar{\eta}_{\text{CHP}}$ only varies with power-to-thermal ratio $C = \eta_{\text{CHP, el}}/\eta_{\text{CHP, th}}$, which becomes the most important characteristic of the technology to focus on.

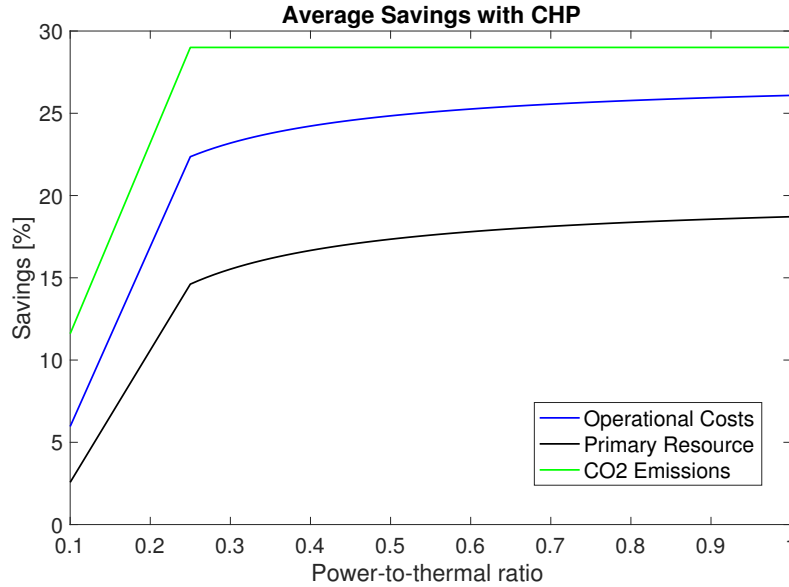


Figure 3-2: Potential benefits for an average customer due to micro-CHP supply with respect to conventional centralised generation

In order to fully exploit the potential of CHP operation, we assume that all the electricity can be produced locally as soon as co-generated heat is not larger than requested yearly demand

$$E_{\text{CHP}}^Y = \min(D_E^Y, CD_Q^Y) \quad (3-7)$$

In this way, operational supply has a different impact according to the relation between power-to-thermal ratio C of the prime mover and customer ratio between electric and thermal consumption C_{cust} :

- when C is smaller than C_{cust} , CHP yearly supply is limited by thermal demand

- when C is larger than C_{cust} , CHP yearly supply has the potential to completely cover electrical demand and lead to more cost-effectiveness for microgrid operation

Additional thermal and electrical demand that cannot be provided by the micro-CHP are respectively supplied by the conventional 100%-efficient auxiliary boiler and the utility grid. Performance indices are computed for an average household as expressed in (2-14)-(2-16), where the values for the microgrid are substituted by the following parameters for primary energy consumption, emissions and costs:

$$\begin{aligned} \text{PE}_{\text{CHP}} &= \frac{E_{\text{CHP}}^Y}{\eta_{\text{CHP,el}}} + \frac{(D_{\text{Q}}^Y - E_{\text{CHP}}^Y/C)}{\eta_{\text{BOIL}}} + \frac{(D_{\text{E}}^Y - E_{\text{CHP}}^Y)}{\eta_{\text{GRID}}} \\ \text{Em}_{\text{CHP}} &= \text{ef}_{\text{GAS}} \cdot (E_{\text{CHP}}^Y/C) + \text{ef}_{\text{GAS}} \cdot (D_{\text{Q}}^Y - E_{\text{CHP}}^Y/C) + \text{ef}_{\text{GRID}} \cdot (D_{\text{E}}^Y - E_{\text{CHP}}^Y) \\ C_{\text{CHP}} &= c_{\text{CHP}} \cdot E_{\text{CHP}}^Y + c_{\text{GAS}} \cdot (D_{\text{Q}}^Y - E_{\text{CHP}}^Y/C) + c_{\text{EL}} \cdot (D_{\text{E}}^Y - E_{\text{CHP}}^Y) \end{aligned} \quad (3-8)$$

In Figure 3-2, the three relative savings with respect to conventional residential supply are represented, as functions of the varying power-to-thermal ratio. We can clearly observe that savings increase with electrical efficiency, making potential benefits from fuel cells ($C = 1$) the highest. However, present high investment cost for fuel cells (about double w.r.t. other prime movers) cannot compete with more widespread traditional technologies. For these reasons we decided to consider an **Internal Combustion Engine (ICE)** ($C = 0.3$) in both our case studies.

Investment An installation cost of 3000 €/kW_e is considered as a good linear approximation for the reference price of a gas-fired micro-CHP prime mover [11]. When a Dutch household invests this amount of money for an engine with an expected 15 years lifetime, a minimum yearly electricity consumption is required to pay back the investment.

In Figure 3-3, economical savings obtained when electricity is produced by an installed micro-CHP are plotted in blue over power-to-thermal ratio of the prime mover. The curve represents the difference between standard cost of electricity in the Netherlands and cost of CHP local supply defined in (3-6).

In the same figure, red line shows the amount of electricity that the smallest (and cheapest) micro-CHP available on the market (1kW_e) has to supply per year to the final customer in order to pay back the initial investment within CHP lifetime. The investment is annualized at an interest rate of 3%/year through the formulation expressed in (3-3). Clearly, when this minimum yearly supply is less than cumulated user demand, investment in micro-CHP will not make any sense from an economic perspective. Since a Dutch household averagely consumes 3.3 MWh of electricity per year (Enerdata, [19]), it seems that investment in micro-CHP is not profitable for single households in the Netherlands.

Moreover, it is important to consider that up to now we have considered optimal conditions for CHP supply, where no operational or technical constraints are taken into account and the heat storage has potentially infinite capacity. However, when instantaneous demand is larger than nominal power rate of CHP during run-time operation, electricity has necessarily

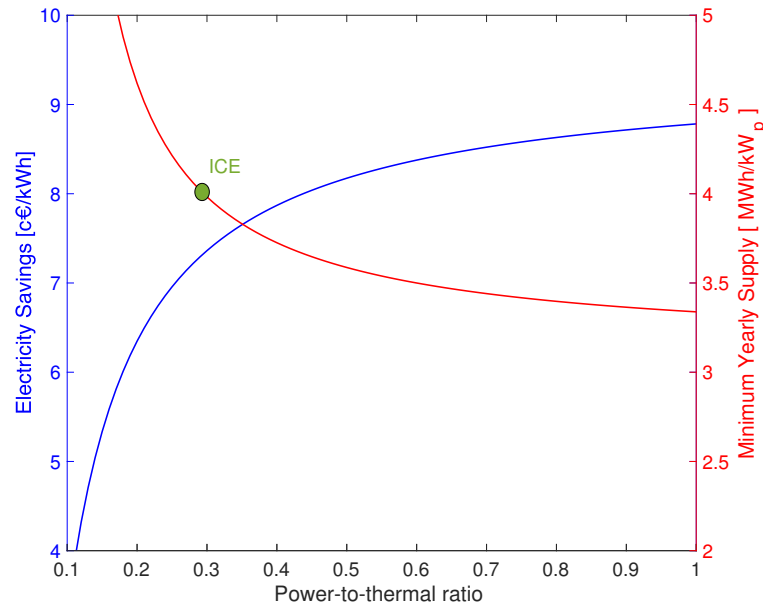


Figure 3-3: Economical benefits of micro-CHP installation in the Netherlands. Blue line shows cost savings of electrical local supply w.r.t. conventional grid supply - Red line shows the minimum yearly consumption which pays back the investment within CHP lifetime.

to be supplied from the utility grid. This means that actual demand to motivate the investment should be largely higher than the computed value for minimum supply, and only very high-demanding households could economically benefit from the installation of micro-CHP at present time. Hence, a more beneficial option would be to install the CHP system in multi-family apartment complexes.

To this purpose, we have investigated the effects of micro-CHP systems employed to cover domestic needs of a larger number of families. In this analysis we have used Liander dataset and considered the following limits for a given size of a CHP gas-fired engine:

- Minimum suppliable electricity to pay back the installation costs: through previous comparison between operational savings and up-front investment we considered that a micro-CHP system based on ICE has to supply at least 4MWh of electric power per year (Figure 3-3).
- Maximum suppliable electricity: when an engine runs continuously for a whole year, it clearly reaches the physical limitation of 8760 operational hours (number of hours in a year).
- Maximum satisfiable demand: electric demand that exceeds the maximum power rate of a CHP system is excluded from the computation of satisfiable demand.

In Figure 3-4, satisfiable demand is plotted for an increasing number of families. Optimal size of the engines for each number of families are represented by red marks and are computed as the values that produce the maximum gap between satisfiable demand and minimum

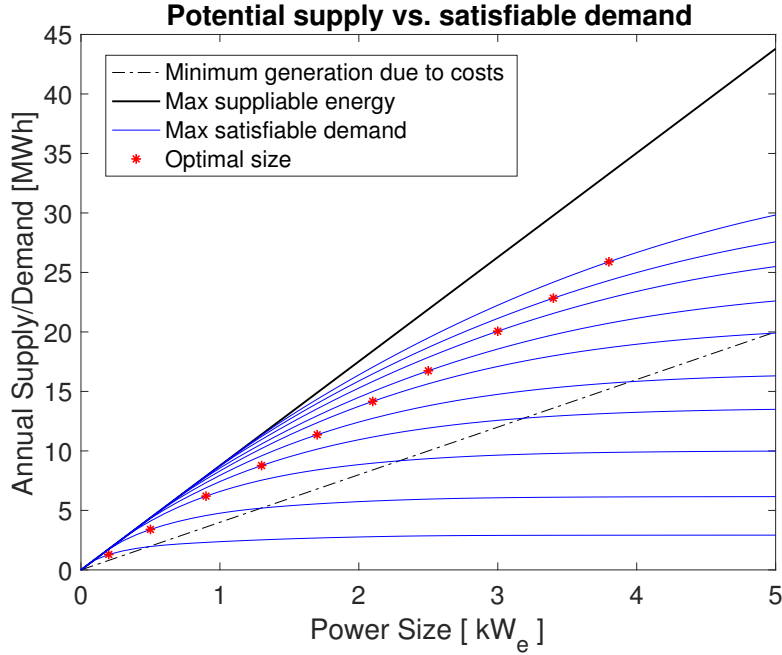


Figure 3-4: Potential supply versus satisfiable demand. Optimal size of CHP engines for increasing number of families

generation. Indeed, for these values the potential economic savings are maximised for the investors. As we observe from the plot, a residential microgrid composed by 1-3 families should invest in CHP engines with a size smaller than 1kW_e , but this technology is not available on the market. Moreover, considering that the investigation was performed in the ‘optimal’ scenario of perfect knowledge about hourly consumption of the households, even the scenario with 4 average families would require an engine size too close to the market limit to allow a profitability gap in the investment. Hence, in order to justify the investment for a micro-CHP in the residential sector, we proceed in this thesis work by assuming the customer to be composed by **5 average households** willing to share the investment in distributed energy resources in a multifamily building.

3-2-2 Potential Benefits of Solar Panels

Installation of PV panels was considered in order to integrate a renewable energy resource in the residential microgrid. For this reason, a model to simulate power supply of the modules based on weather variables was defined in (2-5).

However, the simplest model for PV supply is represented through the approximation of a fixed efficiency of the photovoltaic conversion η_{PV} , independent from cell temperature. Hence, if we set the coefficient temperature $\alpha = 0$ in (2-5), and we make the dependence from the area of the module A_{PV} explicit, we obtain the direct proportionality between the incident radiation on the module surface and the supplied power:

$$P_{PV}(t) = \eta_{PV} \cdot A_{PV} \cdot G_c(t) \quad (3-9)$$

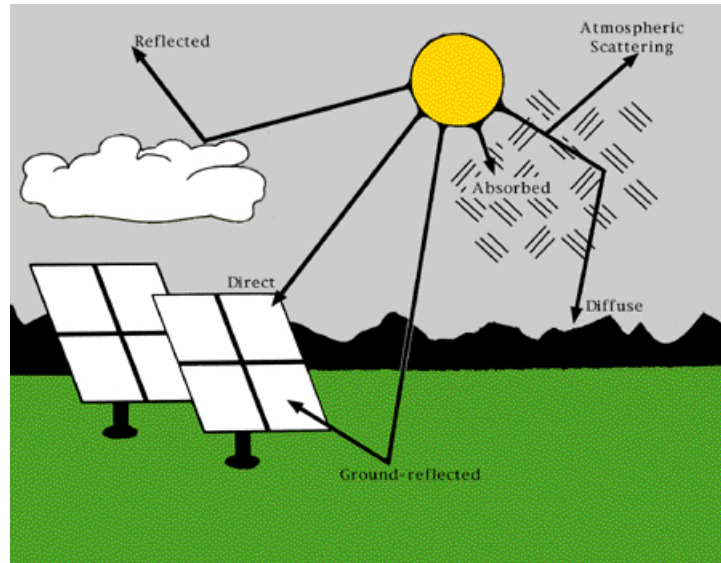


Figure 3-5: Components of solar radiation on PV panels: direct, diffuse and ground-reflected [61]

In this way the photovoltaic efficiency is expressed as the ratio between the nominal power yield per unit area of the module and the standard solar radiation $G_{STC} = 1\text{kW}/\text{m}^2$, as follows:

$$\eta_{PV} = \frac{P_{STC}/A_{PV}}{G_{STC}} \quad (3-10)$$

The climatological database from the ‘Ministerie van Infrastructuur en Milieu’ [42] has been used to provide hourly measurements of global irradiation, the main parameter affecting solar power supply. The closest meteorological station to Amsterdam that we have selected for the simulation is located in Schiphol.

Tilted Angle When PV panels are mounted on a rooftop the geometry of their surface is characterised by a tilt angle with respect to the ground (γ) and an azimuth angle with respect to the south (ϵ). Both these variables are usually adjusted in order to maximise the optimal yield of the module over an entire year, thus increasing the profitability of the up-front investment.

However, in order to compute global radiation incident on a tilted surface, it is necessary to highlight that solar radiation can be modelled as the combination of a direct and a diffuse component (the reflected component is usually neglected), which act in a different way on a flat surface (Figure 3-5). The direct radiation, or beam radiation B follows the direction of solar rays and describes the solar radiation travelling on a straight line from the sun down to the surface of the earth. On the other hand, the diffuse component D describes the radiation that has been scattered by molecules and particles in the atmosphere, and it is often modelled as uniformly distributed in the sky. Hence, the amount of direct radiation is maximised when the surface of PV panels is perpendicular to sun rays, whereas the diffuse radiation only depends on tilted angle and is always maximum for horizontal panels, which receive sunlight from the whole hemisphere. Solar radiation data are usually available for horizontal surfaces.

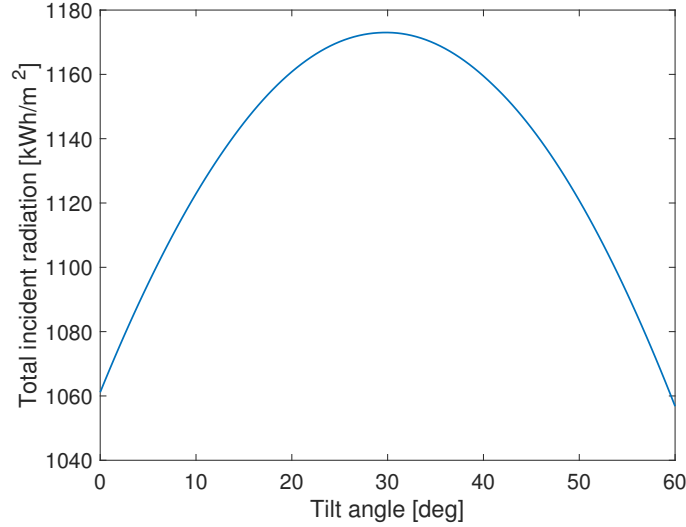


Figure 3-6: Yearly incident radiation on a PV module in Amsterdam w.r.t. its tilt angle γ . The azimuth angle is fixed at $\epsilon^* = 2^\circ W$

Indeed, also in our case, the employed dataset from the ministerial database provides the global irradiation measurements for horizontal surfaces. Hence, a procedure to decompose direct and diffuse components (B_0, D_0) of solar radiation is applied on the dataset, according to [16].

Finally, the optimal panel angles (γ^*, ϵ^*) have been numerically computed by optimising the sum of global irradiation incident on an arbitrarily oriented surface for a period of 5 years (2006-2011). Indeed, the hourly global irradiation is a function of both solar coordinates (varying with time of the day and day of the year) and panel coordinates [77]. We considered, for our case studies, that the choice of the angles could be arbitrary and independent from building structure or orientation. Clearly, if this is not the case, limited choices of angles have to be imposed, thus decreasing the optimal yield of the PV system.

For our scenario the selection of $\gamma^* = 30^\circ$ and $\epsilon^* = 2^\circ W$ leads to an increase of more than 10% in the annual incident irradiation with respect to horizontal panels. A simplified one-dimensional plot is shown in Figure 3-6 to highlight the variation of the incident radiation on the inclined surface with respect to the tilt angle γ , when the azimuth angle is kept fixed.

In the following of this thesis we have employed the selected panel orientation to compute the hourly incident solar radiation $G_c(t)$ leading to PV power supply for case study ‘B’.

Investment When a customer invests in a PV system, it has to properly choose the amount of modules, the electric interconnection between them, their geometric orientation, and the electrical characteristics of power and voltage output of the single panels [48]. In a simplified analysis, we assume that the considered panels have an approximately fixed efficiency $\eta_{PV} = 0.16$ (good market availability, [11]), the orientation is set according to the analysis of previous paragraph, and the only decision parameter left for system description is the effective area covered by the modules A_{PV} . Indeed, the interconnection topology only affects voltage output (not explicitly considered in this thesis), while the amount of panels is strictly correlated to the defined area.

PV Lifetime	l^{PV}	20	years
PV Investment	I_u^{PV}	1800	€/kW _p
PV Efficiency	η_{PV}	16%	

Table 3-2: Techno-economical parameters of PV module [11]

As we highlighted in (3-10) the conversion efficiency η_{PV} links the peak power supplied under STC (P_{STC}) and the effective area covered by the PV system. This means that we can equivalently select the area or the nominal power peak of the system. For instance, an efficiency η_{PV} of 16% implies that a module of 1m² produces an electric peak power of about 160W_p when irradiated in STC.

Nowadays, an average installation cost for a 16%-efficiency PV system is about 1800€/kW_p, including the necessary devices for power conversion and electronic interfaces [11]. The same system, optimally oriented on a rooftop in Amsterdam, yields approximately an yearly supply P_{PV}^Y of 1.1MWh, the numeric equivalent to the incident solar radiation per squared meter shown in Figure 3-6. Since a PV system does not lead to extra operational costs during its lifetime, a rough estimation of photovoltaic generation cost in the Netherlands can be easily performed as:

$$c_{PV} = \frac{I_u^{PV}}{l^{PV} \cdot P_{PV}^Y} \approx 8c€/kWh \quad (3-11)$$

Economical savings with respect to the purchase of electricity from the utility grid ($c_{EL} = 18.5c€/kWh$, Table 2-3) are evident. However, it is fundamental that the PV supply is mostly locally consumed and that the system is correctly sized.

3-3 Optimal Sizing of Energy Resources

Once the technologies to be installed in the residential microgrid have been selected and the typology of beneficiaries have been defined in terms of specified electrical and thermal demand, we are left with the objective to optimally choose the size of each energy resource, based on the potential economical savings that their operation would lead for the investors. The problem of optimal sizing is built as a simulation of microgrid operation (2-6)-(2-12) where sizes of the energy resources are left as decision variables. Under the simplified assumption of perfect knowledge of both consumption and renewable supply on hourly basis, the difference between yearly operational savings and annualized up-front investment is minimised.

It is well known that mixed integer programming problems are NP-complete and their computational complexity mainly depends on the number of integer variables [63]. Hence the optimisation problem increases its complexity with the amount of time steps considered in the simulation. In order to reduce problem complexity a choice of representative ‘typical days’ is performed before solving the actual sizing problem.

3-3-1 Selection of Typical Days

The basic idea of typical days is to select some representative days of the year that, repeated, can reproduce the energy demand of the whole year [62]. For this reason, hourly electrical

and thermal demand of the customers are discretized in N_{el} and N_{th} intervals of equal width. The distribution of occurrences in each interval defines two cumulative energy density curves: CED^{el} and CED^{th} . In the next discussion we will use the nomenclature

$$\text{CED}_{i,j}^k$$

to define the number of occurrences of demand $k \in \{\text{el}, \text{th}\}$ in the j -th interval of the distribution for the i -th day. Therefore, the selection of typical days is mathematically defined as the search for a reduced subset of days that, repeated with their corresponding weights (RP_i), approximate the yearly cumulative energy density.

Mathematical formulation An optimisation problem which selects T typical days over a specific period of N days is set as a mixed-integer-linear problem where δ_i binary variables define whether day i is considered or not among the typical ones. Hence, the repetition factors RP_i are allowed to be strictly positive if and only if the corresponding binary variable is equal to 1 (selected day). Moreover, the choice of T days is considered as an upper bound, instead of a perfect equivalence, because of a decreased computation complexity in the optimization problem. Hence, the two following constraints describe the selection procedure:

$$\begin{aligned} \text{for } i = 1, \dots, N : \quad & \text{RP}_i \leq N \cdot \delta_i \\ & \sum_{i=1}^N \delta_i \leq T \end{aligned} \quad (3-12)$$

The objective of the optimisation is to minimise the difference between the CED of the whole period and the CED of the repeated typical days, for both the typologies of demand (thermal and electrical). Relative errors for each interval of the two distributions are defined at this purpose, and their sum is minimised as follows:

$$\min_{\text{RP}_i, \delta_i} \sum_{j=1}^{N_{\text{el}}} |e_j^{\text{el}}| + \sum_{j=1}^{N_{\text{th}}} |e_j^{\text{th}}| \quad (3-13)$$

$$\text{for } j = 1, \dots, N_{\text{th}} : \quad e_j^{\text{th}} = \frac{\sum_{i=1}^N \text{RP}_i \cdot \text{CED}_{i,j}^{\text{th}}}{\sum_{i=1}^N \text{CED}_{i,j}^{\text{th}}} - 1 \quad (3-14)$$

$$\text{for } j = 1, \dots, N_{\text{el}} : \quad e_j^{\text{el}} = \frac{\sum_{i=1}^N \text{RP}_i \cdot \text{CED}_{i,j}^{\text{el}}}{\sum_{i=1}^N \text{CED}_{i,j}^{\text{el}}} - 1$$

In the equalities (3-14) the denominators are set equal to 1 in the cases in which no occurrences of hourly demand happen for the specific intervals during the N days, in order not to

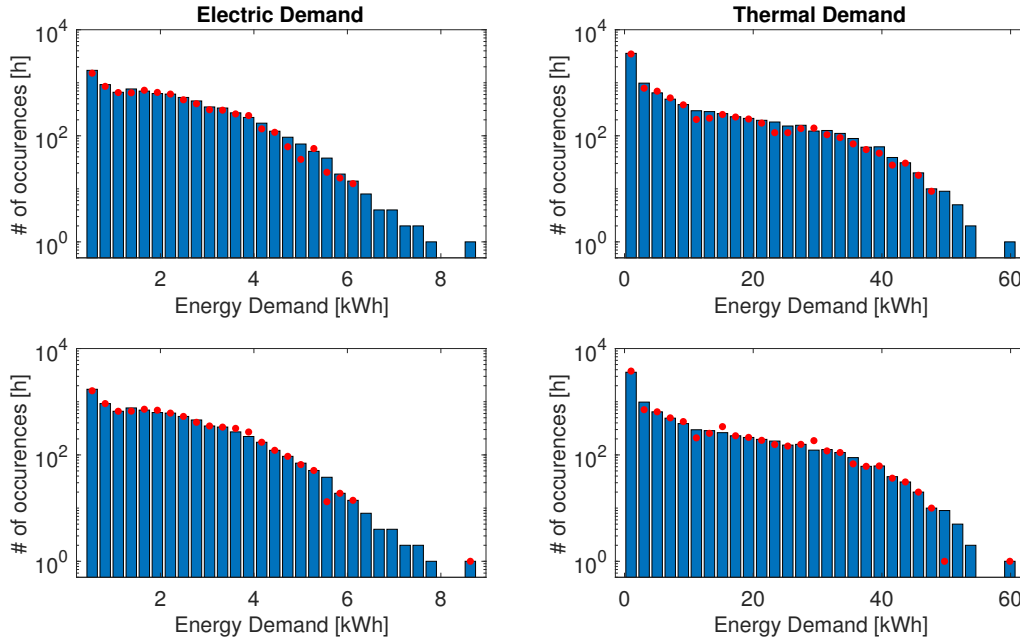


Figure 3-7: Comparison between CED of the whole year (blue bars) and CED of typical days approximation (red dots). Top figures represent the first approximation with 24 days (average error 29%). Bottom figures represent the approximation after recombination procedure with peak days (average error 21%)

incur in infinite values.

To conclude, minimisation of (3-13) subject to the constraints (3-12) and (3-14) represents the mathematical formulation to solve the selection of typical days and find their optimal repetition factors. For computational purpose, in algorithmic implementation the cost function (3-13) is transformed into a linear cost through the application of a common ‘trick’ used for absolute values. The slack variables e are substituted by a set of positive variables e^+ and e^- , such that

$$e = e^+ + e^-$$

and the absolute values can be removed.

Procedure and results Due to the high computational complexity related to the amount of binary variables when a whole year is considered (365 binary variables), the problem has been reduced and slightly approximated. A single year has been divided into six periods of two months. For each period 4 typical days have been chosen by solving problem (3-12)-(3-14) with $T = 4$. Finally, peak days of both electric and thermal demand were added and recombined with the 24 typical days, in order to include the most demanding, even though rarest, situations in the simulation period for optimal sizing [62]. In the recombination procedure, the problem (3-12)-(3-14) is simplified in a linear version without the use of binary variables: days are already chosen, only their repeating factors are recomputed. Final results lead to an approximation within 21% of average error, improving the first result of 29% when no recombination is applied. The comparison between yearly CED and its approximation is plotted in Figure 3-7. Logarithmic scale has been chosen to better analyse the results.

TES Lifetime	l^{TES}	15	years
TES Investment	I_u^{TES}	3	€/l

Table 3-3: Economical parameters of TES [11]

3-3-2 Sizing Problem

The optimal sizing problem is formulated and implemented under the assumption that repeated typical days represent operation over an entire year.

The objective of the optimal sizing problem is to choose the sizes (S^j) of the energy resources that the investor decides to purchase, in order to maximise the economical benefits of microgrid operation during their lifetime l^j . The operational costs C_{MG} are computed through the simulation of the microgrid during a whole year, represented by selected typical days. The up-front investment for energy resources are approximated as costs that increase linearly with resource size and annualized as in (3-3).

The simulation of microgrid operation is modelled as in Section 2-3, thus defining problem constraints. However, the constraints (2-8) and (2-12) are extended in order to include size variables S^j . The minimum operating times T^{UP} and T^{DOWN} of the CHP, showing up in constraints (2-10), are respectively set to 1 and 0 hours [38]. In case ‘B’, the supply of PV modules is described by (3-9), where incident radiation $G_c(t)$ has already been precomputed in Section 3-2-2. Finally, in order to distinguish between electricity flows from or to the utility grid the electric imbalance G is decomposed into two positive variables, as follows:

$$G = G^+ - G^-$$

With the defined constraints, the cost function of the optimisation problem is aimed to minimise the sum of both the yearly operational costs and the annualized investment costs:

$$\min \sum_{i=1}^T \sum_{k=1}^{24} \text{RP}_i \cdot C_{\text{MG}}(i, k) + \sum_{j \in \text{DER}} I_{\text{ann}}^j(S^j) \quad (3-15)$$

Microgrid costs at any time step are computed as the sum of four different components: the cost for the burned fuel (both f_{CHP} and f_{BOIL}), the maintenance cost of the CHP engine (computed with respect to its supplied electricity), the cost of electricity purchased from the utility grid (G^+), and the revenue (negative cost) of the electricity sold back to the grid (G^-). Therefore, C_{MG} is mathematically defined, for each hour i of the day k , as:

$$C_{\text{MG}}(i, k) = \left(f_{\text{CHP}}(i, k) + f_{\text{BOIL}}(i, k) \right) \cdot c_{\text{GAS}} + \left(\eta_{\text{CHP, el}} f_{\text{CHP}}(i, k) \right) \cdot c_{\text{O\&M}} + G^+(i, k) \cdot c_{\text{EL}} - G^-(i, k) \cdot c_{\text{FIT}} \quad (3-16)$$

Investment parameters of each energy resource ($\text{DER} \in \{\text{CHP}, \text{PV}, \text{TES}\}$) are respectively defined in Table 3-1, Table 3-2 and Table 3-3. Maximum power rate of the CHP engine (S^{CHP}) and volume of the thermal energy storage (S^{TES}) are left as optimisation variables for both the case studies; area of PV modules (S^{PV}) is included for case study ‘B’. The size of auxiliary boiler is not included in the optimisation procedure because we assume that gas-fired

Internal Combustion Engine	1.3 kW _e
TES	815 l (≈ 57 kWh _{th})
Up-front Investment	6358 €
Cost Savings	774€ (9.4%)
considering investment:	249€ (3.0%)
Primary Energy Savings	9.4%
Emission Savings	14.5%

Table 3-4: Case A: CHP+TES

Internal Combustion Engine	1 kW _e
TES	815 l (≈ 57 kWh _{th})
PV panels	4.4 kW _p (≈ 27.4 m ²)
Up-front Investment	13320€
Cost Savings	1407€ (17.0%)
considering investment:	435€ (5.3%)
Primary Energy Savings	15.9%
Emission Savings	18.1%

Table 3-5: Case B: CHP+TES+PV

boilers are already available in most houses and do not represent an extra investment cost. Its maximum power rate is considered equal to the thermal peak of the aggregated demand of customers (60kW_{th}), since the installed boilers should already be able to satisfy the demand in the worst case.

3-3-3 Definition of Case Studies

The results of the sizing problem for the two case studies are here presented, respectively in Table 3-4 and Table 3-5. Together with the cost savings, representing the explicit objective of the sizing procedure, all the main performance indices described in Section 2-3-4 (primary energy savings and emission reduction) are also showed.

Potential savings obtained by the optimization have to be considered as overestimated due to the assumed known consumption of the households and known photovoltaic generation. Therefore, the results will serve as theoretical benchmarks on which to evaluate the performance of the control strategies discussed and implemented in the next chapters.

The installation of distributed energy resources indicates potential benefits for both the case studies. However, we highlight that the employment of a PV system in case ‘B’ is strongly motivated by larger economical savings on the long run, even considering the higher up-front investment. Moreover, the size of the CHP engine is reduced in case of PV panels integration, because of their capacity to supply energy at lower cost with respect to the micro-cogeneration system. We want to observe, however, that the installation of the CHP engine is convenient even in case of solar panels employment, due to its capacity of dispatchable supply.

3-4 Conclusions

In this chapter we have analysed and discussed the profitability of investment in residential microgrids at the actual market conditions, and through the data of real domestic consumption of Dutch families.

A first important conclusion for our research regards the investment conditions in micro-CHP systems. We have highlighted that the high cost of the technology does not allow a profitable investment for a single Dutch family. However, a small ICE appears to be economically competitive in multifamily buildings (with at least 5 families), even though its market price should decrease in order to express the full potential of the technology.

Then, we analysed the economic benefits of roof-mounted solar panels and evaluated their lifetime yield. Finally, by means of the previous considerations, we have defined two case studies (with or without solar panels) and applied a method to optimally size the employed resources in the corresponding microgrids. The conclusive results of this chapter represent the initial step in order to begin to evaluate the practical effects of operational control strategies implemented in a residential EMS.

Forecasting of Stochastic Processes

It is envisioned that the smart grid of the future will support large penetration of distributed, intermittent generation resources, large-scale demand response, and plug-in hybrid electric vehicles [3, 64]. Interconnected microgrid environments will employ intelligent and adaptive elements that require advanced control techniques in order to work optimally. Hence, it seems clear that research and development are taking a main direction: the integration of forecasting technologies as a key input element to support the increasing ICT of the smart grid.

In our context, residential microgrid management and scheduling can considerably benefit from accurate net demand forecasting, because economy of operations and control of power systems are quite sensitive to information regarding future behaviour of the network. Moreover, an accurate prediction of power flows from prosumers can also help the aggregator on the distribution level to obtain better information and impose real-time prices to implement demand response policies.

Proceeding in our work, once the two case studies have been defined, the first step in order to design and implement a local EMS is to build forecasting models of the uncertain processes affecting the microgrid. Hence, on one side, we consider energy demand, represented by heating and electricity consumption of the households, while, on the other side, we focus on the forecasting of renewable energy supply, which strongly depends on weather conditions.

In this chapter, we first analyse state-of-the-art forecasting methodologies and techniques Section 4-1. Then, more attention is given to the specific topics of forecasting of energy demand patterns (Section 4-2) and of solar power generation (Section 4-3).

4-1 Literature Background

Forecasting models are employed when it is reasonable to assume that some of the patterns in past numerical data of a measured process are expected to continue into the future. Hence, the predictions are based on solid and realistic data, and they can be considered accurate as long as the derived model correctly represents the historical performance.

Given a specific time-dependent variable y , measured at discrete time steps t , we define its k -steps-ahead prediction as:

$$\hat{y}(t+k|k) = f_k(X(t), X(t-1), \dots, X(t-N)) \quad (4-1)$$

where f_k represents the general k -step-ahead forecasting model and $X(j)$ is a vector containing measured information at time step j of variables that are correlated to the variable of interest y . Variables X are commonly called predictors and could contain both past values of y or external explanatory variables. In cases in which the variable $y(t)$ is self-correlated to values adjacent in time (as it is the case for energy demand and renewable generation), the process is said to be a **time series**.

With respect to the output form one aims to predict, two main typologies of forecasting methodologies can be distinguished: in point forecasting the predicted output $\hat{y}(t+k|k)$ has the form of a single numeric value representing the most probable event at time $t+k$, whereas in probabilistic forecasting the whole probabilistic distribution of the dependent variable is modelled and the uncertainty of its outcome is considered.

In general, there is not yet any single technique that is known to dominate all others for a specific problem; data often determine which technique we should use, rather than the other way around. For many techniques that rely on explanatory variables, an important preliminary step is determining which input variables to use in forecasting models and their functional forms. Then, forecasting models are built through a minimisation of prediction errors, once a parametric relation between input and output of the model is assumed. Here we want to present an overview of the most used basic forecasting approaches in the state-of-the-art literature, inspired by the survey papers [33, 35].

4-1-1 Point Forecasting

Point forecasting methodologies can be considered as the traditional tool to estimate the expected value of future events, based on available past and present data. The scientific literature is rich in studies showing how to apply different techniques in order to obtain precise and effective predictions, and a mature understanding of the topic has been reached during the years. In the following, we present the most applied point forecasting techniques, and finally we present the common metrics used to evaluate the prediction results.

Regression Model The regression framework includes the estimation of parameters in input/output model whose functional form has been already predefined. Usually, linear regression is assumed in the model, due to the simplicity of the related estimation procedure based on ordinary least-square method. Here, the linearity only refers to the dependence on the parameters, whereas the independent variables can be any nonlinear function of the measured variable determined by means of statistical analysis.

When nonlinear relationship with the parameters is allowed and defined, a more complex estimation method has to be used [33].

Time Series Model Time series analysis is based on the assumption that adjacent points in time of sampled recorded data are correlated.

Most of the studies about time series are related to the assumption of stationarity in the investigated process. A stationary time series is a stochastic process where the autocorrelation does not depend on the specific time window in which it is measured. Hence, only the lag between two points in time determines the autocorrelation between them [79]. Under this assumption, the description of a stationary stochastic process is made by combination of polynomials of three different forms:

- Autoregressive (AR) : it defines the dependence on p past values of the estimated variable.
- Moving average (MA) : it defines the dependence on q values of a zero-mean white noise series $\{w(t)\}$.
- Exogenous input (X): it defines a linear combination of b past explanatory variables.

A complete ARMAX(p, q, b) model is showed below for a better understanding, composed of the three described polynomials:

$$y(t) = \underbrace{\alpha_1 y(t-1) + \dots + \alpha_p y(t-p)}_{AR} + \underbrace{\theta_1 w(t-1) + \dots + \theta_q w(t-q)}_{MA} + \underbrace{\beta_1 u(t-1) + \beta_b u(t-b)}_X + w(t) \quad (4-2)$$

In our research we only focus on **non-stationary** time series such as energy consumption and solar power generation, whose patterns are highly correlated to the specific hour of the day that we want to forecast. In many situations, to face this non-stationarity issue, time series can be thought of as being composed of two components: a non-stationary trend component and a zero-mean stationary component. To this purpose ARIMA models are designed as a broadening class of ARMA to include differencing operation (Δ), which is recursively defined as follows:

$$\begin{aligned} \Delta y(t) &= y(t) - y(t-1) \quad ; \\ \Delta^2 y(t) &= \Delta y(t) - \Delta y(t-1) = y(t) - 2y(t-1) + y(t-2) \end{aligned} \quad (4-3)$$

The differencing of data at higher order allows the partial or total elimination of non-stationarity [79]. Hence, ARIMA model can be build by using the series obtained after differencing each of the polynomials in (4-2). Moreover, when data patterns are related to a high seasonal fluctuation, some modification to the models can be made to include seasonal lags. In this way SARIMA models are defined, that include the most complete description of seasonal time series as load demand and solar generation.

Artificial Neural Network Artificial Neural Networks ANN are the most widespread tool in machine learning thanks to their powerful computation ability. ANNs are computational models whose structure is inspired by biological neurons [41]. Since the model is treated as an input-output nonlinear black box, they are able to learn, to generalize, or to cluster data. During the training phase, application of the *back-propagation* algorithm for a multi-layer neural network is one of the key reasons that allows the network to include nonlinear

functions in its structure [31]. With respect to statistical techniques, supervised ANNs can discover nonlinear relations between input and output, such that the knowledge base of the underlying model is inherently reduced. Hence, the steps to follow in order to design an ANN are few: a correct choice of input parametrization, and a topological definition of the network in its layer structure.

Support Vector Regression Support vector regression distinguishes itself from other methods of predicting continuous variables by exhibiting a high degree of generalization when introduced to previously unseen data [40]. The algorithm aims at finding a nonlinear mapping (kernel) of the input data into a higher dimensional space and then solving a linear regression problem in this feature space. The estimated target is described by a linear combination of preprocessed input mapped in the feature space.

Fuzzy Regression The fundamental difference between the assumptions of linear and fuzzy regression relates to the interpretation of deviations between the observed and estimated values. Whereas linear regression assumes that these values are measurement errors, fuzzy regression assumes that they are due to the indefiniteness of the system structure. Hence, instead of singletons, the regressors are assumed to be fuzzy parameters with a symmetrical structure defined by their ‘centres’ and their ‘spreads’. When improving the underlying linear model, one could observe a reduction in the fuzziness, which was originally recognized by a deficient model [36]. An identification of the parameters can be formulated as a linear programming. For more details, the reader is referred to [81].

Evaluation Metrics

Once a forecasting model has been trained on a specific dataset, through the estimation of its parameters, prediction performance is validated by analysis of residuals (forecast errors defined as $e(t) = y(t) - \hat{y}(t)$) on a different dataset. If the model fits well, the standardized residuals should behave as a Gaussian distribution. One of the big problems with non-normality in the residuals is that the amount of error in the forecasting model is not consistent across the full range of the observed data. This means that the predictive ability is not the same across the full range of the dependent variable [87].

The most common computations of aggregate errors used to evaluate the prediction accuracy of a forecasting models are:

- Mean Absolute Percentage Error (MAPE)

$$\text{MAPE} = \frac{100}{N} \cdot \sum_{t=1}^N \left| \frac{e(t)}{y(t)} \right| \quad (4-4)$$

This measure is not defined when the actual value $y(t)$ can be null, as in case of thermal demand. Hence, a weighted version named WAPE can be employed as an useful alternative in these cases:

$$\text{WAPE} = 100 \cdot \frac{\sum_{t=1}^N |e(t)|}{\sum_{t=1}^N |y(t)|} \quad (4-5)$$

- Root Mean Square Error (RMSE), whose metrics is strictly related to the standard deviation of the residual distribution:

$$\text{RMSE} = \sqrt{\frac{\sum_{t=1}^N e^2(t)}{N}} \quad (4-6)$$

4-1-2 Probabilistic Forecasting

The main drawback in point forecasting is its inability to report a probabilistic answer to prediction accuracy. Hence, point forecasting could be particularly failing when the process we want to predict is highly stochastic as in the case of electrical load or heat demand in a residential environment.

Probability represents an important tool in decision making frameworks because it provides a mechanism for measuring, expressing and analysing the uncertainties associated with future events. To improve the decision making and operational planning in a stochastic system, the modeller should be aware of uncertainties associated with the forecasts, since the impact of the uncertainty is reflected in a range of possible outcomes. Hence, despite the mature developments in point forecasting methods, a stochastic process should better be defined through a model that has the ability to explicitly take its intrinsic uncertainty into account. These kind of models are named as probabilistic forecasting.

In the last years, researchers have been moving from the traditional deterministic decision making framework to its probabilistic counterpart [35]. In the scientific literature, the uncertainty of point forecasting model is usually defined by the distribution of residuals. This distribution can only be analysed *ex post*, when the values of the dependent variable are actually observed. However, most of the probabilistic forecasts have been based on immature methodologies, such as simulating residuals using a normal distribution assumption [87].

In the following subsections a complete guideline to how probabilistic forecasting can be categorized and evaluated is presented, based on the study in [35].

Output Form

A probabilistic forecasting can have different output forms for the estimated conditional distribution of the dependent variable: known density function, discrete empirical distribution, or prediction intervals. While from the continuous density function we can always retrieve both the other two forms, the opposite is not possible. However, as it will be analysed in Section 5-4, a continuous density function is not useful from a practical point of view, since it makes a numerical optimization procedure intractable. Hence, forecasting methods that produce directly either empirical distribution or prediction intervals for the random variables are usually considered.

Empirical Distribution Empirical (or discrete) distribution is used to describe a sample of N_s realizations of a given random variable. The intuition is that if the samplings are representative of the original population, then the empirical distribution can be used to make inference about the true one.

Scenario generation is the technique used to create a limited discrete distribution to approximate the true distribution of a stochastic process. Scenario generation methods can

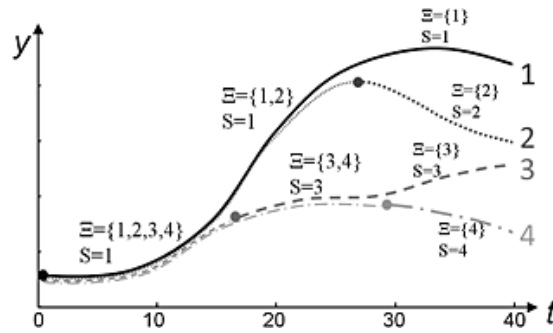


Figure 4-1: Example of tree structure with four scenarios [70]

well approximate distributions when the number of outcomes go to infinity, but can perform poorly when using only a few outcomes [13].

An important consideration is that forecast trajectories of stochastic processes have generally small differences at the initial stage of the forecast, then they tend to diverge because of the increasing prediction horizon. For this reason, methods to reduce the number of representative scenarios are applied in many situations with the purpose of improve problem tractability. For instance **scenario trees** can be generated by an ensemble data by aggregating trajectories over time, such that only significant branches are considered (Figure 4-1, [70]). A tree serves the scope of embedding ensemble data while exploiting more information about its structure, since it specifies moments when some of the uncertainties in the scenarios are resolved in branching points. At any bifurcation of the tree, the entire set of possible scenarios splits in mutually exclusive subsets, called branches. Indeed, from that moment on, an observation of the random variable will have unequivocally recognized which relative ensemble member has occurred.

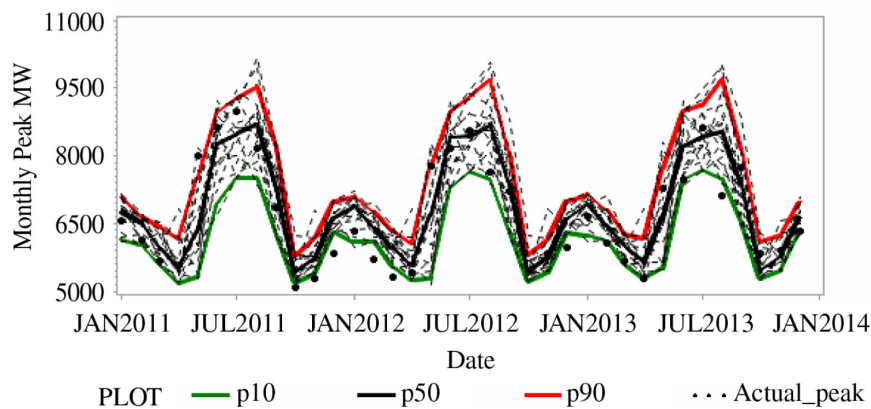


Figure 4-2: Quantile forecasts of monthly peak load for a US utility [35].

Prediction Intervals Prediction intervals are an alternative and more compact way to describe the output of a probabilistic forecasting. A prediction interval is comprised of upper and lower bounds that bracket a future unknown value with a prescribed probability level. In order to better analyse prediction intervals, the notation regarding quantile forecasts has to be introduced. A q -quantile forecast is a specified quantile of the forecast distribution. It

is a single-value prediction representing a cut-point that splits the cumulative distribution function F of the predicted data around the probability level q [35]. It can be computed as the minimum value such that the estimated distribution of Y , conditioned on the measured predictors $U(t)$, is larger than the fixed level q :

$$\hat{y}^q(t+1) = \inf \left\{ y : F_{Y|U(t)}(y) \geq q \right\} \quad (4-7)$$

Consequently, a prediction interval (PI) can be built by using symmetric quantile forecasts as interval extremes, as follows

$$(1 - \alpha)\% \text{ PI} = [\hat{y}^{(\alpha/2)}(t+1), \hat{y}^{(1-\alpha/2)}(t+1)] \quad (4-8)$$

An example of prediction interval is plotted in Figure 4-2, where $\alpha = 0.2$ has been chosen for the quantile forecasts. The 80% prediction interval is therefore comprised between the 10-th quantile (green line) and the 90-th one (red line). Prediction intervals take into account the tails of the distribution as well as the centre. As a result, they have great sensitivity to the assumption of normality.

Methodologies

Many probabilistic forecasting techniques and methodologies have heavy computational requirements. However, since point forecasting has reached a solid maturity in the scientific literature, it is usually more useful to focus on extending those techniques traditionally based on point forecasting.

Indeed, the requested probabilistic framework can be formulated once a simple point forecasting model has been applied to identify a stochastic process. In the post-processing, either a distribution on residuals is estimated to simulate the unmodelled uncertainty, or many single-value forecasts can be combined together in a probabilistic fashion. In the first case, residual distribution can either be parametrized when its shape is assumed to be known, e.g. Gaussian, or computed through discrete approximation in non-parametric form. On the other hand, a combination of point forecasts can result in an interesting and valid approach in order to build a probabilistic forecast. For instance, bootstrap method is one of the most common techniques in probabilistic framework, based on the combination of an ensemble of single-value forecast models. This technique is applied for neural networks in order to build prediction intervals [41], or for nonlinear regression models to build empirical distributions [23].

On the other hand, methodologies applied to directly produce a probabilistic forecast are also widely researched and are worth to be mentioned here. They can be distinguished into two different groups, based on their original purpose: methods in which point forecasting techniques are extended to deal with probabilistic framework in the identification process [46], and methods entirely based on stochastic analysis (i.e. Bayesian networks [28] and Markov processes [69]), commonly based on the discretisation of the forecast probability distribution. The simplest methodology in this context is the approximation of the predicted distribution by means of the relative frequency distribution, built through historical data for each time slot of interest [58].

4-2 Energy Consumption Patterns

Energy demand is a major source of uncertainty in microgrid short-term scheduling. Within the innovative context of smart buildings, it is essential to retrieve information about the energy behaviour (electricity and heat demand) of the household.

Two types of approaches for energy estimation in buildings are possible [26]:

- The forward approach ('white-box') utilizes the equations modelling the physical behaviour of the system to predict the energy demand. However, the model would require availability of information about building design data and household habits.
- The data-driven approach ('black-box') utilizes the data containing the records of input and output variables which govern the performance of the system. Data-driven techniques have the advantage of identifying and discovering models from large datasets by means of the forecasting techniques previously described.

In the following discussion, a data-driven approach will be tacitly assumed.

Demand forecasting can be classified according to the *scope* and the *aim* of the prediction. The *scope* indicates the period of time to be predicted, i.e. the prediction horizon. A rough classification in short and long term load forecasting, with a cut-off horizon of two weeks is usually adopted [35]. On the other hand, the *aim* of the prediction indicates the number of variables which have to be predicted. In this context, we distinguish between prediction of a single variable (e.g. load of next hour or next day) and prediction of multiple values. Our main interest for the purpose of this thesis is to consider short term load forecasting for multiple temporal intervals, such as hourly forecast of next day. This kind of forecast is defined as *load profile*.

Even though load forecasting has been a fundamental business problem since the origin of the electric power industry, most of the research until now traditionally refers to predict the expected electricity demand at aggregated levels, since it represents the most useful information for centralised network management [33]. Traditional load point forecasting has been widely applied through both statistical and machine learning techniques in order to estimate future load profiles of single households. However, as the spatial scale of prediction decreases (disaggregated consumption), the intrinsic stochastic behaviour of the end users becomes more difficult to predict and a larger amount of data are requested for the identification of the forecasting model. The massive smart meter deployment over the past decade has provided the industry with a huge amount of data that is highly granular, both temporally and spatially. Hence, more user-specific models have been built with the purpose to integrate accurate information in local EMS.

Indeed, in these conditions of high granular stochastic process, both on temporal and spatial scale (5 aggregated households), we need to focus our attention on probabilistic forecasting. A measurement of prediction uncertainty is really valuable when it comes to predict stochastic time series of small scale energy demand.

As first step of our forecasting procedure we want to compare performance of different prediction techniques on the hourly electrical and thermal load. Then, we start from that basis in order to identify a probabilistic forecasting model.

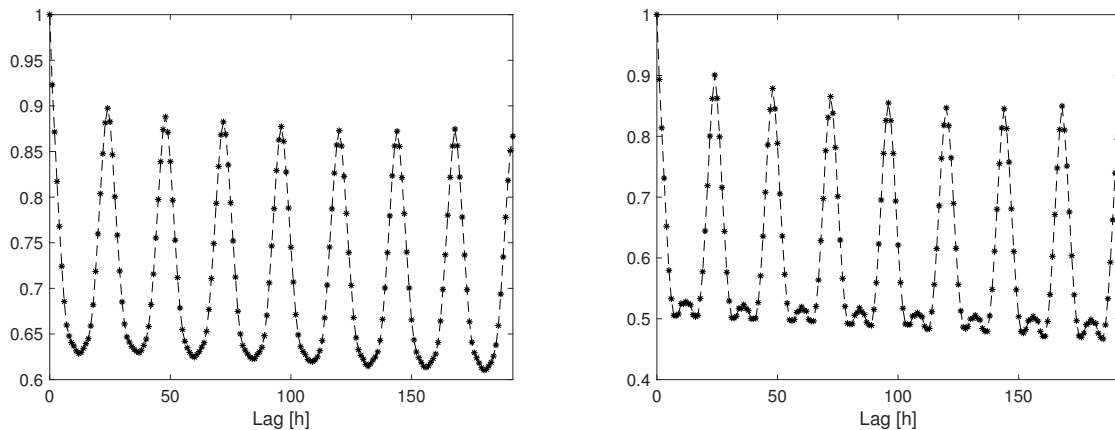


Figure 4-3: Autocorrelation of demand, plotted over hourly lags. Electrical consumption on the left and thermal consumption on the right.

4-2-1 Prediction Factors

Domestic demand can be considered as a non-stationary time series with strong seasonality. Three seasonal patterns are often being investigated in energy consumption: hour of a day, day of a week and month of a year. Moreover, many studies have proved that weather variables, such as average temperature and global solar irradiation, are highly correlated with electrical consumption [32]. Similarly, energy consumption related to the heat demand in a residential building is dependent on a huge number of external factors. Among them we can highlight two main variables: average outside temperature and behavioural patterns of the occupants in the house, which represent the strongest cause of stochasticity [74].

Independently from the model we want to use for prediction, a fundamental step for build any forecasting model is to properly select its input signals, called prediction factors. Due to the high volatility of the analysed processes, a point forecasting model that does not consider external explanatory predictors (e.g. temperature, sunlight, occupancy at home) is not expected to be very accurate. However, the consideration of explanatory factors would force the EMS to highly increase its complexity due to either a communication link with a meteorological service or the presence of additional local sensors to be installed in the building. Hence, the forecasting methodologies implemented in this thesis are **only founded on local measurements of energy consumption** in Dutch houses, and no external information is employed or integrated in the EMS.

We start our analysis with the observation of the autocorrelation function of the time series in Figure 4-3. The time series is the aggregated sum of electrical consumption of 5 different households in Amsterdam (from dataset [5]) and represents the electrical demand in the microgrid that we have selected for our case studies.

Firstly, we highlight the strong volatility of the time series, as the correlation factor is largely above 0.5 for many time instants in the past. This means that the autoregressive patterns are not particularly strong and could not be sufficient to obtain an accurate forecasting model. However, the main predictor factors can be observed from the plot: autoregressive components for the last hours, and daily autoregressive components for the previous day (24-hour lag). In the following the three main seasonal patterns are separately analysed and discussed.

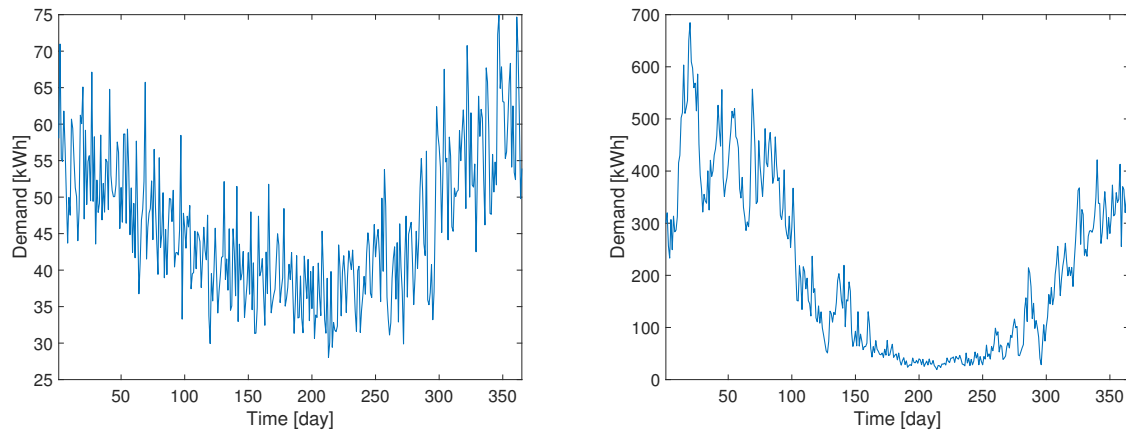


Figure 4-4: Daily demand along the year, data from [5]. Electrical consumption is shown on the left and thermal consumption on the right.

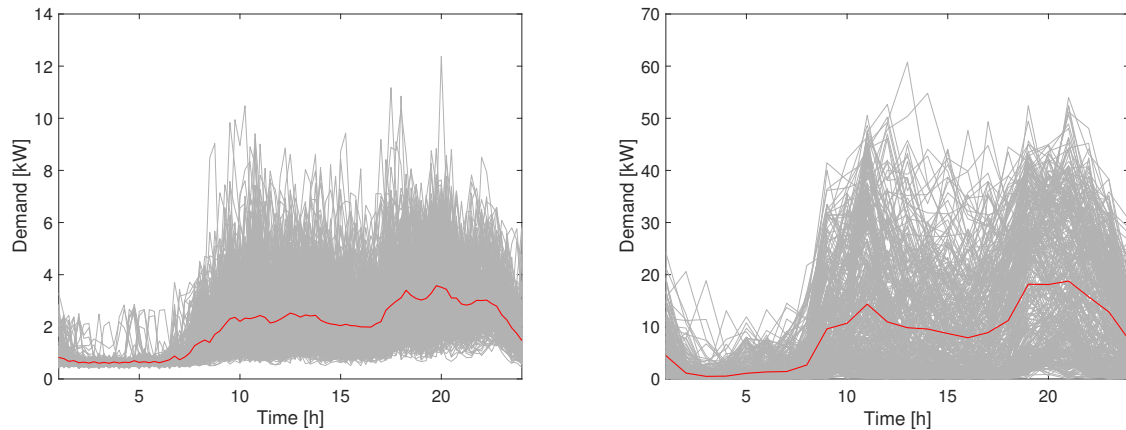


Figure 4-5: Demand for every day of the year. Electrical consumption on the left and thermal consumption on the right. Red lines represent the average daily patterns.

Yearly Pattern Yearly seasonality can be more clearly studied if we analyse daily cumulative demand during the year (Figure 4-4). The electrical demand varies substantially along the year with a sinusoidal-like behaviour with a peak during winter season. The seasonality is more evident for thermal demand, due to the correlation between space heating and environmental temperature. Moreover, larger intra-seasonal oscillations in thermal demand could be explained by peaks of colder periods.

In forecasting model the yearly pattern can be learnt by using predictors as day of the year, over a period of 365 days, but due to our reduced dataset (a single year of measurements) this pattern cannot be explicitly identified.

Daily Pattern Daily seasonality is the strongest characteristic of load curves. We can plainly distinguish ‘morning’ and ‘evening’ peaks which are repeated on a daily basis for both the energy needs. Apart from a strong volatility of demand behaviour (partially explained by yearly seasonality) a daily pattern is visible for both the energy consumptions (red lines in

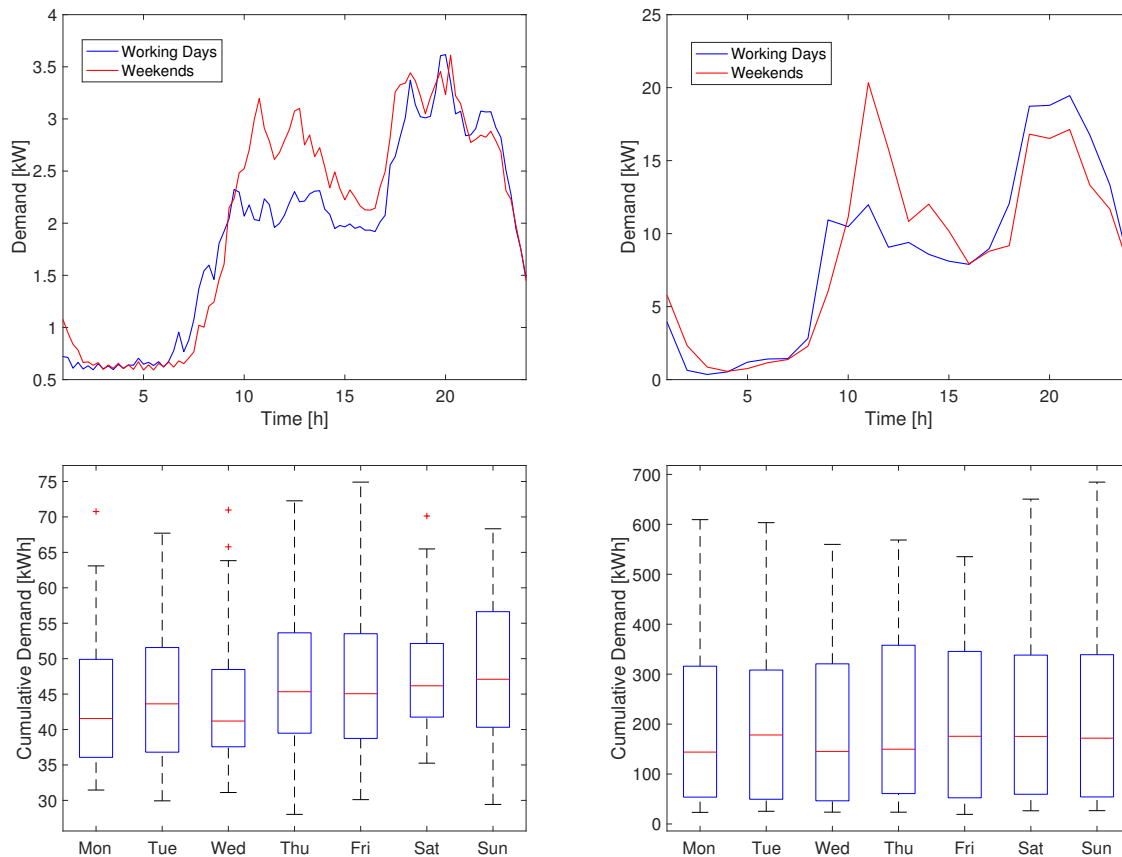


Figure 4-6: Daily consumption for different weekdays. Electrical consumption on the left and thermal consumption on the right. Top figures show average daily profiles, while bottom figures cumulative daily demand.

Figure 4-5). This pattern cannot easily be represented by a known function and appears to be highly nonlinear. Moreover, thermal consumption presents a visible clusterisation in two groups, due to high-demanding winter and low-demanding summer days.

Weekly Pattern As regards the weekdays, we have not found any interesting pattern in the datasets, as already observed in the autocorrelation plots of Figure 4-3. Indeed, the use of day of week as a predictor in the identified models was found not to influence the accuracy performance.

However, we can demonstrate the presence of clear correlation between consumptions and typology of considered day (working days or weekends). As observed in Figure 4-6, the difference is more evident for electrical consumption (left side). The cumulative demand per weekdays (bottom figures) highlights that the consumptions during working days are statistically equivalent.

Due to this analysis, we conclude that a boolean variable representing the typology of day has the potential to improve forecasting models, even though it is not linearly correlated to the demand.

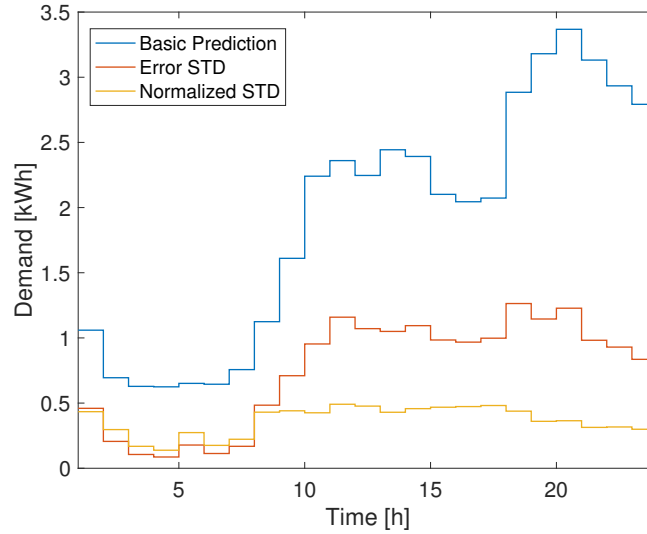


Figure 4-7: Naive forecasting model for electrical demand: average hourly consumption. The 'blue' line represents the consumption assumed by the model; the 'red' line shows the standard deviation of the prediction error for every hour, and the 'yellow' line the same value normalised with respect to the predicted value.

4-2-2 Benchmark: Naive Forecasting

Before proceeding with the identification and validation of forecasting models for the aggregated energy demand in our case studies, we want to provide the reader with two benchmark forecasting strategies (for electric and thermal consumption), which are inspired by the scientific literature and employed to compare the prediction accuracy of our models.

The performance of forecasting models for electric consumption is evaluated with respect to a naive methodology which assigns a specific *load profile* to every day. This benchmark case, named **time-of-the-day** model, is built by computing the average values of the electrical hourly consumption. We observe that, when a time-of-the-day model is applied, the prediction error for every hour is strictly proportional to the actual value of consumption: the higher the hourly demand, the wider the probability distribution of its occurrences throughout the whole year. Indeed, the 'yellow' line in Figure 4-7, which represents the normalised error deviation with respect to the naive prediction, is almost constant for any hour of the day.

On the other hand, since gas usage highly varies with seasons (due to space heating) a time-of-the-day model results in very bad estimation. Hence, we assumed a **persistence forecasting** model which assigns a daily *load profile* based on the consumption of the previous day. Performance accuracy of the two models are presented in Table 4-1 in terms of RMSE and MAPE. For thermal demand, due to hourly intervals of null consumption, the latter cannot be defined

	MAPE (WAPE)	RMSE
Electrical Demand	27.3%	840 Wh
Thermal Demand	(42.8%)	5.95 kWh

Table 4-1: Performance of the benchmark models

Technique	Electrical Demand			Thermal Demand		
	MAPE [%]	RMSE [Wh]	n-RMSE [-]	WAPE [%]	RMSE [kWh]	n-RMSE [-]
SARIMA	42.8 ± 1.3	982 ± 26	1.17	52.6 ± 1.3	6.01 ± 0.22	1.01
Lin. Regression	26.5 ± 0.4	748 ± 10	0.89	36.2 ± 1.5	4.72 ± 0.13	0.79
ANN	26.9 ± 1.2	712 ± 22	0.85	36.1 ± 0.9	4.71 ± 0.14	0.79

Table 4-2: Point forecasting performance for energy demand (± 1 standard deviation). The value 'n-RMSE' represents the normalized index with respect to the benchmark models.

and it is substituted by its weighted version (WAPE). These values represent the benchmark with respect to which we compare performance of point forecasting methodologies discussed in the next.

4-2-3 Point Forecasting Models

Dynamics of energy demand can be modelled in different ways. Firstly, we test traditional techniques for the identification of demand forecasting model. Subsequently, in the next section, we present an innovative periodic model which performs better than the previous ones in terms of both the evaluation metrics and is useful to integrate a detailed uncertainty model in a probabilistic framework. For each of the presented methods, available data for a single year are split into training (60% of data) and validation sets, by considering random days sampled throughout the year. The validation set is further employed for the simulation phase in Chapter 6.

Evaluation is reported in Table 4-2 according to the discussed metrics and a further parameter is computed: n-RMSE represents the correspondent quantity normalised with respect to the performance of the naive forecasting techniques. Each model has been trained and validated for 10 different random choices of the days selection in order to avoid bias in the results. Hence, the performance is expressed as the average of the different tests, with a range error representing the measured standard deviation.

SARIMA

SARIMA is traditionally used for demand forecasting on aggregated level for large scale generation, due to its relatively low complexity. However, the model is based on the strong assumption that seasonal differencing is able to almost completely remove the non-stationarity of time series. Hence, the following differencing is applied as a pre-filter to the analysed time series:

$$\Delta^D y(t) = y(t) - y(t - D) \quad (4-9)$$

where D represents 24 hours seasonality.

Nevertheless, for volatile small-scale systems differencing operation does not lead to the stationarity of the process, thus violating Gaussian assumption and corrupting technique performance. Indeed, the accuracy of the SARIMA model is even worse than naive forecasting, even though the amount of model parameters resulting in the best validated performance are selected for the forecasting.

Linear Regression

A linear model can be developed inspired by the traditional SARIMA model, in case the moving average part is neglected. In this case, the dynamical model of the time series is reduced to a one-step-ahead forecasting model in which no Gaussian assumption is forced on the additive noise. Hence, together with the simple autoregressive components, we consider a second set of predictors in the model in order to take daily seasonality into account: data from the previous day (24 hour lag), which were already proved to be strongly correlated with present measurements, and those of the adjacent hours. Therefore, the final model is described as follows:

$$\hat{y}(t+1) = w(t) + \underbrace{\alpha_1 y(t) + \dots + \alpha_p y(t-p+1)}_{AR} + \underbrace{\theta_0 y(t-24) + \dots + \theta_q y(t-24+q) + \theta_{2q} y(t-24-q)}_S \quad (4-10)$$

The choice of model parameters is the one leading to the best validation performance. Autoregressive term is set to a linear combination of the measurements for the last 3 hours ($p = 3$), while, on the other hand, we also consider as predictors measurements collected between 2 hours before and 2 after the 24-h lagged load ($q = 2$). This model largely increase its prediction performance with respect to the SARIMA model for both thermal and electrical demand.

Neural Network

The greatest advantage of a neural network when modelling a dynamical process is the opportunity to detect underlying non-linearities in the data through its high generalization power. In case of demand forecasting, a linear model is unable to detect the nonlinear daily or weekly pattern that characterizes the processes, as highlighted in Section 4-2-1. Indeed, as input of the ANN, together with autoregressive and seasonal regressive variables, we can include those variables that are not linearly correlated with the value to be forecast even though strongly affect the prediction: hour of the day and typology of weekday. However, as the evaluation metrics suggests, the added information is unable to improve the prediction power of the linear regression model.

The model is structured as a feed-forward neural network with a single hidden layer of 10 neurons. The topology has been chosen with a tuning procedure: extra complexity did not lead to any accuracy improvement.

4-2-4 Probabilistic Forecasting

As expected, point forecasting techniques for residential demand are not very accurate when no external explanatory variables are employed in the models (more than 25% of average prediction error). The main issue in the identification of forecasting models for energy consumption is represented by their high non-stationarity within a daily periodicity. Indeed, regardless of the underlying point forecasting model, the sample variance of prediction errors is always larger during the busiest peak hours.

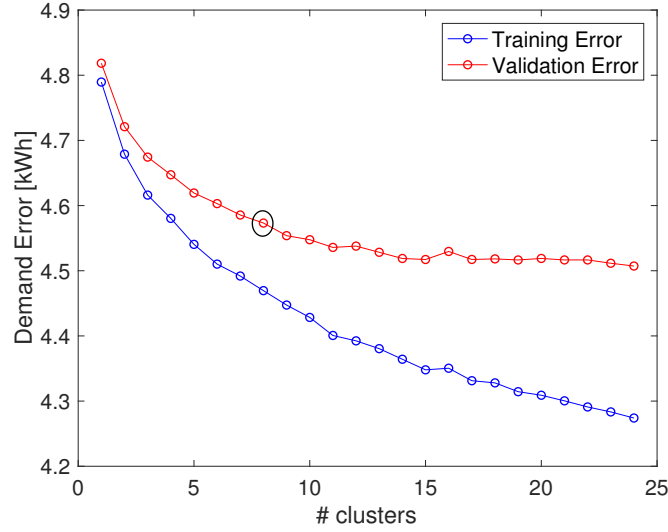


Figure 4-8: One-step-ahead forecasting with periodic model. Validation and training errors are compared for an increasing amount of modes

Since linear regression model and ANN seems to have very similar performance, as showed in Table 4-2, and due to lower complexity of the regression model, we chose to extend the latter in a way that explicitly considers daily patterns, together with their stochastic behaviour.

Periodic Model

Electric and thermal demand predictions are modelled by separating their expected cumulative value during the future time steps from an additive disturbance depending on the behaviour of customers.

A periodic stochastic hybrid system whose modes depend directly on the time of the day is therefore defined in the following form:

$$\begin{cases} x(t+1) = A_i x(t) + B w_i(t) & \text{if } k(t) \in \mathcal{T}_i \quad i = 1, \dots, \bar{N}_m \\ k(t+1) = \text{mod}(k(t) + 1, 24) \end{cases} \quad (4-11)$$

where \mathcal{T}_i are the sets representing specific periods of the day, \bar{N}_m represents the amount of modes and for each of them a compact linear system describes the dynamics (4-10). The state $x(t)$ is a vector of proper dimension including all the relevant past measurements and the matrices A_i are sparse with non-zero values occupying elements of the first row. The disturbances $w_i(t)$ are distributed according to unknown probability distributions \mathcal{W}_i and B is the first vector of the canonical base in the state dimension. The main purpose of the periodic model is to distinguish the uncertainty distribution on a temporal basis, while highlighting the same patterns as in the linear regression model.

For model training, firstly a provisional N_m is set equal to the total number of time steps during the day, i.e. 24. Then, the N_m linear models are clustered through the well-known *k-means* algorithm in \bar{N}_m temporal classes, in order to define the regions \mathcal{T}_i . Finally, the \bar{N}_m regression models are recomputed for each mode by means of linear least squares.

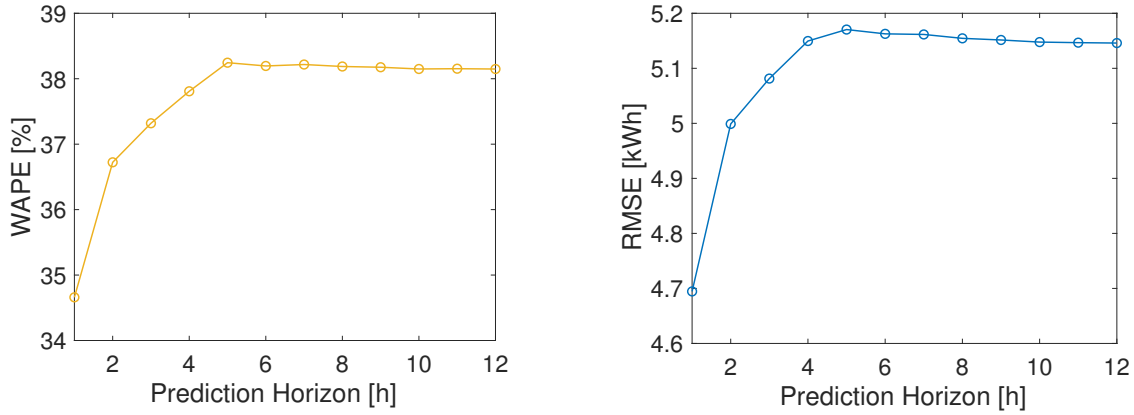


Figure 4-9: Evaluation metrics of the periodic model for multi-step-ahead forecasting of thermal consumption

The choice of \bar{N}_m is performed by analysing the validation error over an increasing number of clusters. When a single cluster is selected the model is equivalent to the standard linear regression (4-10), but performance improves for increasing \bar{N}_m . In Figure 4-8, we observe model performance for thermal demand forecasting: validation error for an number of clusters larger than 8 stays within 10% of the asymptotic performance when 24 different hourly models are considered, while the training error clearly keeps decreasing. Hence, in case of thermal demand, \bar{N}_m is set equal to 8. The same procedure is applied for electrical demand, leading to a choice of \bar{N}_m equal to 10. These choices define the forecasting models that are used for the rest of the thesis.

Results of the model accuracy for one-step-ahead forecasting show better performance with respect to all previous techniques. For larger prediction horizons, prediction accuracy decreases, until an asymptotic performance level is reached, as showed in Figure 4-9 for thermal demand. The latter case is motivated by the irrelevance of present information for improve the accuracy of prediction on the long-term. Specifically, for horizons beyond 6 hours the measurements of past thermal consumption are not adding any significant information to the forecasting.

However, it is important to highlight that the main objective of the periodic model is to disaggregate the description of system uncertainty into different time clusters, such that the probabilistic representation results more accurate.

Empirical Distribution

The *ex-post* distributions $\tilde{\mathcal{W}}_i$ of prediction errors on the training set can well approximate the true probabilistic distributions \mathcal{W}_i for each of the \bar{N}_m modes in the periodic model. However, Kolmogorov-Smirnov test [86] applied on $\tilde{\mathcal{W}}_i$ rejects Gaussian assumption and no parametric formulation of the distributions can be inferred. Hence, the obtained distributions are stored in a non-parametric form as vectors of sample probabilities in equally spaced intervals, representing an empirical distribution. However, the tails of these distributions are cut in order

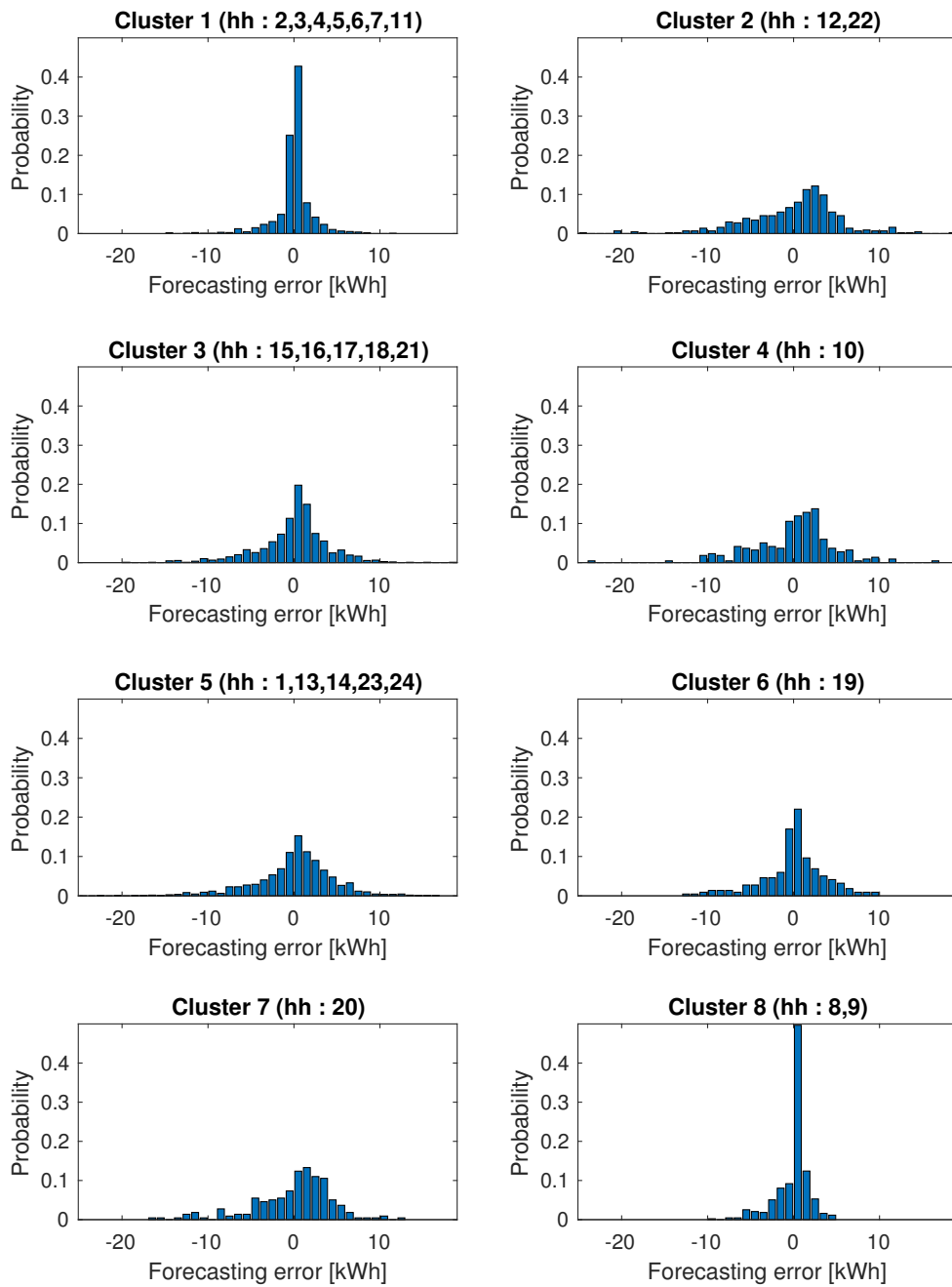


Figure 4-10: Empirical distributions of periodic model uncertainty \mathcal{W}_i for each mode of the system.

to remove outliers in the residuals: the extreme 1% of each probability distribution is not considered for the uncertainty model.

In Figure 4-10 the uncertainty models computed for the 8 modes of thermal demand forecasting are plotted as empirical distributions. Each mode (or cluster) is identified by the hours of day defined in brackets.

4-3 Photovoltaic Generation

Solar energy is subject to considerable temporal and spatial fluctuations. However, with the expansion of photovoltaic generation in the energy supply system, the necessity for accurate solar forecasts is increasing. These forecasts form the basis for the cost-optimised strategy of an EMS, with the aim of integrating solar power generation in microgrids.

In Section 3-2-2, we have explained the high correlation between the solar irradiance incident on a tilted PV panel in a specific location and the output power produced by the correspondent PV array. Due to this correlation, the forecasting model for photovoltaic supply can be similarly computed either for previously measured incident global radiation or directly for past power output. Hence, we can distinguish two main forecasting strategies in the context of solar power prediction: physical and statistical.

The physical strategy is based on ensembles of meteorological data (numerical weather prediction) that are used as predictors to forecast solar irradiance [72]. The PV model (3-9) is successively applied in order to output the generation forecast. This methodology is especially useful as an approximated simulation in the case PV panels are not installed yet at the desired location, and their physical model is only theoretical.

On the other hand, statistical strategy is based on the availability of historical data and the modelling framework of time series. The data are collected and recorded by sensors installed with the purpose to measure PV power output. In this way, the estimated forecasting model can also be adapted on-line in order to obtain a better performance in real world applications, when PV system are subject to changes due to snow cover, leaves or dirt on the panel [6].

The two approaches can easily be combined by considering the numerical weather prediction of the global irradiance as explanatory variable of the statistical model [6, 8]. In this scenario the prediction results to be more accurate on the long run, since the correlation between global irradiance and power output is learnt by the forecasting model instead of being theoretically imposed. In the reviewed works, it is recognized that for short term forecasting (within 2-4 hours), the relevant inputs consist of past observations of PV power output, whereas for longer horizons information from numerical weather predictions is more relevant.

In our case, since the panels are not installed yet and their output would be simulated through the radiation measurements, the two computational strategies would offer exactly the same result. Hence, we proceeded by considering forecasting model for the incident solar radiation, whereas PV supply will be simulated through the physical model (3-9).

4-3-1 Clear Sky Model

It is well-known that global radiation follows seasonal patterns related to Sun-Earth position [48]. While this seasonality is deterministic, stochastic behaviour of solar power supply is due to variability in cloudiness and sky overcasting during the day. For this reason, in many

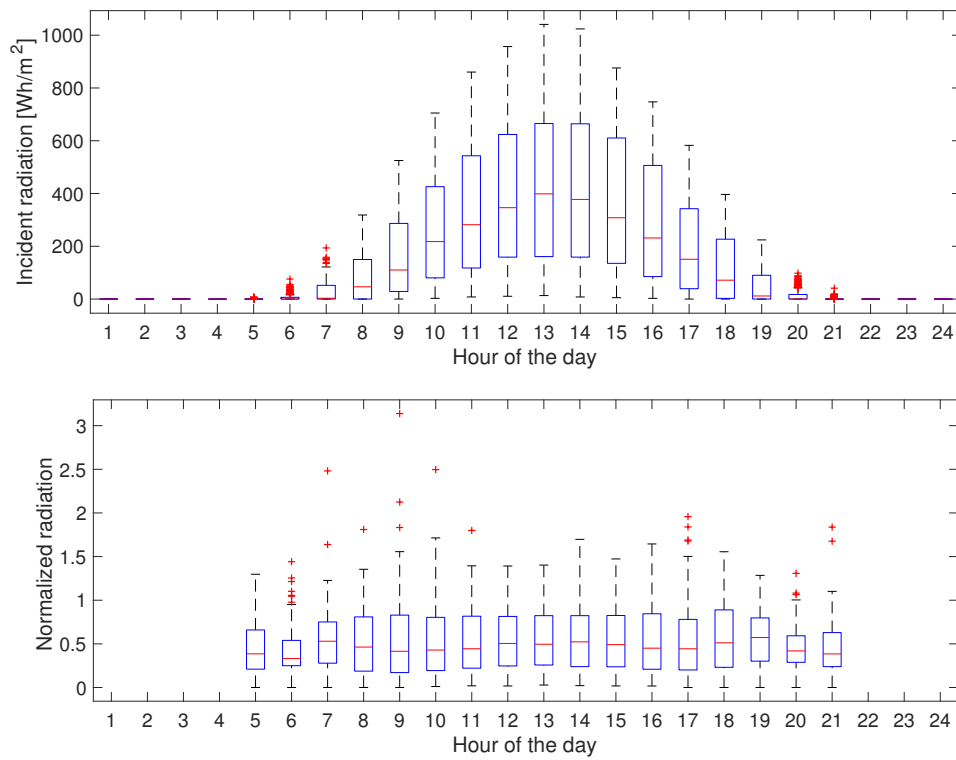


Figure 4-11: Comparison of radiation distributions before and after the normalization. '+' represent outliers

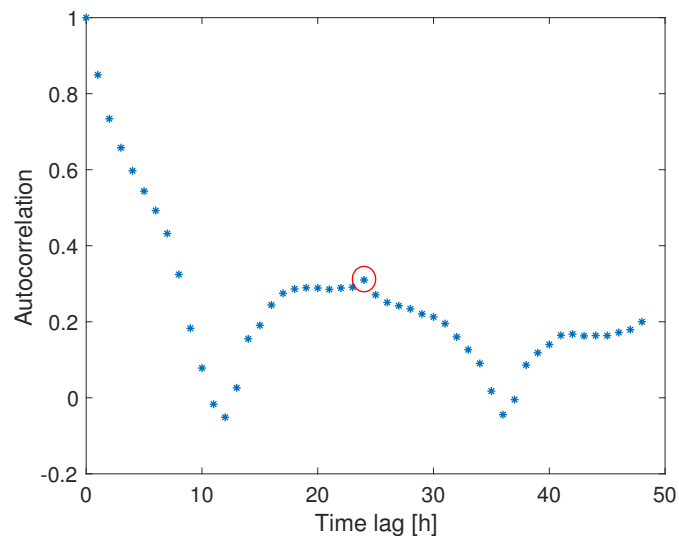


Figure 4-12: Autocorrelation of $\{\tau(t)\}$. The 'red' circle highlights the daily correlation with 24-h periodic lag.

literature studies [6, 8], a so called ‘clear sky model’ is computed and used to estimate the global solar irradiance without taking into account haze/cloud effects, as though the radiation was measured during a clear day. This model aims to separate the stochastic component (transmittance of radiation through clouds) from the deterministic one.

To this purpose, the normalized radiation is defined as the ratio between the measured radiation and the clear sky one:

$$\tau(t) = \frac{G_c(t)}{G_c^{cs}(t)} \quad (4-12)$$

The clear sky radiation (G_c^{cs}) is approximated as a local constant model with respect to the day of the year and the time of the day. Indeed, the latter two variables represent the only source of irradiance variability once the location is set and the sky is assumed clear. The procedure is usually performed through statistical smoothing techniques such as quantile regression [6]. In this way, no physical explanation has to be modelled and the estimation is uniquely referred to the available data. It is important to notice that, when a sparse number of clear sky observations (especially in winter period) is present in the data, the procedure could lead to biased results.

4-3-2 Forecasting Model

The discussed clear sky approach is applied in our case to identify a forecasting model for solar power generation. Firstly, meteorological data from KNMI [42] are used to compute incident solar radiation in Schiphol (closest station to Amsterdam) for a period of 5 years, as explained in Section 3-2-2. Then, a smoothing technique based on weighted quantile regression is applied to build the clear sky model $G_c^{cs}(t)$ for every day/hour couple of the year. Finally, once the clear sky model is estimated, solar power prediction can be performed on the normalized time series.

The normalization procedure makes the series $\{\tau(t)\}$ a stationary process, as we can see by the box-plot in figure 4-11. Indeed, the mean of the process becomes time-invariant. For this reason, traditional time series analysis can be applied to forecast future values of solar radiation incident on the mounted solar panels.

The daily seasonality can still be retrieved in the time series by observing the autocorrelation function of the process in Figure 4-12. Hence, due to the previous observations, a simple seasonal autoregressive model can be assumed to describe the stationary process $\{\tau(t)\}$, as follows:

$$\hat{\tau}(t+1) = a\tau(t) + b\tau(t-23) + w(t) \quad (4-13)$$

Clearly, during night time, when $G_c^{cs}(t)$ is null, the normalized radiation is not defined and no prediction has to be performed for those time steps. Hence, the correspondent data are removed from the training set.

Since the uncertainty in residuals of the trained model does not pass the Kolmogorov-Smirnov test, the Gaussian assumption is rejected also in this case. The obtained *ex-post* distribution of the normalized radiation is stored in a non-parametric form as an empirical distribution, and the model is easily integrated in the probabilistic framework.

During the forecasting procedure, the incident radiation $\hat{G}_c(t+k)$ can be predicted, by inverting (4-12), as:

$$\hat{G}_c(t+k) = \hat{\tau}(t+k) \cdot G_c^{cs}(t+k) \quad (4-14)$$

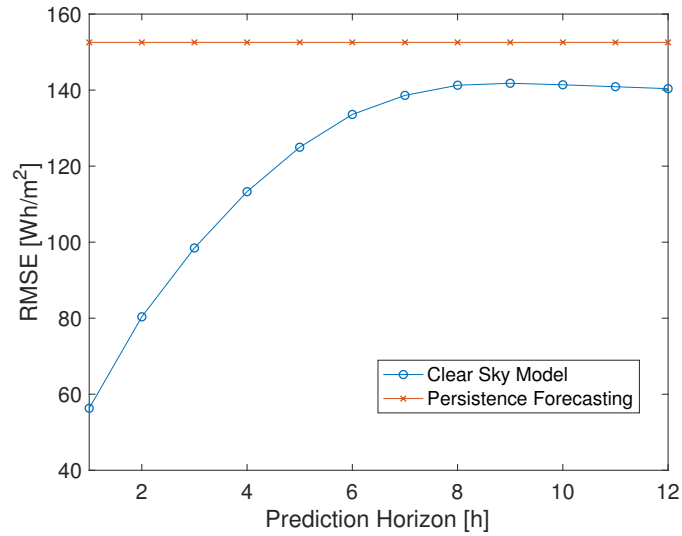


Figure 4-13: Performance of solar radiation forecasting

and subsequently employed to compute PV hourly supply by means of the panels model (3-9). The performance of the clear sky model is evaluated for the incident radiation in terms of RMSE and plotted in Figure 4-13 for an increasing prediction horizon. In the same figure, a comparison with a simple persistence forecasting model, in which the predicted output is assumed equal to the corresponding 24-h lagged measurement, is proposed in order to better understand the results. Similarly to demand forecasting, for horizons larger than 6-7 hours prediction accuracy reaches an asymptotic performance.

4-4 Conclusions

Supervisory control strategies are mainly based on the information they are able to process about future evolution of the microgrid. Indeed, our first step for the implementation of a local EMS has been to focus on the identification of forecasting models for stochastic processes affecting the power balances of the microgrid: thermal and electrical consumption of the customers on one hand, and PV uncontrollable supply on the other hand.

The forecasting techniques analysed in this chapter are exclusively based on data that can be easily collected by the controller, i.e. previously measured values of the considered processes and calendar information. As a consequence, the prediction error, even for the best identified models, results relatively large due to the high volatility of the stochastic processes. We believe that the prediction accuracy could be improved by introducing extra information collected by local sensors, e.g. occupancy, or obtained through web communication with a meteorological database, e.g. outside temperature or numerical weather prediction for solar irradiation, but these measurements were not included in our thesis.

Control Strategies for Energy Management Systems

A local Energy Management System (EMS) takes into account technical and economic considerations and determines power flows within the microgrid and the exchange of electricity with the utility grid to achieve optimal operation. The decisions that the EMS can make are intrinsically hybrid in nature: firstly it has to choose which micro-sources should be switched on/off (unit commitment problem), then it has to fix the amount of production generated from each micro-source or exchanged with the grid at any time step (economic dispatch). Moreover, a crucial feature for the correct control strategy is to consider the technical constraints related to the energy resources integrated in the microgrid.

In this chapter we analyse predictive control strategies that can be applied to supervise the microgrid operation with the specified objective of cost minimisation for the owners. In Section 5-1, we firstly investigate the state-of-the-art Model Predictive Control (MPC) strategies from a theoretical perspective and highlight advantages and disadvantages of different algorithms that aim to deal with systems affected by uncertainties. Then, in Section 5-2 a rule-based benchmark strategy is presented to control the micro-CHP and the auxiliary boiler. Finally, the MPC techniques will be employed and adapted to our case studies. The ‘certainty equivalence’ paradigm is firstly assumed in Section 5-3 such that the predictive strategy can be formulated in a deterministic framework. Lastly, in Section 5-4, the core strategy of this thesis is presented through a reformulation of the original problem with a stochastic approach that explicitly considers the uncertainties affecting microgrid operation.

5-1 Literature Background: Model Predictive Control

Model Predictive Control (MPC) is a control strategy widely applied in process industries and power systems for solving problems where constraints on the manipulated and controlled variables naturally arise and have to be considered in the control design [52]. It is a control strategy in which the current control action is obtained by solving on-line, at each sampling

time, a finite horizon open-loop optimal control problem, using the measured state of the system as the initial state. The optimization yields an optimal control sequence and the first control element in this sequence is applied in a receding horizon fashion [71].

The main advantage of MPC is its ability to handle control problems in which an off-line computation of the control law is difficult or technically impossible. Furthermore, due to the reformulation of the control problem into an optimization one, MPC can easily include constraints. This makes the strategy more powerful with respect to classical control schemes (e.g. PID, H-infinity) [71].

However, on the other hand, necessary conditions for the implementation of MPC algorithms are slow dynamics of the controlled system, such that the optimization can be solved on-line within each time sample, and the availability of a mathematical model that identifies the underlined system dynamics explicitly.

Before a detailed explanation of the control strategies applied for the optimal power flows in the case studies defined in Section 3-3-3, in this section we present the state-of-the-art MPC algorithms used to control perturbed systems.

5-1-1 Classic MPC

Model Predictive Control is traditionally applied on a discrete-time dynamic system (5-1), in which the state and the input are constrained to be confined within specified sets.

$$\begin{aligned} x(t+1) &= f(x(t), u(t)) \\ x &\in \mathbb{X}, u \in \mathbb{U} \end{aligned} \quad (5-1)$$

An MPC strategy converts the control problem into a finite horizon optimization procedure to be solved at each time step, parametrized on the currently measured state x_0 . In the following, the notation ‘ $\hat{\cdot}$ ’ is used to indicate the variables involved in the definition of the optimization problem.

The optimization objective of an MPC is to minimize a specific user-defined cost function V_{N_p} , which considers N_p future control actions $\hat{u}(k)$ that affect the evolution of the system (5-1) in an open-loop fashion. The decision variable $\mathbf{u} = [\hat{u}(0), \dots, \hat{u}(N_p)]^T$ belongs to the decision space \mathcal{U}_{N_p} of feasible control sequences, which have to respect the input bounds ($\hat{u}(k) \in \mathbb{U}$) and, at the same time, keep the controlled state $\hat{x}^{\mathbf{u}}$ inside its constraints ($\hat{x}^{\mathbf{u}}(k+1) \in \mathbb{X}$), for all the time steps $k = 0, \dots, N_p - 1$ within the prediction horizon.

Then, after the optimization problem is solved, a receding horizon scheme is implemented for a closed-loop control at any time step: the implicit MPC law $u(t) = l_{N_p}(x_0)$ applied to the system is defined as the first value $\hat{u}(0)$ of the optimal control sequence \mathbf{u}^* .

From a theoretical perspective, in the MPC framework two main issues have to be assessed: stability and recursive feasibility. These are discussed in the following.

Recursive Feasibility Recursive feasibility is probably the most important property for a MPC strategy, both from a theoretical and practical point of view. It implies that, if the optimization problem can be solved for the initial state $x(0)$, it can be solved for any subsequent state reached by the controlled system [71].

The feasible set of initial states \mathcal{X}_{N_p} for which a solution to the optimization problem exists is

called **region of attraction**, and is defined as the set of states allowing a not empty decision space :

$$\mathcal{X}_{N_p} = \{x \mid \mathcal{U}_{N_p}(x) \neq \emptyset\} \quad (5-2)$$

Hence, recursive feasibility can be mathematically defined in the following form:

$$x(t) \in \mathcal{X}_{N_p} \implies x(t+1) = f(x(t), l_{N_p}(x(t))) \in \mathcal{X}_{N_p} \quad (5-3)$$

thus guaranteeing that the next-time state of the controlled system is kept in the region of attraction when current state belongs to it.

It is fundamental to assure recursive feasibility if we want to implement MPC to control an existing system. If this is not possible, any implementation of the MPC algorithm should be modified to include a feature that enables recovery from faults that cause infeasibility.

Stability As Kalman himself pointed out in one of his classic papers, optimality does not ensure stability:

“ In the engineering literature it is often assumed (tacitly and incorrectly) that a system with optimal control law is necessarily stable. ” *R. F. Kalman* [71]

Indeed, when we apply a finite horizon optimization problem, even when its objective is to regulate the state to the origin, instability issues could arise. This is due to the fact that MPC controller solves an open-loop optimization problem, whereas the control action is implemented in closed-loop. Therefore, the actual controlled state could significantly differ from the predicted one on the long run. In the nominal scenario (deterministic system) these two variables are identical if, and only if, we consider an infinite horizon for the optimization problem. However, apart from very simple systems (linear unconstrained system), where a closed form solution to the infinite horizon problem does exist, in any other case the optimization would be intractable.

For this reason, a dual-mode paradigm was introduced in [53] and further motivated in [51] in order to formalise the discussion over the stabilising ingredients for classical MPC. This paradigm is widely applied in the literature and consists of a double control mode for the decision variables in the optimization procedure on the open-loop system:

- A discrete control sequence \mathbf{u} is applied for the first N_p time steps by means of the implicit control law $l_{N_p}(x)$.
- A pre-defined stabilising control law $l_f(x)$ working in the terminal set \mathbb{X}_f is applied at the end of the prediction horizon. Based on this law, the stabilising ingredients V_f (terminal cost) and \mathbb{X}_f (terminal set) are computed and introduced in the optimization problem.

Eventually, when the dual-mode paradigm is applicable, the new version of the optimal and stable control problem has a reduced region of attraction \mathcal{X}_{N_p} due to the presence of a terminal constraint $\hat{x}^{\mathbf{u}}(N_p) \in \mathbb{X}_f$.

5-1-2 Robust MPC

As we previously highlighted, for a deterministic system the optimal open-loop control problem for a given initial state is equivalent to its closed-loop formulation (dynamic programming) [71]. However, for any perturbed system this equivalence of trajectories does not hold anymore.

In the following we assume system dynamics to be affected by an **additive disturbance** w . Hence, the model (5-1) is modified as follows:

$$\begin{aligned} x(t+1) &= f(x(t), u(t)) + w(t) \\ x &\in \mathbb{X}, u \in \mathbb{U}, w \in \mathbb{W} \end{aligned} \quad (5-4)$$

where the introduced set \mathbb{W} describes the uncertainty range.

Due to the disturbance, the open-loop problem can result in very poor predictions, leading to divergence of the state trajectory from its reference.

For the optimal control problem to give the same solution as that obtained by dynamic programming it is necessary for the decision variable to be a control policy, i.e. a sequence of feedback control laws, instead of a simple control sequence. Pure feedback MPC strategy, based on control policies, is theoretically optimal, but computationally intractable due to the infinite dimension of the policy space. Hence, optimality has necessarily to be sacrificed for tractability, by imposing a parametrization of the control policy.

In this context, robust optimization is usually implemented to deal with the presence of uncertainty in the problem definition. The robust goal is to minimize the cost function V_{N_p} , while guaranteeing that the **operational constraints are satisfied for any permissible realization of the uncertainty**. Hence, robust approach is based on the assumption of a finite and measurable support of system uncertainty. Specifically, in case of additive disturbance, the set \mathbb{W} is assumed to be bounded.

The classic approach in robust MPC synthesis is to employ a minimax strategy, i.e. minimization of a worst-case performance measure, where the worst-case is defined as the disturbance sequence leading to the largest open-loop cost [53]. Hence, the minimax robust strategy solves the following optimization problem (subject to system constraints) :

$$\min_{\mathbf{u}} \max_{\mathbf{w}} \{V_{N_p}(x_0, \mathbf{u}, \mathbf{w}) \mid \mathbf{w} \in \mathbb{W}^{N_p}, \mathbf{u} \in \mathcal{U}_{N_p}\} \quad (5-5)$$

where the cost function is explicitly dependent on the disturbance sequence \mathbf{w} , together with the control sequence \mathbf{u} , due to the perturbed model dynamics (5-4) of state evolution.

The main problem with minimax MPC algorithm is that the controller can become overly conservative, since it has to find a single control sequence that works well in open-loop for all admissible disturbance realizations. On the other hand, closed-loop minimax approach could lead to tractability issues because the amount of cases that have to be investigated to solve the optimization problem (5-5) increases exponentially with the dimension of \mathbb{W} [47].

A fundamental tool to reduce conservatism in robust MPC is the introduction of a feedback parametrization of the input law. One of the most well-known approach, used to control a linear perturbed system subject to input and state constraints, is the *tube-based* MPC [54]. This control strategy is based on the concatenation of two controllers in a cascade scheme:

- A deterministic MPC law, which is used to generate the nominal open-loop trajectories (centres of the *tubes*) and is defined on the nominal system (when no disturbance is assumed) with precomputed tightened constraint sets.

- An outer ancillary controller that aims to steer all the trajectories towards the nominal reference, and parametrizes the control law with respect to the closed-loop error e between the state of the controlled system and its open-loop nominal trajectory.

The main disadvantages of the *tube-based* strategy can be identified in the parametrization of the outer control law and the approximation of the new constraint sets, which could lead to a certain degree of conservativeness and sub-optimality.

Robust MPC law can be quite conservative and lead to poor performance when applied to uncertain systems, since it does not take into account the probabilistic nature of the disturbance and assumes that it can uniformly take any value into the disturbance set. Moreover, robust satisfaction of the constraints may be impossible to enforce if the support of the disturbance is unknown or possibly unbounded. Indeed, in residential microgrids, where energy demand highly fluctuates, the forecasting error for thermal consumption can be even larger than TES size, leading to infeasible operation in the robust framework. Hence, robust MPC strategies cannot be implemented in our case studies.

5-1-3 Stochastic MPC

Due to the previously discussed issues, robust optimization can be relaxed and recast in a stochastic framework by **allowing the constraints to be violated** at a certain degree, with the aim to enlarge the feasibility region of the optimization problem and reduce its conservativeness. The violation rate is aimed to be controlled by fixing a probability risk level p for each relaxed constraint [24].

To show how system constraints can be properly recast in a probabilistic setting, we refer for simplicity to an individual linear state constraint of the form :

$$g^T x(t) \leq h \quad (5-6)$$

If we want to allow a specific rate of *point-wise* violation, the correspondent *chance* constraint in the stochastic formulation of the optimization problem, once all variable dependences are made explicit, is defined as :

$$\begin{aligned} \mathcal{P}\{g^T \hat{x}^{\mathbf{u}, \mathbf{w}}(k) \leq h\} &\geq 1 - p && \text{for } k = 1, \dots, N_p \\ \implies \mathcal{P}\{g^T [\hat{x}^{\mathbf{u}}(k) + e^{\mathbf{w}}(k)] \leq h\} &\geq 1 - p \end{aligned} \quad (5-7)$$

where p is a design parameter to be tuned in order to obtain a trade-off between performance and constraint violation. The second inequality highlights how, for the superposition principle, the effect of the additive disturbance on the state trajectory can be decoupled from its nominal evolution in the form of the closed-loop error e .

More generally, when g is a matrix, for instance when the goal is to express the probability that the state and/or the control are inside a certain set, the constraint is called joint chance constraint. The simplest way to work with a joint chance constraint is, however, to approximate it by splitting the overall set into a sequence of individual chance constraints, whose probability sums up to the original one. This technique is called *risk allocation* and is well described in [24].

Some recent overviews about the state-of-the-art algorithms for stochastic MPC strategies highlight a great interest for the topic in the contemporary literature [55, 24]. These papers helped to categorise the stochastic MPC algorithms in two major schools-of-thought:

- Analytical approaches: based on the reformulation of the chance constraints in deterministic terms, they take explicitly into consideration the stochastic properties of the disturbance.
- Randomized approaches: based on a discretisation of the probability distribution of the disturbance, sampling strategies are considered. Hence, the stochastic formulation is translated on a deterministic multi-scenario problem by means of a statistical approximation.

Analytical Approaches

In analytical approaches, the chance constraint (5-7) can be generally reformulated by considering the action of the disturbance sequence \mathbf{w} as a tightening factor of the nominal constraint set:

$$g^T \hat{x}^{\mathbf{u}}(k) \leq h - q^{\mathbf{w}}(k, 1 - p) \quad \text{for } k = 1, \dots, N_p \quad (5-8)$$

The constraint tightening level $q^{\mathbf{w}}(k, 1 - p)$ is nothing more than the left quantile of the distribution $g^T e^{\mathbf{w}}(k)$ and can be computed based on the available information about the disturbance. It is analytically defined as the minimum value obtained by the following optimization problem :

$$\min_q \left\{ q \mid \mathcal{P} \left\{ g^T e^{\mathbf{w}}(k) \leq q \right\} = 1 - p \right\} \quad (5-9)$$

In the probabilistic framework, the worst-case scenario of the robust approach can still be retrieved by imposing $p = 0$, reconverting the chance constraint in its ‘hard’ form.

A feedback parametrization of the control law $l_{N_p}(x, e)$ is widely employed in the scientific literature in order not to incur in an uncontrolled open-loop evolution of the state trajectories, thus making the input variable $\hat{u}(k)$ always depend on the stochastic disturbance [24]. For this reason we want to highlight that hard constraints on the input can only be imposed in two cases for analytical approaches: when the disturbance is supported on a bounded set, or when assumptions on recursive feasibility can be relaxed. Moreover, on the other hand, the evolution of the error trajectory $e^{\mathbf{w}}$ and subsequently the values of the quantiles computed in (5-9) strictly depend on the input parametrization of the control law, which also affects the computational complexity of the applied algorithm.

Guarantees on recursive feasibility and bounds on the violation level probability have been already provided for linear systems, by adding extra constraints to the optimization problem [45, 43, 44, 29]. On the other hand, analytical approaches for nonlinear system (as in case of the hybrid model described in Section 2-3) have not been deeply researched, due to the impossibility to express the closed-loop error trajectory $e^{\mathbf{w}}$ in closed form and subsequently compute the analytical properties of the quantiles (5-9).

Randomized approaches

The randomized, or scenario-based, methods rely on the on-line random generation of a sufficient number of disturbance realizations ($\mathbf{w}[j]$) in order to reformulate the stochastic

optimization in a tractable deterministic framework. The main objective of the randomized approaches is to compute a lower bound to the number of requested scenarios N_s in order to ensure a prescribed level of constraint violation p .

Each chance constraint of the form (5-7) is enforced by a set of deterministic ones, as follows:

$$\begin{aligned} g^T \hat{x}^{\mathbf{u}, \mathbf{w}[j]}(k) &\leq h \quad \text{for } j = 1, \dots, N_s \\ &k = 1, \dots, N_p \end{aligned} \quad (5-10)$$

Furthermore, in this framework, the cost function is redefined as a sampled average over the N_s realizations:

$$V_N(x_0, \mathbf{u}, \mathbf{w}) = \frac{1}{N_s} \sum_{j=1}^{N_s} V_N(x_0, \mathbf{u}, \mathbf{w}[j]) \quad (5-11)$$

The main advantage of scenario generation approaches is that they are applicable to wide classes of systems (both linear and nonlinear) affected by general disturbances. Moreover, joint chance constraint can be enforced without any extra conservativeness. However, stability and recursive feasibility are not established by none of the investigated works in the scientific literature. Thus, open issues on this area concern the possibility of formally guaranteeing feasibility and stability properties.

The relationship between a lower bound on N_s and the number of decision variable d in a stochastic programming optimization has firstly been analysed in [14]. Here, the relation is carried out by means of the ‘confidence level’ concept: since the optimization procedure depends on a specific multi-extraction of the disturbance realizations $\mathbf{w}[j]$, the computed optimal solution \mathbf{u}^* could lead to actual constraint violation; hence, the confidence level β is defined as the allowed probability that the ‘unseen’ disturbance realizations violate the predicted result. Moreover, when the possibility to remove R of the generated scenarios is introduced in [15], with the aim to reduce potential conservativeness of the result, a definitive inequality was finally presented, which correlates all the variables of interest:

$$\beta \geq \binom{R+d-1}{R} \sum_{i=0}^{R+d-1} \binom{N_s}{i} (1-p)^i p^{N_s-i} \quad (5-12)$$

The formula is independent from any chosen generation and removal algorithm and from any disturbance distribution, as long as the scenarios used in the optimization are representative of the true distribution. Hence, for practical engineering purposes, once a very small value ($\approx 10^{-6}$) of the confidence level has been fixed, and the correspondent minimum number of scenarios is used in the optimization, we may conclude with ‘practical certainty’ that the stochastic formulation of the optimization problem is solvable for any realization of the uncertainty [15]. This fundamental property allows for generalization of unseen scenarios, not used in the computation of the solution.

In [76], the presented result is adapted to the multi-stage optimization for the MPC framework. The classic scenario approach is therefore extended: each constraint may affect only a certain subspace of the whole decision space, due to a strict relation with a single temporal stage. The dimension of this subspace is called **support rank**.

In this context, the number N_s of required disturbance realizations is proved to be just dependent on the support rank of the first-step constraints (ρ_1). Thus, a great mathematical result is achieved: the sample size necessary to implement an MPC randomized approach is

decoupled from the prediction horizon, and the variable d in (5-12) can be substituted by the significantly smaller value ρ_1 .

Furthermore, in the same work [76], the **average-in-time** (instead of point-wise) probability of constraint violation is considered, in order to further reduce conservativeness of the result. Consequently, the confidence level β can be neglected for the expected time-average violation and removed from the computation of lower bound for the scenarios. An admissible sample-removal pair (N_s, R) can be selected by solving the one-dimensional integration of β_{\min} (right hand side of (5-12)) over any possible value of point-wise violation probability v :

$$\int_0^1 \binom{R + \rho_1 - 1}{R} \sum_{i=0}^{R + \rho_1 - 1} \binom{N_s}{i} (1-v)^i v^{N_s-i} dv$$

Then, we have to guarantee that the computed result is smaller than the fixed admissible average-in-time level p . In case no scenario removal is performed ($R = 0$), the integration can be solved analytically, leading to the least restrictive condition for the amount of scenarios in stochastic multi-stage optimization:

$$\frac{\rho_1}{N_s + 1} \leq p \implies N_s \geq \frac{\rho_1 - p}{p} \quad (5-13)$$

5-2 Benchmark Strategy: Rule-Based Control

As explained in Chapter 2, the only energy resources on which the supervisory control can impose its decisions are the dispatchable generators. Micro-CHPs are employed in our case studies with the aim to supply the households with the requested electrical and thermal demands. Since the two forms of power output are physically correlated, the control strategy has to consider that only one of them can be used as a controlled variable.

In the literature, the micro-CHP units are typically controlled according to two different rule-based approaches, called heat-led or electricity-led [57]. As their names suggest, through these strategies, the prime mover is turned on/off according to the heat or power demand, respectively. Since thermal efficiency of a micro-CHP unit is commonly greater than its electrical efficiency (with the exception of fuel cell technologies) and the employment of thermal storage allows decoupling between corresponding supply and consumption, thermal demand is usually chosen as the driving variable.

Due to local consumption, the heat flows out from the storage which thereby decreases in temperature, while heat supplied by both the micro-CHP and the auxiliary boiler increases water temperature. In heat-led framework, the prime mover output is controlled such as to keep the storage temperature at an average value, corresponding with an average energy level \bar{Q}_{TES} . When this strategy is applied, the next hour demand is defined either by means of reference profile [38] or through a point forecasting model as in predictive strategies. As we analysed in Chapter 4, naive ‘time-of-the-day’ models would lead to far worse performance due to poor prediction accuracy. Hence, in the following we apply the periodic forecasting models based on linear regression already described in Chapter 4 for one-step-ahead prediction \hat{D}_Q . Furthermore, the use of the same forecasting procedure will help us to better compare the performance of all the presented control strategies.

Microgrid operation described in Section 2-3 is therefore controlled with the heat-led control law for micro-CHP and the auxiliary boiler, presented in Algorithm 1.

Algorithm 1 Rule-Based Strategy*CHP:*

if $\delta_{\text{CHP}}(t-1) - \delta_{\text{CHP}}(t-2) > 0$ **or** $\frac{T_s}{C} \cdot \min_{\text{CHP}} + Q_{\text{TES}}(t) - \hat{D}_Q(t) < \max_{\text{TES}}$ **then**

$$Q_{\text{CHP}}(t) \leftarrow \frac{1}{T_s} \max \left(\min \left(\bar{Q}_{\text{TES}} - Q_{\text{TES}}(t) + \hat{D}_Q(t), \frac{T_s}{C} \cdot \max_{\text{CHP}} \right), \frac{T_s}{C} \cdot \min_{\text{CHP}} \right)$$

$$\delta_{\text{CHP}}(t) \leftarrow 1$$

else

$$Q_{\text{CHP}}(t) \leftarrow 0$$

$$\delta_{\text{CHP}}(t) \leftarrow 0$$

end if*BOILER:*

if $T_s \min_{\text{BOIL}} + T_s Q_{\text{CHP}}(t) + Q_{\text{TES}}(t) - \hat{D}_Q(t) < \max_{\text{TES}}$ **then**

$$Q_{\text{BOIL}}(t) \leftarrow \frac{1}{T_s} \max \left(\min \left(\bar{Q}_{\text{TES}} - T_s Q_{\text{CHP}}(t) - Q_{\text{TES}}(t) + \hat{D}_Q(t), T_s \max_{\text{BOIL}} \right), T_s \min_{\text{BOIL}} \right)$$

$$\delta_{\text{BOIL}}(t) \leftarrow 1$$

else

$$Q_{\text{BOIL}}(t) \leftarrow 0$$

$$\delta_{\text{BOIL}}(t) \leftarrow 0$$

end if

Firstly, CHP status and power output are selected, then the extra heat supplied by the boiler is subsequently determined. Standard operation is computed through microgrid heat balance (2-6), where demand and TES level at next time step are respectively substituted by the output \hat{D}_Q of thermal forecasting model and the desired thermal level \bar{Q}_{TES} . The generation process is conditioned for both the engines, when it could lead to violation of the maximum allowable temperature in the thermal storage. Moreover, a further constraint on the choice of CHP status is related to the switching between ‘on’ and ‘off’ modes in consecutive hours, as expressed in (2-10).

The rule-based strategy explicitly considers technical constraints related to CHP and boiler operation. Indeed, the range of heat generation for the two engines (when they are ‘on’) is limited by their nominal size on one hand and their minimum output on the other hand.

However, this naive strategy does not exploit the full potential of cost minimisation when energy demand has to be met, and more advanced techniques can be implemented.

5-3 Certainty Equivalence: MPC

When future predictions of system dynamics are considered by the controller, a supervisory strategy is said to be ‘intelligent’, since all relevant information about the consequences of choosing actions are taken into account [37]. In many literature works [17, 38, 49, 66, 65, 82, 10, 75, 85] the idea to propose more advanced control schemes is developed through the formulation of optimization problems, which consider the heat coverage as a constraint of the cost minimization problem on a prediction horizon longer than a single time step. Therefore, the framework of MPC strategy, deeply analysed in Section 5-1, can be perfectly adopted in the EMS for a residential microgrid.

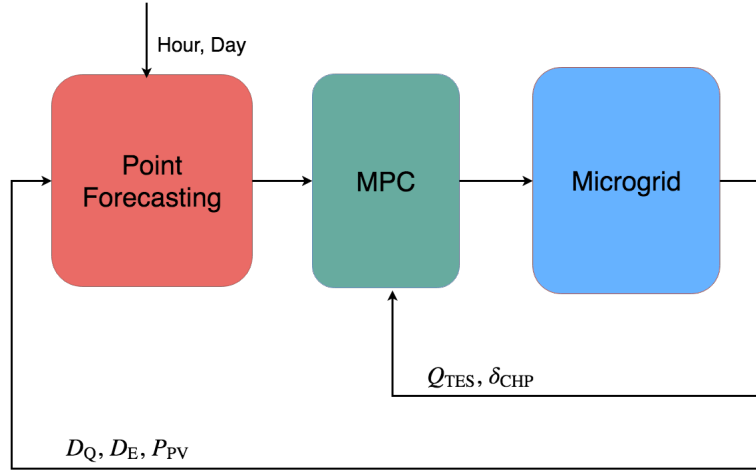


Figure 5-1: Nominal MPC scheme

In the largest part of literature, the uncertainties related to renewable energy generation and to load demands are not modelled in their stochastic dynamics [38, 65, 82, 10, 75]. According to the certainty equivalence paradigm the forecasts are assumed to be deterministically predicted with point forecasting methodologies. Hence, the scheme implemented for conventional MPC strategy is presented in Figure 5-1: the microgrid has been defined for the two case studies in Section 3-3-3, while the forecasting models for energy demand and PV supply have been presented in Chapter 4. Hence, in this section we discuss the receding horizon strategy corresponding to the MPC block, which receives as input N_p predictions of the stochastic processes and the current status of TES and generators.

5-3-1 Deterministic Formulation

The economic objective of the control strategy is represented by the minimization of operational costs over the prediction horizon, in a way similar to the sizing procedure presented in Section 3-3-2, but re-adapted to a receding horizon structure.

More in detail, the cost function is represented by the operational costs of the microgrid (3-16) along a fixed prediction horizon N_p , evaluated at any time step. However, in order to take into account the benefits of the limited-in-time operation management beyond the considered horizon, a terminal cost is added to the function (5-14). Indeed, the heat stored in the TES after the N_p time steps can be consumed in the future, thus avoiding to buy and burn additional gas in the auxiliary boiler to supply thermal energy. For this reason, we decided to consider as terminal cost for our predictive strategy the negative price (revenue) of the saved gas. The optimization problem to be solved at any time step is therefore defined as :

$$\min_{\mathbf{f}, \delta} \sum_{k=0}^{N_p-1} \left[(c_{\text{GAS}} + c_{\text{O\&M}} \cdot \eta_{\text{CHP}}) \cdot \hat{f}_{\text{CHP}}(k) + c_{\text{GAS}} \cdot \hat{f}_{\text{BOIL}}(k) + c_{\text{EL}} \cdot \hat{G}^+(k) - c_{\text{FIT}} \cdot \hat{G}^-(k) \right] - \underbrace{c_{\text{GAS}} \cdot (\hat{Q}_{\text{TES}}(N_p) - \min_{\text{TES}})}_{\text{terminal cost}} \quad (5-14)$$

The constraints of the optimization problem are expressed by the equations (2-6)-(2-12) representing the model of microgrid operation for N_p time steps, starting from t . The initial state for the optimization $\hat{Q}_{\text{TES}}(0)$ is given by the measured state $Q_{\text{TES}}(t)$, while the energy demands (and the PV supply for case study ‘B’) are provided from the point forecasting model for the next N_p time steps. Therefore, the problem can be solved as a Mixed Integer Linear Programming problem and the controlvariables related to the first time step ($k = 0$) are effectively applied to the system for the next hour.

Due to the effect of the uncertainties in consumption and renewable supply (when present), large perturbations of the nominal system can lead to problem infeasibility when heat coverage of the TES is not guaranteed. Hence, a recovery strategy has to be introduced, which substitutes the computation of the optimal supply in case of infeasibility. We decided to employ the benchmark rule-based strategy to recover from these kind of faults.

5-3-2 Practical Disadvantages

When deterministic MPC strategy is applied to a stochastic system, no constraints satisfaction nor recursive feasibility can be guaranteed [52]. From a practical point of view, in our case studies, large violations of the thermal constraints in the water storage tank occur. This means that inevitable disturbances and forecast errors deteriorate the actual performance of the controller and lead to several *ex post* constraint violations, especially in small scale environments, where the stochastic component is highly volatile.

This behaviour would imply the necessity of a lower-level controller to recompute input of the generators within the time step and reduce the constraint violations. This two-level strategy would strongly affect the computed economic savings of the deterministically scheduled microgrid operation. However, due to absence of available data samples for thermal demand within the hourly time step T_s , the lower-level control cannot be implemented neither the overall performance exactly evaluated.

Recovery and saturation A rough estimate of performance deterioration can be computed by assuming a recovery strategy for lower bound violation of the thermal constraint (2-12) and a saturation process for the upper bound violation of the same constraint. On one hand, we can assume that the auxiliary boiler is capable to react fast enough to avoid any lower bound violation of the temperature in the TES, such that the scheduled boiler supply is augmented in the following way:

$$Q_{\text{BOIL}}(t) = \min\left(\eta_{\text{BOIL}} \cdot \hat{f}_{\text{BOIL}}(0) + \underbrace{\min\left(\min_{\text{TES}} - Q_{\text{TES}}(t+1), 0\right)}_{\text{lower bound violation}}, \max_{\text{BOIL}}\right) \quad (5-15)$$

The external minimum is applied to take into account technical limit of maximum generation of the boiler. Clearly, boiler generation should practically be adjusted on-line, within the time step, in order to know the actual level $Q_{\text{TES}}(t+1)$.

On the other hand, the overproduced heat, which cannot be stored in the TES, is assumed to be dumped. Hence, the following saturation condition holds:

$$Q_{\text{TES}}(t+1) = \min\left(Q_{\text{TES}}(t) + T_s \cdot Q_{\text{CHP}}(t) + T_s \cdot Q_{\text{BOIL}}(t) - D_Q(t), \max_{\text{TES}}\right) \quad (5-16)$$

5-4 Stochastic Reformulation

Stochastic methods are considered as the right balance between the conservativeness of robust design and the poor performance of deterministic approach, in cases in which uncertainties affect the controlled system. Stochastic control strategies aim to recast the problem into a probabilistic framework by explicitly taking uncertainty into account, such that undesired unmodelled effects do not lead to suboptimal performance and deteriorate theoretical properties.

Without requiring an explicit probability distribution, the uncertainty of disturbance can be characterized more flexibly. For this reason, the most common stochastic approach for supervisory control in microgrids are, undoubtedly, scenario-based methods, which can characterize the uncertainty by means of historical data. However, in the majority of the scientific literature no probabilistic bounds on the amount of constraint violation are explicitly considered and the number of generated scenarios is empirically selected [66, 49, 4]. Moreover, the uncertainty in the system is often assumed or theoretically modelled instead of being evaluated and quantified as in our work.

5-4-1 Scenario-Based Approach

In the scenario-based approach one single control sequence of the decision tuple (\mathbf{f}, δ) along the prediction horizon has to be determined, such that the optimization problem is solved for a fixed amount N_s of generated uncertainty realizations. The deterministic optimization problem (5-14) is extended to deal with stochastic trajectories of the forecast processes related to demand and PV supply.

The theoretical result showed in (5-13) provides a lower bound to N_s related to the support rank ρ_1 of the relaxed constraint and the allowed probability p of constraint violation. Since microgrid dynamics are defined by a single state (TES level), the support rank of the system corresponds to $\rho_1 = 1$; hence, an allowed risk of 5% average-in-time violation of the temperature in the thermal storage leads to a requested amount of scenarios:

$$N_s = \frac{\rho_1 - p}{p} = 19$$

The stochastic processes affecting the controlled system are represented by the forecast demand and, for case study 'B', the forecast photovoltaic supply. For this reason N_s tuples of $(\hat{D}_Q^{[j]}, \hat{D}_E^{[j]}, \hat{P}_{PV}^{[j]})$ have to be generated through the probabilistic forecasting models defined in Chapter 4. These variables affect power balance equations (2-6)-(2-7) and, subsequently thermal constraint (2-12) regarding TES level. Therefore, each of these constraints is repeated in the optimization problem for the generated scenarios, whereas the constraints that only involves decision variables are considered analogously to the deterministic approach. Finally, the recovery strategy in case of infeasibility is considered to be, as in deterministic approach, the benchmark rule-based controller.

It is important to highlight that, due to large uncertainty in thermal demand model, the level of TES for multiple realizations can easily spread on an interval wider than the range D^* allowed by the installed water tank. In these cases the optimisation problem, which requires

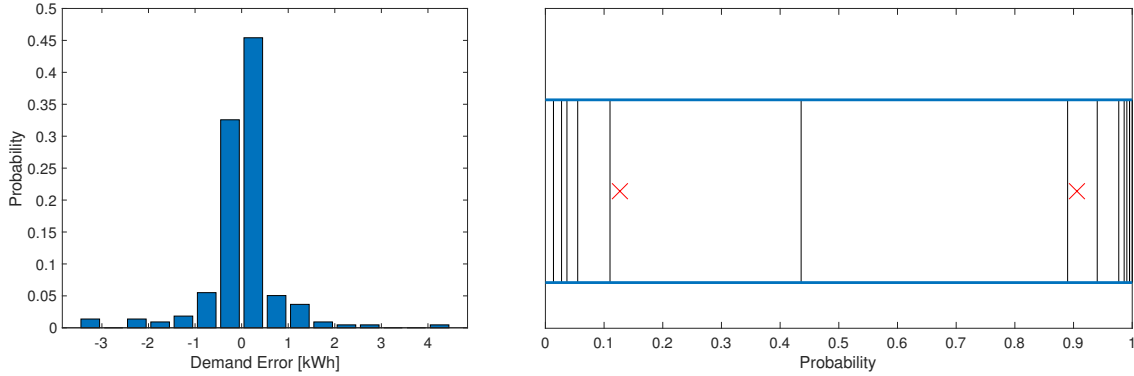


Figure 5-2: Roulette Wheel Mechanism for the uncertainty model of electrical demand. The unit interval is sliced in probability levels (on the right) according to the empirical distribution (on the left). The red 'X's represent two independent samples generated from a uniform distribution: their position on the roulette wheel determine the subintervals where to extract the realizations of forecast error

all the constraints to be satisfied for all the generated scenarios, will result to be infeasible.

$$\exists k : \max_j \hat{Q}_{\text{TES}}^{[j]}(k) - \min_j \hat{Q}_{\text{TES}}^{[j]}(k) > \underbrace{\max_{\text{TES}} - \min_{\text{TES}}}_{D^*} \implies \text{unfeasible problem} \quad (5-17)$$

Hence, the main issue with the scenario-based approach consists of a large infeasibility rate due to wide probabilistic distributions of the uncertainties related to thermal demand. A possible way to decrease this rate would be to use a higher sampling frequency for the supervisory strategy. Indeed, the absolute values of demanded thermal energy for shorter time steps would decrease, and the probability of a large range due to forecast error would decrease consequently. However, more granular data are not available and we have to deal with the forecasting errors produced for time steps of one hour.

Scenario Generation

The forecasting models of thermal and electrical demand were defined through a periodic linear regression system affected by an additive disturbance, which is described by a set of empirical distributions \mathcal{W}_i for each temporal mode. A complete formulation of the model was presented in Section 4-2-4.

The procedure we employ to generate the requested amount of scenarios in the stochastic framework is based on the so called **roulette wheel mechanism** [56]. This mechanism is widely applied when one wants to sample from a non-parametric empirical distribution, which assigns given probabilities to each interval of the possible outcomes, named bin. A roulette wheel divides the probability unity $[0,1]$ in slices whose width corresponds to the specific probability level of each bin (Figure 5-2). Then, a random number is generated from a unitary uniform distribution for each scenario. The value of the random number falls in one of the slices of the roulette wheel, thus determining a specific range for the error forecast. Once a specific bin is selected, the value of $w_i(k)$ is uniformly sampled within the extracted bin. Hence, the degree of approximation due to discretisation is strictly dependent on the

width of bins. The sampled uncertainty is propagated through the forecasting model for each of the N_s scenarios.

On the other hand, as regards PV supply, a simpler generation method can be applied. Indeed, the decomposition of the supply between the deterministic clear-sky component and the stochastic normalized component allow us to employ the Gaussian error of the AR model to propagate the forecasting error.

5-4-2 Tree-Based Approach

When the original ensemble of scenarios is provided, an exploitation of a tree structure, as explained in Section 4-1-2, has the potential to better describe the uncertainty distribution. While in scenario-based MPC a unique control sequence is required to satisfy system constraints for any realized scenario, in tree-based MPC each control sequence has to satisfy only the constraints related to the disturbance in its branch. Indeed, a different control sequence for each root-to-leaf path has to be considered, leading to an increase of the decision space with respect to the classical scenario-based approach. However, the increment of computational complexity is paid off by a less conservative result, due to a more representative uncertainty approximation.

In order to define a tree structure it is sufficient to assign a parent member $P[i]$ and a branching point $B[i]$ to each ensemble member [70]. The branching point represents the time step when a scenario is considered to be separated from its parent. The branching point is ‘infinite’ in case when a scenario is undistinguishable from its parent until the end of the prediction horizon. Moreover, the parent of the root scenario is conventionally chosen as 0.

In order to reduce the large amount of decision variables corresponding to each separate scenario, it is necessary to introduce the so called non-anticipative constraints by exploiting the information given in the tree structure: two control sequences will be equal before the bifurcation point of their respective branches [70]. The non-anticipativity constraints are defined for each generated scenario except for the tree root:

$$\hat{u}^{[j]}(k) = \hat{u}^{[P[j]]}(k) \quad \text{for } k = 1, \dots, \min\{B[j] - 1, N_p\} \quad (5-18)$$

$$\forall j \in \{1, \dots, N_s\} \setminus \{j : P[j] = 0\}$$

In this way the input tree will exactly have the same structure as the disturbance tree. Since the tree has a unique root, the first component of any control sequence will be the same and the MPC algorithm can be implemented in a receding horizon fashion.

Tree Construction

In order to deal with the large infeasibility rate due to uncertainty in thermal demand, we decided to build a scenario tree whose branching is based on the condition that the cumulative ‘distance’ between scenario couples cannot be larger than the allowed energy range in the thermal energy storage D^* , as expressed in (5-17).

The tree construction is inspired by the algorithm in [70] and leads to the minimum number of branches with the fixed distinguishability condition. Hence, a symmetric distinguishability matrix D is first computed, having as entries the branching time in which a couple of scenarios (i, j) have to be considered as belonging to different branches. Here, branching time is the

minimum time in which the cumulative ‘distance’ between scenario couples results to be larger than D^* :

$$D_{ij} = \min \left\{ t : \underbrace{\left| \sum_{k=1}^t \hat{D}_Q^{[i]}(k) - \hat{D}_Q^{[j]}(k) \right|}_{\Delta Q_{\text{TES}}(t)} \geq D^*, \quad 2 \leq t \leq N_p \right\} \quad i, j = 1, \dots, N_s \quad (i \neq j) \quad (5-19)$$

Branching time has to be necessarily larger than 1, because all the branches are required to have the same root at the first time step, and is at most equal to the prediction horizon N_p , since no information is available after that point in time. However, it can happen that two trajectories are close enough to each other so that, even at the end of the horizon, when all the available observation will have been collected, one ensemble member is not distinguishable from the other. In this specific case, D_{ij} has an infinite value. On the other hand, the entries on the main diagonal ($i = j$) are not defined, since they represent the distance of a scenario from itself.

Once the distinguishability matrix D has been computed, the following algorithm is applied to build the tree:

1. The maximum element of D is retrieved at the position (i, j) . The correspondent parameters of the row member are assigned:

$$P[i] = j \quad B[i] = D_{ij}$$

2. The element (and its symmetric) is removed from the matrix by means of a ‘NaN’ assignment. Indeed, a removal would modify the matrix structure.
3. The distinguishability properties of the member i are propagated to its parent, in order not to lose any information:

$$D_{:j} = \min\{D_{:i}, D_{:j}\}$$

4. Eventually, i -th row and column are both set to ‘NaN’, such that the child member is not reconsidered anymore.
5. Steps 1-4 are repeated until the tree parameters are assigned for any scenario.

The number of scenarios used to build the tree has to be coherent with the allowed probability risk p . As example, we show in Figure 5-3 the tree structure built from $N_s = 19$ scenarios of thermal demand forecasting, computed at 6 a.m. during a winter day. Scenarios plotted with the same colour are considered to belong to the same branch, thus they have to be controlled by the same control sequence. To better understand the distinguishability criteria, in the bottom figure we also plotted the cumulative thermal demand along the increasing prediction horizon. This variable directly affects the storage level Q_{TES} due to the linear relation of the heat balance (2-6) and represents the storage loss when no supply is provided to the system. Hence, we can clearly see how our construction of the disturbance tree separate scenarios with different demand level. In this example, D^* is equivalent to 25kWh.

The feasibility rate of a tree-based MPC algorithm highly increases with respect to scenario-based method, at the expense of a greater computational complexity due to augmentation of

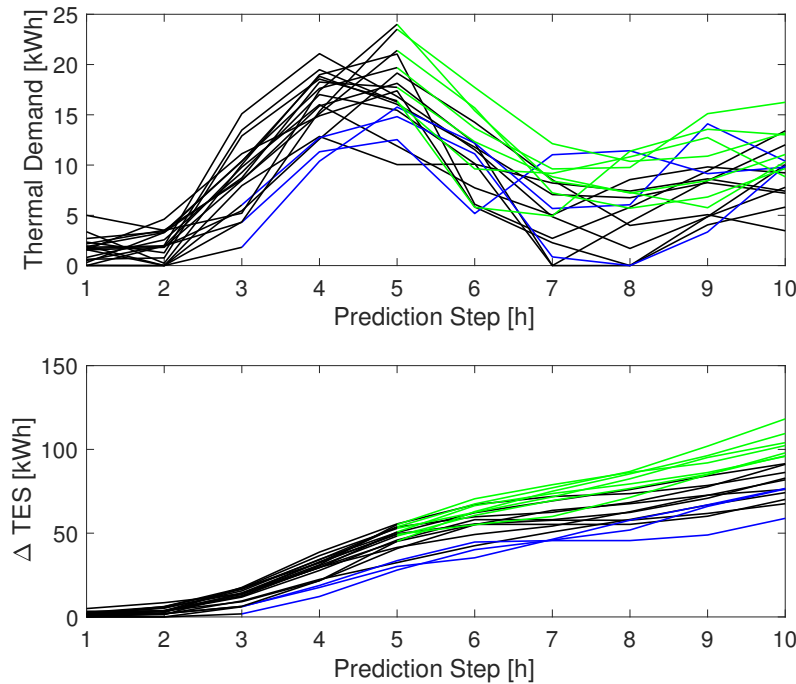


Figure 5-3: Tree structure built from $N_s = 19$ scenarios of thermal demand forecasting. Scenarios plotted with the same colour are considered to belong to the same branch

the decision space. However, we can afford this extra complexity without any practical issue due to our model simplicity. Indeed, with a 2,7 GHz Intel processor, the optimisation is still solvable in at most 0.6 seconds, whereas the sampling time of the implemented supervisory control is 1 hour.

5-5 Conclusions

The heat-led rule-based controller described in Section 5-2 is considered as the benchmark control strategy to be implemented in a local EMS. Then, a deterministic MPC strategy, based on the *certainty equivalence* paradigm of forecasts, is implemented, in order to explicitly optimise the operational costs of the microgrid on the long run. Indeed, when future predictions of system behaviour are considered by the controller, the strategy is said to be ‘intelligent’ since all relevant information about the consequences of choosing actions are taken into account. The disadvantages of deterministic strategies to the residential microgrid are related to frequent violations of the thermal comfort constraints, hence the necessity to integrate model uncertainty into a more complete stochastic framework is highlighted.

Subsequently, stochastic MPC strategies are formulated in a randomised approach that numerically approximates disturbance uncertainty by means of scenario realizations of the stochastic processes involved. Finally, a method to build a tree structure for the thermal demand forecasting is presented, with the purpose to implement a tree-based MPC and improve the feasibility rate of the stochastic control strategy.

Simulation and Comparison

The purpose of the investigated supervisory control strategies is to select set-points for the supply of the generators in the microgrid (gas engine and auxiliary boiler). This final chapter presents and compares the results obtained by the different control strategies described in Chapter 5, when applied on the two case studies defined in Section 3-3-3.

Before presenting our final results, we want to briefly recap our problem statement by means of the following conditions:

- electric and thermal local demand have to be satisfied at any time step within the microgrid
- water temperature of the thermal energy storage, used to decouple thermal supply and demand, has to be kept within predefined bounds
- the technical constraints regarding operation of the generators have to be considered
- the operational cost of the microgrid has to be optimised in order to maximise economical savings for the households that invested in the distributed resources

The four proposed control strategies have been tested on the same 40% days selected throughout the whole year, representing the validation set of the forecasting models for energy demand and solar power supply. All the models have been implemented and simulated on MATLAB 2017b. Performances are evaluated in terms of cost savings, primary energy savings, and emissions savings with respect to the conventional case of centralised electric generation and standard domestic boiler. Moreover, violation rate of thermal constraints in the TES represents an additional fundamental parameter to be evaluated.

The necessity to satisfy thermal demand for comfort of the households at any time instant would require a lower-level controller to recompute the set-points of the generators within the hourly time step. This two-levels strategy would strongly affect the computed savings of the scheduled microgrid operation. A rough estimate of performance deterioration is computed for all the investigated cases by assuming, on one hand, that supplied heat violating upper bounds of the thermal storage would be dumped and lost, whereas, on the other hand, that

Control Strategy	Rule-Based	Classic MPC	Scenario MPC	Tree MPC
Cost Savings	6.14 %	6.60 %	6.25 %	6.17 %
Primary Energy Savings	5.85 %	6.30 %	5.93 %	5.86 %
Emission Savings	11.78 %	12.60 %	12.12 %	11.91 %
Violation Rate (Up/Down)	8.6/1.5 %	6.11/16.24 %	2.5/1.6 %	0.7/3.6 %
Infeasibility Rate	-	1.6 %	26.7 %	2.9 %

Table 6-1: Control strategies comparison. Prediction horizon N_p is set to 6 hours for all MPC controllers.

the auxiliary boiler is capable to react fast enough to avoid lower bound violations within the time step, at the price of additional gas consumption. Hence, the recomputed performance indices are showed in a separate table for the two cases studies, thus highlighting larger savings obtained when stochastic strategies are applied.

We recall that, for predictive strategies, infeasibility issues are addressed by considering the rule-based controller as back-up strategy. Moreover, for all the predictive strategies, the horizon N_p **has been fixed to 6 hours** because this choice offers the best performance. For larger horizons, the increasing uncertainty in the forecasting deteriorates the results of the MPC optimization.

6-1 Case Study ‘A’: Micro-CHP

For the first case study, described in Table 3-4, the supervisory control considers the forecast energy demand of the end-users and makes hourly decisions about the production of both the CHP engine and the gas-fired boiler connected to the microgrid.

Four different simulations have been run for the proposed control strategies and their results are showed in Table 6-1. Since the cost savings represent our explicit objective, only the best performance according to this index is highlighted in the table.

We want to make clear that the performance indices of the four methods belong to a quite narrow range, thus highlighting the limited benefits of the control strategy applied in a local EMS, when unit commitment and economic dispatch represent the only decisions to make. However, the following discussion helps to understand the differences between the tested strategies.

All the considered indices are the lowest in the case in which the rule-based controller is applied. The result is completely reasonable if we consider that this controller does not make any ‘smart’ decision about the production schedule of the microgrid resources. Indeed, it just selects the CHP supply based on the TES level, without even considering electricity needs. On the other hand, the classic MPC framework displays the best performance in terms of operational savings.

However, the effect of stochastic strategies can be proved by the reduced rate of constraint violations in the TES. The decisions made by scenario and tree-based MPC are more conservative due to the explicit consideration about uncertainty in energy demand evolution: the amount of constraint violation is drastically reduced with respect to the deterministic framework, at the price of a lower optimised cost. Finally, the main difference between the two stochastic strategies consists of the ability of the tree-based MPC to deal with conditions

Control Strategy	Rule-Based	Classic MPC	Scenario MPC	Tree MPC
Cost Savings	5.80 %	5.79 %	6.00 %	6.02 %
Primary Energy Savings	5.49 %	5.45 %	5.69 %	5.70 %
Emission Savings	11.44 %	11.71 %	11.70 %	11.71 %

Table 6-2: Control strategies comparison when thermal violations are avoided. Prediction horizon N_p is set to 6 hours for all MPC controllers.

that would be infeasible in cases in which a scenario-based strategy is implemented.

In the Figures 6-1–6-4, we show the power flows within the microgrid when the different control strategies are implemented in the EMS. Only six days, which are representative of the whole dataset (144 days), are shown for matter of clearness. Each day is randomly selected in a single bimester in order to cover the seasonality of the year.

The figures consists of 4 different plots, where the ones on the left represent the thermal network of the microgrid and the ones on the right the electrical network. Moreover, the top plots display the energy balances between local supply (coloured bars) and demand (black line), whereas the bottom plots display the correspondent network imbalances: the TES level for the thermal network and the amount of bought (or sold) electricity from (to) the utility power grid as regards the electrical network.

We observe that rule-based controller operates the CHP engine at its maximum or minimum power supply (when the TES is close to its full capacity) for most of the time. Indeed, it does not regulate the supply based on information regarding the electrical demand. Moreover, due to its myopia about the future network evolution it often incurs in forced switching off of the CHP engine which can be avoided with predictive strategies.

When MPC strategies are implemented, the controller takes into account both future dynamics and electricity needs, managing to choose a more beneficial action in the enlarged decision space. Moreover, the evident difference between deterministic and stochastic strategies is the behaviour of the TES: when the forecasting uncertainty is explicitly considered in stochastic MPC strategies, the storage level is averagely pushed at a larger distance from the bounds.

The benefits of implementation of stochastic strategies and the subsequent reduction in constraint violations can be better understood if we look at the same simulation results when all the violations are explicitly penalized and assumed to be solvable. Hence, an upper saturation of thermal level in the water storage, as in (5-16), can be considered for the evaluation, and a recovery strategy is assumed on the auxiliary boiler in order to compensate for the lower bounds violation, as in (5-15).

In these updated conditions, we can observe the results showed in Table 6-2. Performance of classic MPC are consistently reduced and they appear to be even worse than the simple rule-based controller. On the other hand, stochastic strategies, which aim to reduce the thermal violation rate, keep their performance closer to the standard problem. Tree-based MPC becomes the best among all the proposed control strategies in this context. However, we have to highlight that the larger computational complexity of the tree-based algorithm seems not to pay off the slightly larger performance with respect to scenario-based MPC, which would probably be the chosen algorithm to implement in a local EMS.

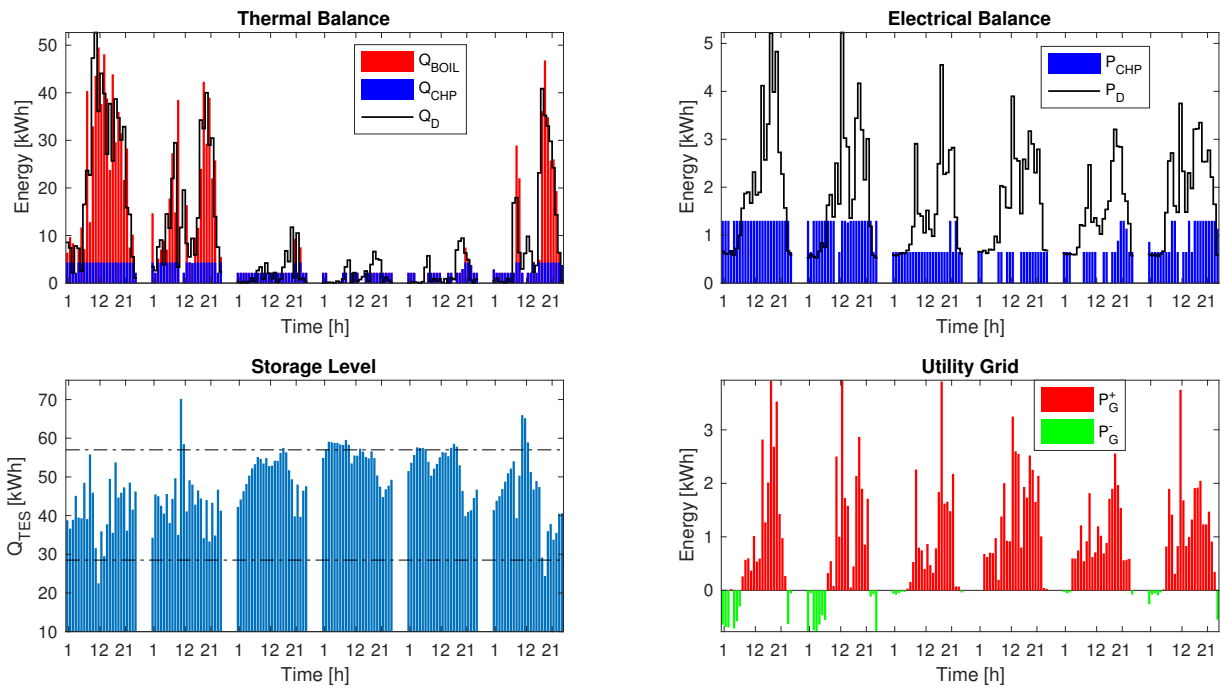


Figure 6-1: Rule-based control strategy applied to case study 'A'

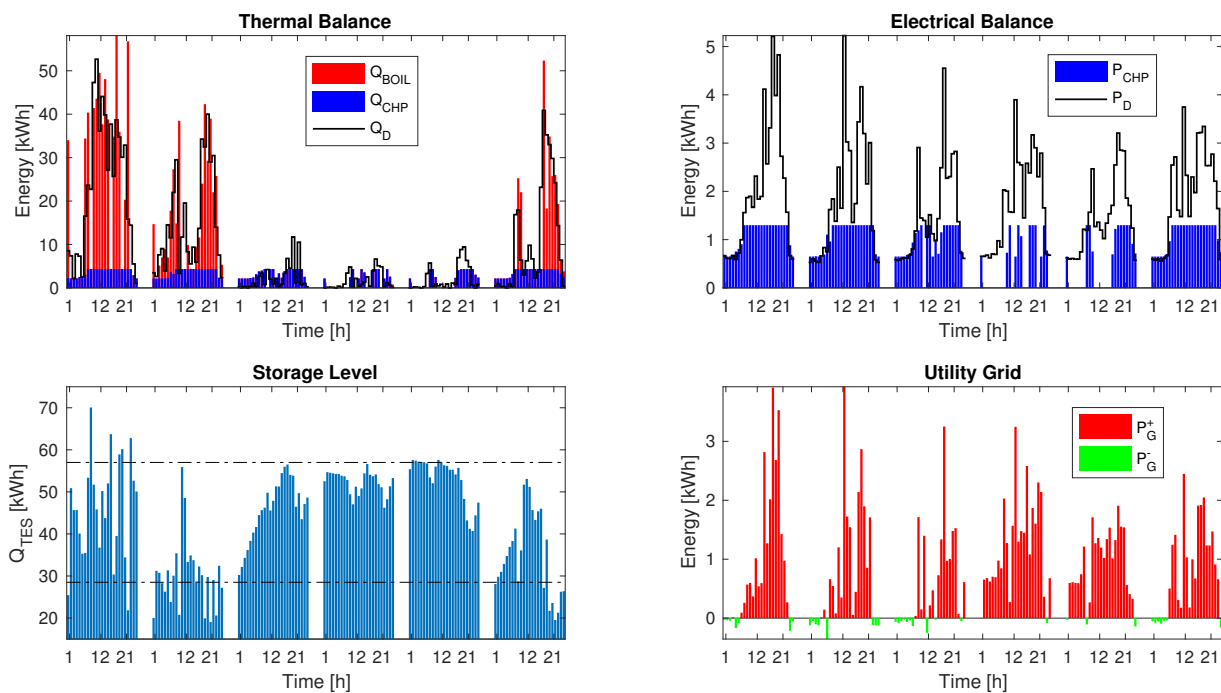


Figure 6-2: Deterministic MPC strategy applied to case study 'A'

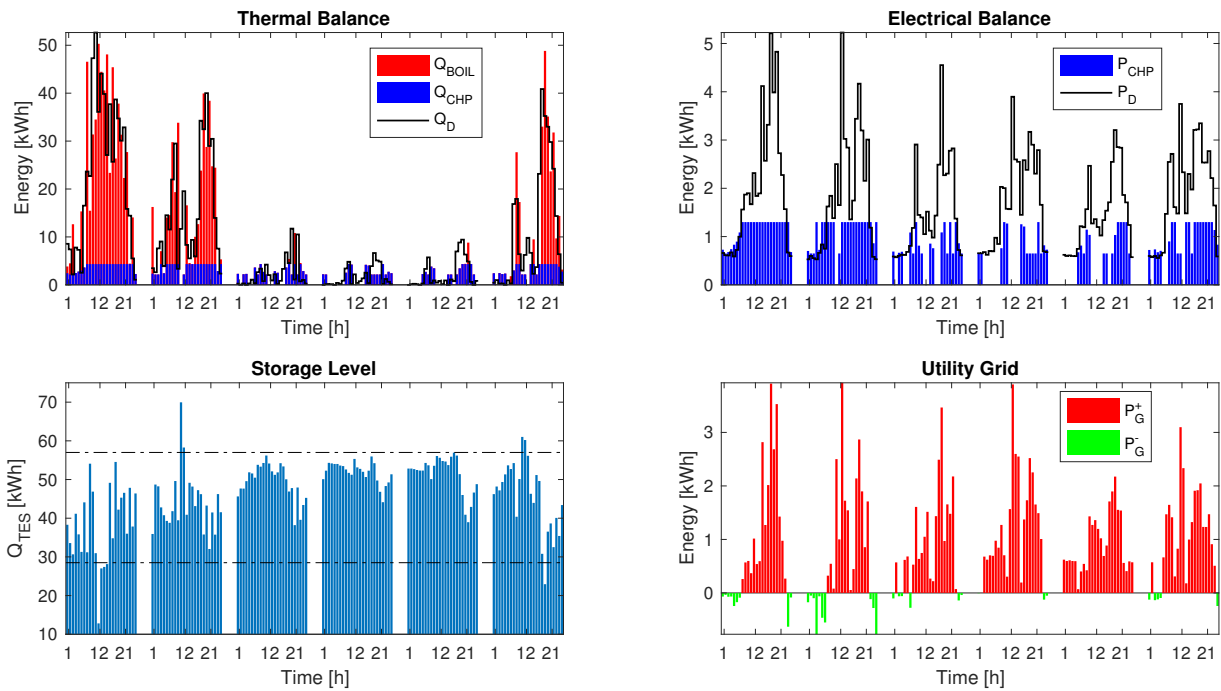


Figure 6-3: Scenario MPC strategy applied to case study 'A'

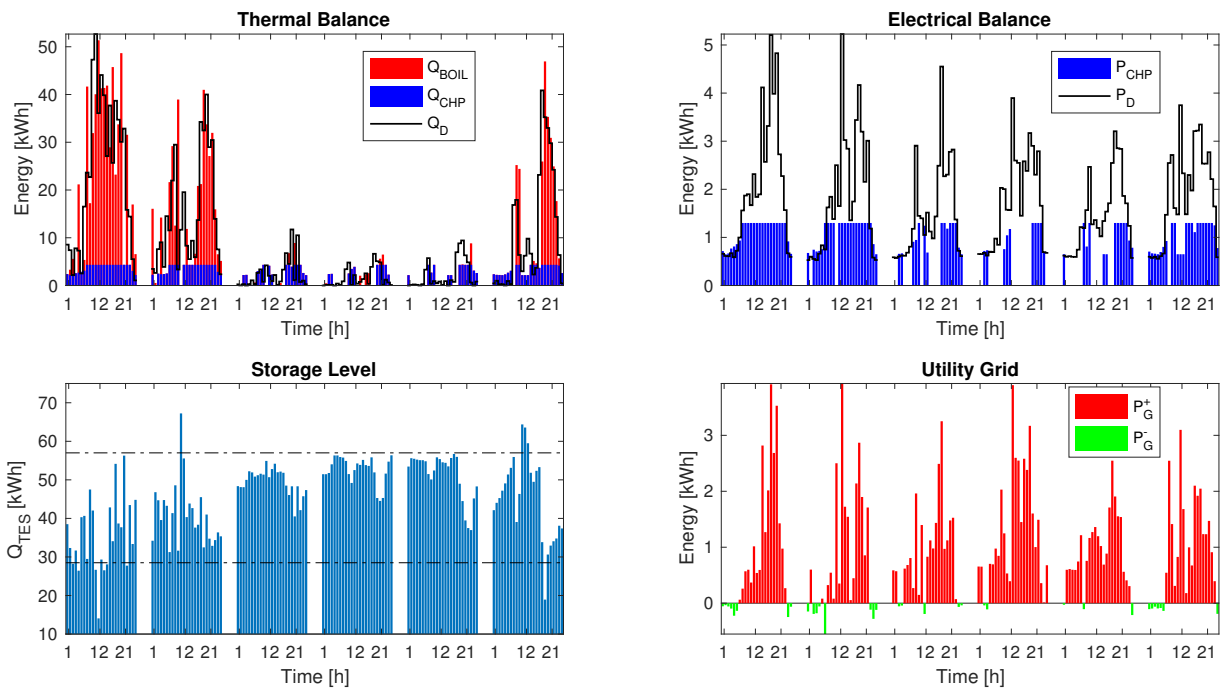


Figure 6-4: Tree-based MPC strategy applied to case study 'A'

6-2 Case Study ‘B’: Micro-CHP and PV Generation

In case study ‘B’ we have assumed that the previous microgrid scenario is modified and enlarged with an interconnected PV system. The optimal sizing procedure for the energy resources led us to the microgrid defined in Table 3-5. Since the PV system is not controllable and its power output entirely depends on atmospheric conditions, the implemented control strategies only differs from case study ‘A’ due to a more complex forecasting model that attempts to predict net electricity demand in the microgrid. Indeed, the clear-sky model proposed in Section 4-3-1 is used to forecast PV power production within the prediction horizon for all the MPC strategies. The added information is considered in the optimization procedure by computing the reduced electric demand with respect to the case study ‘A’.

Figures 6-5 – 6-8 show the simulation results for the same six days of the previous case study. The fundamental difference in microgrid operation regards, on the electrical side, a new local source of energy supply: the electricity produced by the PV panels represented in yellow bars. The rule-based controller behaves quite similarly to case study ‘A’, because its decisions are not based on the dynamics of the modified electrical network. Predictive strategies, on the other hand, can better adapt the micro-CHP production during sunny days, when the supplied PV power can almost completely satisfy the internal demand.

Conclusions about the proposed control strategies are very similar to the previous case. Indeed, classic MPC offers the best performance when constraint violations are not penalized (Table 6-3), whereas a tree-based algorithm highly improves its rank when up saturation and low bound recovery are considered to avoid violation of thermal bounds (Table 6-4).

Control Strategy	Rule-Based	Classic MPC	Scenario MPC	Tree MPC
Cost Savings	12.63 %	12.99 %	12.91 %	12.94 %
Primary Energy Savings	10.87 %	11.43 %	11.29 %	11.36 %
Emission Savings	16.59 %	16.45 %	16.53 %	16.48 %
Violation Rate (Up/Down)	3.8/1.5 %	3.4/16.7 %	1.1/2.4 %	0.5/2.7 %
Infeasibility Rate	-	0.38 %	26.8 %	0.5 %

Table 6-3: Control strategies comparison. Prediction horizon N_p is set to 6 hours for all MPC controllers.

Control Strategy	Rule-Based	Classic MPC	Scenario MPC	Tree MPC
Cost Savings	12.40 %	12.13 %	12.75 %	12.77 %
Primary Energy Savings	10.63 %	10.53 %	11.13 %	11.15 %
Emission Savings	16.35 %	15.49 %	16.34 %	16.36 %

Table 6-4: Control strategies comparison when thermal violations are avoided. Prediction horizon N_p is set to 6 hours for all MPC controllers.

6-3 Conclusions

In the last chapter of this thesis, we showed the results of the proposed control strategies for the two residential microgrids selected as our case studies.

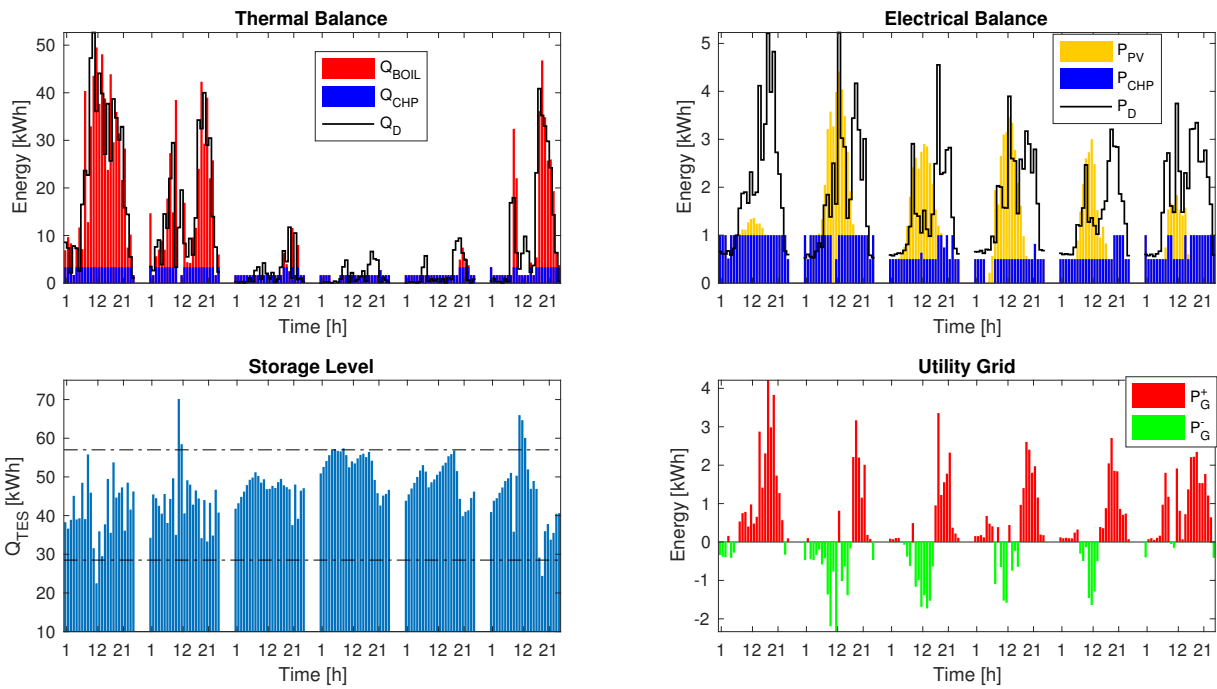


Figure 6-5: Rule-based control strategy applied to case study 'B'

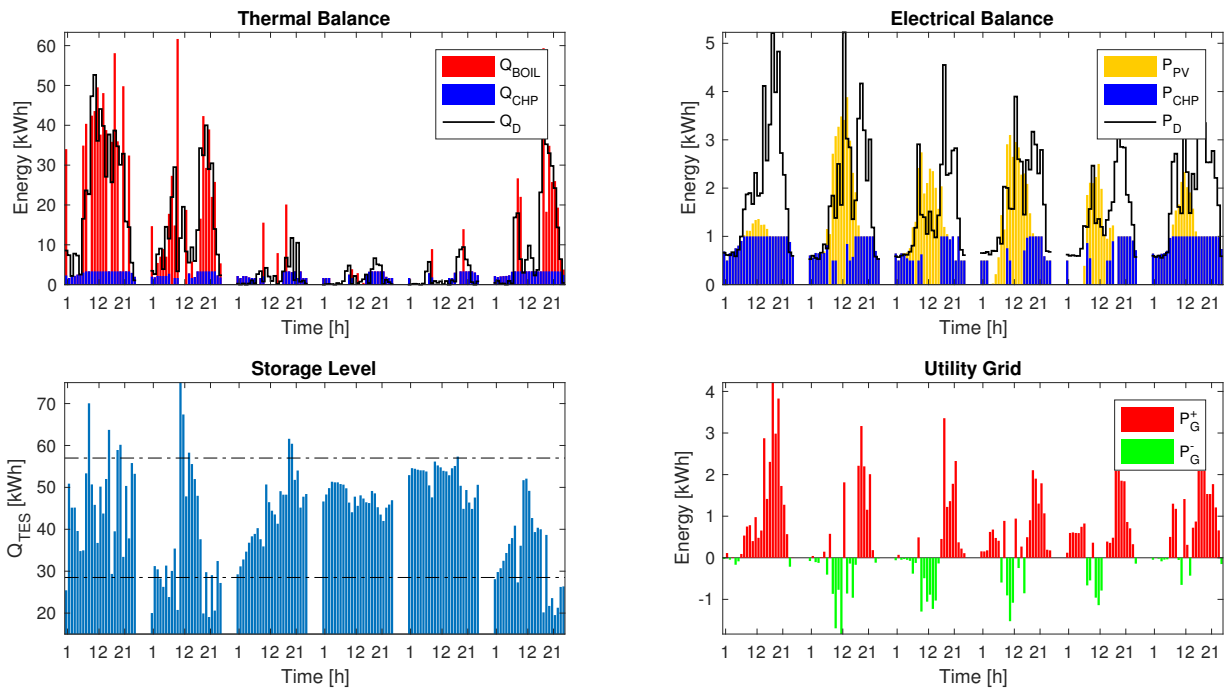


Figure 6-6: Deterministic MPC strategy applied to case study 'B'

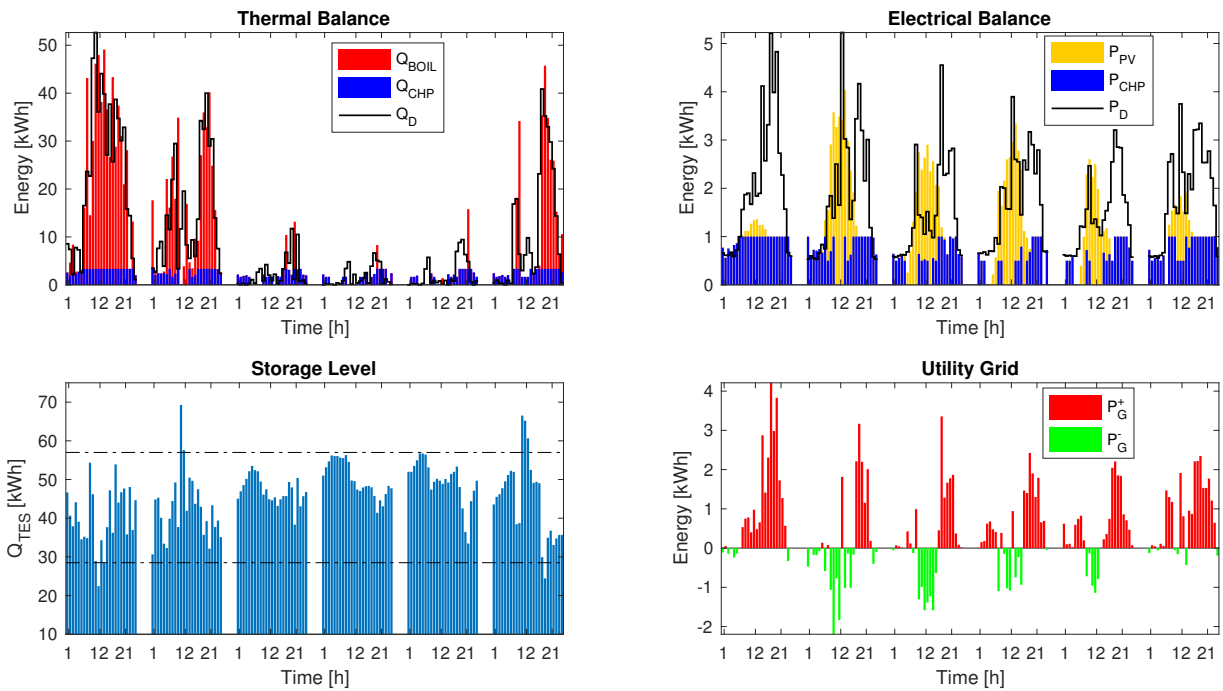


Figure 6-7: Scenario MPC strategy applied to case study 'B'

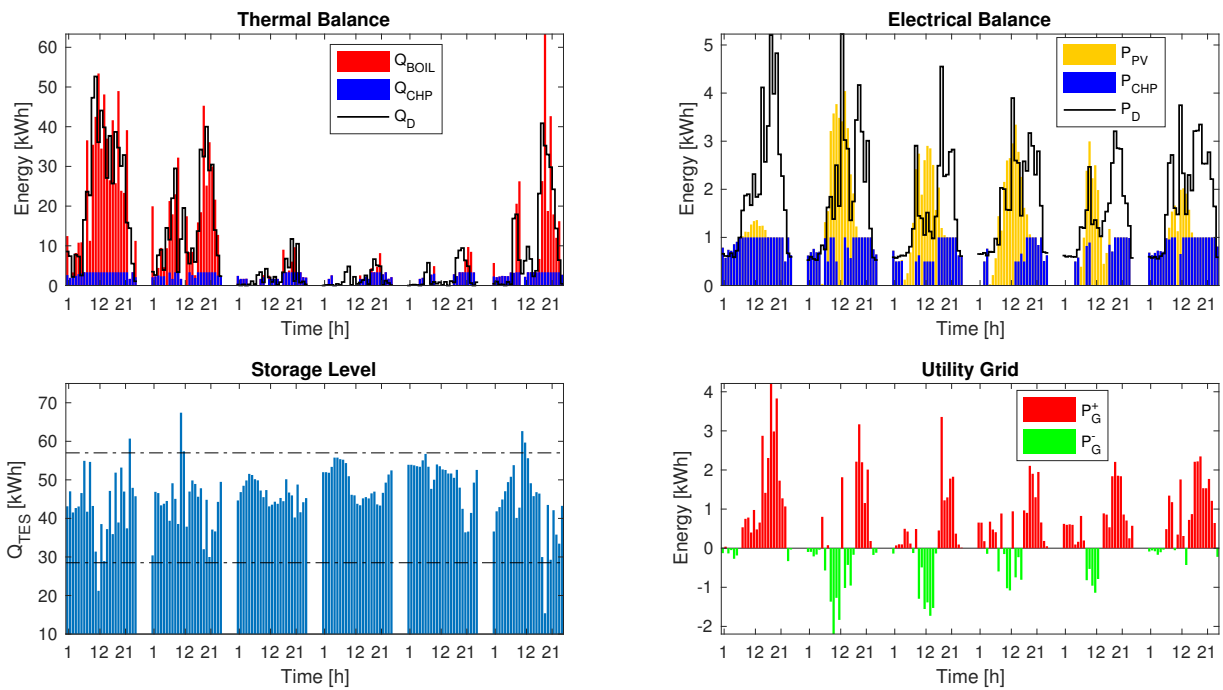


Figure 6-8: Tree-based MPC strategy applied to case study 'B'

In the small scale context of a residential microgrid, deterministic optimization is strongly affected by the uncertainty of forecasting models and, consequently, leads to aggressive decisions of the supervisory controller that do not take system uncertainty into account. Hence, from a practical point of view, deterministic MPC strategy incurs in several constraint violations of the thermal comfort bounds in the hot water TES. When the consequences of these violations are considered, it emerges that stochastic strategies, as tree-based MPC, can actively control the violation limit and offer the best performance between the tested algorithms.

Conclusions & Recommendations

7-1 Summary

In this thesis we have investigated the profitability of investment and employment of distributed generation technologies in residential microgrids. Our look has been focused on actual market conditions and has been limited to the Dutch scenario. Specifically, we developed an economic profitability analysis for the installation of a micro-CHP system, whose power and heat production reduce the primary fuel consumption in residential environments, and solar roof PV panels. Hence, two case studies have been defined, on which to perform our analysis: case study ‘B’ is different from case study ‘A’ due to the presence of an integrated non-controllable PV system in the microgrid, together with the micro-cogeneration engine. In both cases the resources were optimally sized with respect to the maximum economic profitability they could lead to the customers during their lifetime.

Subsequently the thesis has been developed with the purpose to evaluate the effects of the strategy implemented to control the power generated by the distributed energy resources composing the residential microgrid.

Supervisory control strategies are mainly based on the information they are able to process about future evolution of the microgrid. Indeed, our first step consisted of the implementation of forecasting models for stochastic processes affecting the power balance of the microgrid: thermal and electrical consumption of the customers on one hand, and PV uncontrollable supply on the other hand. The forecasting are exclusively based on data which can be easily collected by the controller, i.e. previously measured values of the considered processes and calendar information. As a consequence, the prediction error, even for the best identified models, results relatively large due to the high volatility of the stochastic processes. We assume that prediction accuracy could be improved by introducing extra information collected by local sensors, e.g. occupancy, or obtained through web communication with a meteorological database, e.g. outside temperature. However, on small scale forecasting, the effect of the behaviour of the customers represents the largest and most unpredictable source of uncertainty, and it would be impossible to reduce the prediction error below a certain physical threshold.

After forecasting models have been identified, we designed and implemented predictive control strategies that are based on the MPC framework and are adapted to our case studies. The main target of our work, at this point, was to measure the beneficial effects of stochastic strategies, which take model uncertainty explicitly into account into the optimization procedure, with respect to the standard deterministic framework. Stochastic MPC strategies are formulated in a randomised approach that numerically approximates disturbance uncertainty by means of scenario realizations of the stochastic processes involved. A scenario-based MPC and a tree-based MPC were adapted and implemented on the defined case studies and the simulation results were discussed.

7-2 Conclusions

The first results of this thesis have showed that micro-CHP engines have not reached a mature enough development to justify their widespread installation in residential buildings. Indeed, their high technology cost is never practically compensated by the operational savings obtained by the households during CHP lifetime. Only very high-demanding customers or, more likely, clusters of 4-5 families willing to share the investment can have the economical motivation to establish a residential microgrid. However, in these cases, the CHP engine would be undersized with respect to the potential operational savings it could lead to the investors, because of its large market cost: an increase in the engine size represents a cost that cannot be balanced by adequate economical savings. Hence, we conclude that the investment decision should be helped through government subsidies, which can be motivated by the beneficial effects in emissions reduction and efficiency improvement led by micro-CHP employment. Additionally, this reasoning is further magnified when we consider fuel cells as CHP prime mover. In this case, the technology cost (almost double with respect to other CHP engines) represents the fundamental obstacle to even more promising results in terms of operational savings.

On the other hand, the integration of solar panels for local electricity supply in a residential microgrid results to be highly recommended from an economic point of view, even in less sunny countries as the Netherlands. Indeed, the incredible growth of PV market in the last years has dramatically reduced the technology cost and made their employment profitable.

Our second research question, regarding the benefits of stochastic strategies, is then answered through simulations performed on MATLAB on the previously built case studies. Indeed, predictive strategies based on MPC perform better than standard rule-based control laws in terms of cost, primary energy, and emissions savings. However, in the small scale context of a residential microgrid, deterministic optimization is strongly affected by the uncertainty of forecasting models and, consequently, leads to aggressive decisions that do not take system uncertainty into account and incur in several constraint violations of the thermal comfort bounds in the hot water TES. When the consequences of these violations are practically considered, it emerges that stochastic strategies, as tree-based MPC, can actively control the violation limit and offer the best performance between the tested algorithms.

However, it is fundamental to highlight that all the evaluated results for the operational cost savings are enclosed in a really small range, which consists of about 0.5% of the total yearly expenses (≈ 40 €/year). One of the main reasons of this result can be retrieved in the undersized CHP engine, whose decision space is not large enough to develop the full

potential of microgrid operational savings. Indeed, the high investment cost of the considered technology represents a fundamental obstacle to its market maturity and to a more beneficial sizing procedure.

7-3 Future Work

In this section, recommendations for future work are listed.

1. Since we have identified in the high installation cost of micro-CHP technologies the main obstacle if we want to take full advantage of its operational savings (especially in terms of primary energy consumption and emissions), it would be fundamental to evaluate the effects of the proposed strategies on larger CHP engines. Indeed, we are aware that an increased decision space can lead to larger benefits of predictive strategies over rule-based controllers. To this purpose, the sizing procedure should follow different targets than pure economic reasoning, e.g. minimisation of primary energy consumption, and could also include the integration of a battery bank for electrical storage.
2. More factors could be considered to enlarge the beneficial gap of predictive strategies in the residential microgrid context. For instance, a variable real-time pricing scheme for the electricity cost, the use of demand response for electrical flexible loads, or, more easily, a more flexible space heating strategy which considers the building thermal model, have the potential to be included in this work and offer a larger decision space for the supervisory controller.
3. We have estimated that about 15% of yearly potential benefits (in case of perfect prediction) are lost due to forecasting errors. Hence, any improvement in forecasting models for the stochastic processes involved in the microgrid system could lead to a beneficial increase in operational savings. The inclusion of external explanatory variables, such as house occupancy and outside temperature, should be considered to improve the forecasting models and evaluate the effect of the enhanced prediction accuracy on the performance of the controlled system.
4. To the same purpose of the previous point, it would be interesting to repeat and improve our results with a reduced sampling time to measure sensor information and impose control decisions. Indeed, on a time scale of 15 or 20 minutes the prediction error would be reduced in absolute terms. Moreover, the results could be evaluated more accurately, due to the not considered intra-hour dynamics of domestic consumption. However, more granular data are needed for this goal.

Bibliography

- [1] International Energy Agency. Energy Policies of IEA Countries - The Netherlands. <http://www.iea.org/publications/freepublications/publication/Netherlands2014.pdf>, 2014.
- [2] International Energy Agency. Netherlands - Energy System Overview. <http://www.iea.org/media/countries/Netherlands.pdf>, 2016.
- [3] F. Alavi, E. P. Lee, N. van de Wouw, B. De Schutter, and Z. Lukszo. Fuel cell cars in a microgrid for synergies between hydrogen and electricity networks. *Applied Energy*, 192:296–304, 2017.
- [4] M. Alipour, B. Mohammadi-Ivatloo, and K. Zare. Stochastic scheduling of renewable and CHP-based microgrids. *IEEE Transactions on Industrial Informatics*, 11(5):1049–1058, 2015.
- [5] Alliander NV. Beschikbare data: Slimme meter. <https://www.liander.nl/over-liander/innovatie/open-data/data/>, 2013.
- [6] P. Bacher, H. Madsen, and H. A. Nielsen. Online short-term solar power forecasting. *Solar Energy*, 83(10):1772–1783, 2009.
- [7] A. Bemporad and M. Morari. Control of systems integrating logic, dynamics, and constraints. *Automatica*, 35(3):407–427, 1999.
- [8] R. J. Bessa, A. Trindade, C. S. P. Silva, and V. Miranda. Probabilistic solar power forecasting in smart grids using distributed information. *International Journal of Electrical Power & Energy Systems*, 72:16–23, 2015.
- [9] M. Bianchi, A. De Pascale, and P. R. Spina. Guidelines for residential micro-CHP systems design. *Applied Energy*, 97:673–685, 2012.
- [10] F. Brahman, M. Honarmand, and S. Jadid. Optimal electrical and thermal energy management of a residential energy hub, integrating demand response and energy storage system. *Energy and Buildings*, 90:65–75, 2015.

- [11] C. Brandoni and M. Renzi. Optimal sizing of hybrid solar micro-CHP systems for the household sector. *Applied Thermal Engineering*, 75:896–907, 2015.
- [12] G. Bruni, S. Cordiner, V. Mulone, V. Rocco, and F. Spagnolo. A study on the energy management in domestic micro-grids based on Model Predictive Control strategies. *Energy Conversion and Management*, 102:50–58, 2015.
- [13] G. C. Calafiore and M. C. Campi. The scenario approach to robust control design. *IEEE Transactions on Automatic Control*, 51(5):742–753, 2006.
- [14] M. C. Campi and S. Garatti. The exact feasibility of randomized solutions of uncertain convex programs. *SIAM Journal on Optimization*, 19(3):1211–1230, 2008.
- [15] M. C. Campi and S. Garatti. A sampling-and-discarding approach to chance-constrained optimization: feasibility and optimality. *Journal of Optimization Theory and Applications*, 148(2):257–280, 2011.
- [16] M. Collares-Pereira and A. Rabl. The average distribution of solar radiation-correlations between diffuse and hemispherical and between daily and hourly insolation values. *Solar Energy*, 22(2):155–164, 1979.
- [17] S. R. Cominesi, M. Farina, L. Giulioni, B. Picasso, and R. Scattolini. Two-layer predictive control of a micro-grid including stochastic energy sources. In *American Control Conference (ACC)*, pages 918–923. IEEE, 2015.
- [18] Energieonderzoek Centrum Nederland (ECN). ECN Phyllys Classification - Groningen Natural Gas. <https://www.ecn.nl/phyllis2/Biomass/View/929>, 2018.
- [19] Enerdata. World Energy Council - Energy Efficiency Indicators. <https://wec-indicators.enerdata.net/household-electricity-use.html>, 2014.
- [20] Odyssee-Mure (Enerdata). Energy Efficiency Country Profile: Netherlands. <http://www.odyssee-mure.eu/publications/profiles/the-netherlands-efficiency-trends-english-version.pdf>, 2015.
- [21] EnerTwin. CHP system with a micro turbine. <http://www.enertwin.com/>.
- [22] Eurostat. Energy Consumption By Sector In The EU. <https://epthinktank.eu/2016/07/08/energy-efficiency-in-buildings/energy-consumption-by-sector/>, 2014.
- [23] S. Fan and R. J. Hyndman. Short-term load forecasting based on a semi-parametric additive model. *IEEE Transactions on Power Systems*, 27(1):134–141, 2012.
- [24] M. Farina, L. Giulioni, and R. Scattolini. Stochastic linear Model Predictive Control with chance constraints – A review. *Journal of Process Control*, 44:53–67, 2016.
- [25] A. H. Fathima and K. Palanisamy. Optimization in microgrids with hybrid energy systems—a review. *Renewable and Sustainable Energy Reviews*, 45:431–446, 2015.
- [26] A. Fouquier, S. Robert, F. Suard, L. Stéphan, and A. Jay. State of the art in building modelling and energy performances prediction: A review. *Renewable and Sustainable Energy Reviews*, 23:272–288, 2013.

-
- [27] Fraunhofer Institute for Solar Energy Systems. Photovoltaic Report. <https://www.ise.fraunhofer.de/content/dam/ise/de/documents/publications/studies/Photovoltaics-Report.pdf>, 2016.
- [28] N. Friedman, D. Geiger, and M. Goldszmidt. Bayesian network classifiers. *Machine Learning*, 29(2-3):131–163, 1997.
- [29] L. Giullioni. *Stochastic Model Predictive Control with application to distributed control systems*. PhD thesis, Polytechnic of Milan, 2015.
- [30] J. M. Grosso, P. Velarde, C. Ocampo-Martinez, J. M. Maestre, and V. Puig. Stochastic model predictive control approaches applied to drinking water networks. *Optimal Control Applications and Methods*, 38(4):541–558, 2017.
- [31] M. T. Hagan and M. B. Menhaj. Training feedforward networks with the marquardt algorithm. *IEEE Transactions on Neural Networks*, 5(6):989–993, 1994.
- [32] L. Hernández, C. Baladrón, J. M. Aguiar, L. Calavia, B. Carro, A. Sánchez-Esguevillas, D. J. Cook, D. Chinarro, and J. Gómez. A study of the relationship between weather variables and electric power demand inside a smart grid/smart world framework. *Sensors*, 12(9):11571–11591, 2012.
- [33] L. Hernandez, C. Baladron, J. M. Aguiar, B. Carro, A. J. Sanchez-Esguevillas, J. Lloret, and J. Massana. A survey on electric power demand forecasting: future trends in smart grids, microgrids and smart buildings. *IEEE Communications Surveys & Tutorials*, 16(3):1460–1495, 2014.
- [34] Honda. Household Gas Engine Cogeneration Unit. <http://world.honda.com/power/cogenerator/>.
- [35] T. Hong and S. Fan. Probabilistic electric load forecasting: A tutorial review. *International Journal of Forecasting*, 32(3):914–938, 2016.
- [36] T. Hong and P. Wang. Fuzzy interaction regression for short term load forecasting. *Fuzzy Optimization and Decision Making*, 13(1):91, 2014.
- [37] M. Houwing. *Smart heat and power: Utilizing the flexibility of micro cogeneration*. PhD thesis, TU Delft, 2010.
- [38] M. Houwing, R. R. Negenborn, and B. De Schutter. Demand response with micro-CHP systems. *Proceedings of the IEEE*, 99(1):200–213, 2011.
- [39] International Energy Agency. World Energy Outlook. <http://www.iea.org/weo/>, 2017.
- [40] R. K. Jain, K. M. Smith, P. J. Culligan, and J. E. Taylor. Forecasting energy consumption of multi-family residential buildings using support vector regression: Investigating the impact of temporal and spatial monitoring granularity on performance accuracy. *Applied Energy*, 123:168–178, 2014.
- [41] A. Khosravi, S. Nahavandi, D. Creighton, and A. F. Atiya. Comprehensive review of neural network-based prediction intervals and new advances. *IEEE Transactions on Neural Networks*, 22(9):1341–1356, 2011.

- [42] Koninklijk Nederlands Meteorologisch Instituut. Climatology - Hourly weather data for the Netherlands. <http://projects.knmi.nl/klimatologie/uurgegevens/selectie.cgi>, 2017.
- [43] M. Korda, R. Gondhalekar, J. Cigler, and F. Oldewurtel. Strongly feasible stochastic Model Predictive Control. In *50th IEEE Conference on Decision and Control - European Control Conference (CDC-ECC)*, pages 1245–1251, 2011.
- [44] M. Korda, R. Gondhalekar, F. Oldewurtel, and C. N. Jones. Stochastic MPC framework for controlling the average constraint violation. *IEEE Transactions on Automatic Control*, 59(7):1706–1721, 2014.
- [45] B. Kouvaritakis, M. Cannon, S. V. Raković, and Q. Cheng. Explicit use of probabilistic distributions in linear predictive control. *Automatica*, 46(10):1719–1724, 2010.
- [46] B. Liu, J. Nowotarski, T. Hong, and R. Weron. Probabilistic load forecasting via quantile regression averaging on sister forecasts. *IEEE Transactions on Smart Grid*, 8(2):730–737, 2017.
- [47] J. Lofberg. Approximations of closed-loop minimax MPC. In *Decision and Control, 42nd IEEE Conference on*, volume 2, pages 1438–1442. IEEE, 2003.
- [48] E. Lorenzo. Energy collected and delivered by PV modules. *Handbook of Photovoltaic Science and Engineering*, pages 905–970, 2003.
- [49] J. M. Maestre, L. Raso, P. J. Van Overloop, and B. De Schutter. Distributed tree-based model predictive control on a drainage water system. *Journal of Hydroinformatics*, 15(2):335–347, 2013.
- [50] M. M. Maghanki, B. Ghobadian, G. Najafi, and R. J. Galogah. Micro combined heat and power (MCHP) technologies and applications. *Renewable and Sustainable Energy Reviews*, 28:510–524, 2013.
- [51] D. Q. Mayne. An apologia for stabilising terminal conditions in model predictive control. *International Journal of Control*, 86(11):2090–2095, 2013.
- [52] D. Q. Mayne. Model predictive control: Recent developments and future promise. *Automatica*, 50(12):2967–2986, 2014.
- [53] D. Q. Mayne, J. B. Rawlings, C. V. Rao, and P. O. M. Scokaert. Constrained model predictive control: Stability and optimality. *Automatica*, 36(6):789–814, 2000.
- [54] D. Q. Mayne, M. M. Seron, and S. V. Raković. Robust model predictive control of constrained linear systems with bounded disturbances. *Automatica*, 41(2):219–224, 2005.
- [55] A. Mesbah. Stochastic model predictive control: An overview and perspectives for future research. *IEEE Control Systems*, 36(6):30–44, 2016.
- [56] S. Mohammadi, S. Soleymani, and B. Mozafari. Scenario-based stochastic operation management of microgrid including wind, photovoltaic, micro-turbine, fuel cell and energy storage devices. *International Journal of Electrical Power & Energy Systems*, 54:525–535, 2014.

-
- [57] S. Murugan and B. Horák. A review of micro combined heat and power systems for residential applications. *Renewable and Sustainable Energy Reviews*, 64:144–162, 2016.
- [58] R. Nanda. A Bayesian Approach for Forecasting Heat Load in a District Heating System (Master Thesis, Lulea University of Technology), 2015.
- [59] United Nations. Paris Agreement. http://unfccc.int/files/essential_background/convention/application/pdf/english_paris_agreement.pdf, 2015.
- [60] Navigant Research. Market Data: Microgrids. <https://www.navigantresearch.com/research/market-data-microgrids>, 2016.
- [61] NREL. Solar Radiation. <https://www.nrel.gov/rredc/>.
- [62] J. Ortiga, J.C. Bruno, and Coronas A. Selection of typical days for the characterisation of energy demand in cogeneration and trigeneration optimisation models for buildings. *Energy Conversion and Management*, 52(4):1934–1942, 2011.
- [63] J. Ostrowski, M. F. Anjos, and A. Vannelli. Tight mixed integer linear programming formulations for the unit commitment problem. *IEEE Transactions on Power Systems*, 27(1):39–46, 2012.
- [64] S. Parhizi, H. Lotfi, A. Khodaei, and S. Bahramirad. State of the art in research on microgrids: A review. *IEEE Access*, 3:890–925, 2015.
- [65] A. Parisio, E. Rikos, and L. Glielmo. A model predictive control approach to microgrid operation optimization. *IEEE Transactions on Control Systems Technology*, 22(5):1813–1827, 2014.
- [66] A. Parisio, E. Rikos, and L. Glielmo. Stochastic model predictive control for economic/environmental operation management of microgrids: An experimental case study. *Journal of Process Control*, 43:24–37, 2016.
- [67] A. Picciariello, J. Reneses, P. Frias, and L. Söder. Distributed generation and distribution pricing: Why do we need new tariff design methodologies? *Electric Power Systems Research*, 119:370–376, 2015.
- [68] I. Prodan and E. Zio. A model predictive control framework for reliable microgrid energy management. *International Journal of Electrical Power & Energy Systems*, 61:399–409, 2014.
- [69] M. L. Puterman. *Markov decision processes: discrete stochastic dynamic programming*. John Wiley & Sons, 2014.
- [70] L. Raso, N. Giesen, P. Stive, D. Schwanenberg, and P. J. Overloop. Tree structure generation from ensemble forecasts for real time control. *Hydrological Processes*, 27(1):75–82, 2013.
- [71] J. B. Rawlings and D. Q. Mayne. *Model Predictive Control: Theory and Design*. Nob Hill Publishing, 2009.

- [72] Y. Ren, P. N. Sugathan, and N. Srikanth. Ensemble methods for wind and solar power forecasting – A state-of-the-art review. *Renewable and Sustainable Energy Reviews*, 50:82–91, 2015.
- [73] L. R. Rodríguez, J. M. S. Lissén, J. S. Ramos, E. Á. R. Jara, and S. Á. Domínguez. Analysis of the economic feasibility and reduction of a building’s energy consumption and emissions when integrating hybrid solar thermal/PV/micro-CHP systems. *Applied Energy*, 165:828–838, 2016.
- [74] O. G. Santin, L. Itard, and H. Visscher. The effect of occupancy and building characteristics on energy use for space and water heating in Dutch residential stock. *Energy and Buildings*, 41(11):1223–1232, 2009.
- [75] N. Saraf. Predictive control for residential capacity controlled heat pumps in a smart grid scenario (Master Thesis, TU Delft), 2015.
- [76] G. Schildbach, L. Fagiano, C. Frei, and M. Morari. The scenario approach for Stochastic Model Predictive Control with bounds on closed-loop constraint violations. *Automatica*, 50(12):3009–3018, 2014.
- [77] M. Sharafi and T. Y. ELMekkawy. Multi-objective optimal design of hybrid renewable energy systems using PSO-simulation based approach. *Renewable Energy*, 68:67–79, 2014.
- [78] ShareAmerica. Distributed Generation Growing More Popular. <https://share.america.gov/distributed-generation-growing-more-popular/>, 2016.
- [79] R. H. Shumway and D. S. Stoffer. *Time series analysis and its applications*, volume 3. Springer, 2000.
- [80] Sunpower. The 1kW Stirling Engine. <http://sunpowerinc.com/1kw-stirling-engine/>.
- [81] H. Tanaka and J. Watada. Possibilistic linear systems and their application to the linear regression model. *Fuzzy Sets and Systems*, 27(3):275–289, 1988.
- [82] M. Tasdighi, H. Ghasemi, and A. Rahimi-Kian. Residential microgrid scheduling based on smart meters data and temperature dependent thermal load modeling. *IEEE Transactions on Smart Grid*, 5(1):349–357, 2014.
- [83] The Renewable Energy Hub. Internal Combustion Engine CHP Generators. <http://www.renewableenergyhub.co.uk/micro-combined-heat-and-power-micro-chp-information/internal-combustion-engine-chp-generator.html>.
- [84] VaasaETT. Household Energy Price Index. <https://www.energypriceindex.com/latest-update/>, 2018.
- [85] P. Velarde, L. Valverde, J. M. Maestre, and C. Ocampo-Martinez. On the comparison of stochastic model predictive control strategies applied to a hydrogen-based microgrid. *Journal of Power Source*, 343:161–173, March 2017.

- [86] R. Wilcox. Kolmogorov–smirnov test. *Encyclopedia of Biostatistics*, 2005.
- [87] Ji Xie, T. Hong, T. Laing, and C. Kang. On normality assumption in residual simulation for probabilistic load forecasting. *IEEE Transactions on Smart Grid*, 8(3):1046–1053, 2017.

Glossary

List of Acronyms

CHP	Combined Heat and Power
ICE	Internal Combustion Engine
PV	PhotoVoltaic
STC	Standard Test Conditions
TES	Thermal Energy Storage
EMS	Energy Management System
MPC	Model Predictive Control
MLD	Mixed Logical Dynamical
MAPE	Mean Absolute Percentage Error
WAPE	Weighted Absolute Percentage Error
RMSE	Root Mean Square Error
ANN	Artificial Neural Network
ICT	Information and Communication Technologies
IEA	International Energy Agency

